

UNIVERSITÄTSKLINIKUM HAMBURG-EPPENDORF

Institut für Tumorbiologie

Prof. Dr. med. K. Pantel

CTC-enrichment of larger sample volumes utilizing a slanted spiral microfluidic device and subsequent culture in microwells

Dissertation

zur Erlangung des Grades eines Doktors der Medizin
an der Medizinischen Fakultät der Universität Hamburg.

vorgelegt von:

Luisa Stegat
aus Münster

Hamburg 2023

(wird von der Medizinischen Fakultät ausgefüllt)

**Angenommen von der
Medizinischen Fakultät der Universität Hamburg am: 22.04.2024**

**Veröffentlicht mit Genehmigung der
Medizinischen Fakultät der Universität Hamburg.**

Prüfungsausschuss, der/die Vorsitzende: Prof. Dr. Volkmar Müller

Prüfungsausschuss, zweite/r Gutachter/in: PD Dr. Simon Joosse

Table of Contents

List of Figures	1
List of Tables	1
Abbreviations	2
1 Working hypothesis	4
1 Introduction	5
2.1 Cancer and Carcinogenesis	5
2.1.1 Genetic mutations - the basis of tumor development	5
2.1.2 Cancer risk factors	6
2.1.3 Passenger and driver mutations	7
2.1.4 Epigenetic modifications	8
2.1.5 The achievement of unlimited cell growth	9
2.1.6 Overcoming defensive mechanisms	10
2.1.7 The role of the immune system	10
2.1.8 Angiogenesis and tumor metabolism	11
2.1.9 Individual tumor characteristics	12
2.1.10 Cell types within the cancer microenvironment	13
2.2 Metastasis and the role of circulating tumor cells	15
2.2.1 Migration and intravasation	16
2.2.2 Circulating Tumor Cells	17
2.2.3 Extravasation and Colonization	18
2.3 Liquid biopsy	19
2.4 CTC enrichment methods	22
2.5 CTC culture and its role in personalized medicine	25
2.6 Study design	27
3 Material and Methods	28
3.1 Materials	28
3.2 Methods	31
3.2.1 Sample collection and processing	31
3.2.2 Enrichment with the slanted spiral microfluidic device	32
3.2.3 CellSearch® analysis	33
3.2.4 Culture of MCF7 cell line cells	33
3.2.5 CTC immunofluorescence detection	33
3.2.6 Culture of spiral-enriched cancer cells	33
3.2.7 Whole Genome Amplification (WGA)	35
3.2.8 Next generation sequencing	35
3.2.9 Statistical Analyses	35
4 Results	36
4.1 Development of the slanted spiral enrichment protocol	36
4.1.1 PBMC removal efficiency depending on cell concentrations and flowrate	36
4.1.2 Tumor cell line (MCF7) recovery rate of the slanted spiral	38
4.1.3 The influence of repetitive enrichment cycles on sample volume, CTC recovery and PBMC clearance	41

4.2	Viability of MCF7 cells after spiral enrichment and suitability of the culture conditions in microwells	44
4.3	CTC enrichment and microwell culture from patient samples	46
4.3.1	CTC categorization after sample enrichment with the slanted spiral depending on fluorescence appearance	47
4.3.2	CTC enumeration from patient samples after spiral enrichment	48
4.3.3	Confirmation of CTC status by next generation sequencing	52
4.3.4	Comparison of CTC counts obtained by slanted spiral and CellSearch® system	53
4.3.5	Culture of breast cancer CTCs	55
4.3.6	Culture of ovarian cancer CTCs	58
5	Discussion	61
5.1	Optimal performing conditions of the slanted spiral microfluidic device and potentials in diagnostic leukapheresis enrichment	61
5.2	Recovery rate and impact of internal and external factors	62
5.3	CTC enrichment from patient samples	65
5.4	CTC culture in microwells	67
6	Conclusion	71
7	Summary	72
8	Zusammenfassung	73
9	References	74
10	Acknowledgements	84
11	Entfällt aus datenschutzrechtlichen Gründen	
12	Eidesstattliche Versicherung	85

List of Figures

Figure 1 The Cells of the Tumor Microenvironment	14
Figure 2 The Metastatic Cascade	16
Figure 3 CTC detection rates depending on analyzed blood volume	21
Figure 4 Illustration of the slanted spiral	25
Figure 5 Production of the microwell agar chips	34
Figure 6 Influence of PBMC concentration on the spiral's PBMC removal efficiency	37
Figure 7 PBMC removal efficiency of the slanted spiral depending on cell concentration and flowrate	38
Figure 8 Exemplary pictures of cells categorized as "intact" and "torn"	40
Figure 9 Tumor cell line (MCF7) recovery of the slanted spiral	41
Figure 10 Effects of multiple enrichment cycles on CTC recovery rate	43
Figure 11 Increase of CTC recovery after enrichment of the discarded fraction	44
Figure 12 Development of the spiral enriched MCF7 cells in microwells	45
Figure 13 Development of MCF7 cells in culture after spiral enrichment	46
Figure 14 Exemplary pictures of CTCs detected in CTC+ patients after spiral enrichment	51
Figure 15 Copy number alterations in cells confirmed as CTCs	53
Figure 16 Cell cluster detected in one patient after breast cancer microwell culture	56
Figure 17 Breast cancer CTC development in culture (Patient 1)	57
Figure 18 Ovarian CTC progression in microwell culture	59
Figure 19 Fluorescence microscopy of cells cultured from ovarian cancer patients	60
Figure 20 Clogged spiral cross section	65

List of Tables

Table 1 Consumable materials	28
Table 2 Reagents	29
Table 3 Antibodies	29
Table 4 Kits	30
Table 5 Devices	30
Table 6 Software	31
Table 7 External services	31
Table 8 Tumor cell recovery rates from existing publications	39
Table 9 Tumor cell recovery rates after a secondary enrichment	42
Table 10 Breast cancer patient cohort	47
Table 11 Different cell types detected in the patient samples by fluorescence microscopy after slanted spiral enrichment	48
Table 12 Classification of cells enriched by slanted spiral from patient samples	49
Table 13 Comparison of keratin-positive CTCs detected in breast cancer patients with CellSearch® and slanted spiral	54
Table 14 Microwell culture of breast cancer cells after slanted spiral enrichment	55
Table 15 Microwell culture of ovarian cancer cells after slanted spiral enrichment	58

Abbreviations

2D	Two-Dimensional
3D	Three-Dimensional
ANOVA	Analysis Of Variance
ATP	Adenosine Triphosphate
BAM	Binary Alignment Map
BR	Broad Range
BRCA1	Breast Cancer 1
CAF	Cancer Associated Fibroblasts
CD45	Cluster of Differentiation 45
CDK	Cyclin Dependent Kinase
CNAs	Copy Number Alterations
CO ₂	Carbon Dioxide
CSC	Cancer Stem Cells
DAPI	4',6-Diamidin-2-phenylindol, Dihydrochloride
DLA	Diagnostic Leukapheresis
DMEM	Dulbecco's Modified Eagle Medium
DNA	Desoxyribonucleic Acid
DPBS	Dulbecco's Phosphate-Buffered Saline
dsDNA	Double-Stranded DNA
DTCs	Disseminated Tumor Cells
ECM	Extracellular Matrix
EDTA	Ethylenediaminetetraacetic Acid
EGFR	Epidermal Growth Factor Receptor
FDA	Food And Drug Administration
FGF5	Fibroblast Growth Factor 5
G2	Second Degree of Malignancy
GAPDH	Glyceraldehyd-3-Phosphat-Dehydrogenase
GFP	Green Fluorescent Protein
HER2	Human Epidermal Growth Factor Receptor 2
HS	High Sensitivity
K	Keratine
MCF7	Michigan Cancer Foundation 7
MET	Mesenchymal-To-Epithelial-Transition
MHC I	Major Histocompatibility Complex I
PBMC	Peripheral Blood Mononuclear Cell
PCR	Polymerase Chain Reaction
PDMS	Polydimethylsiloxan
PFA	Paraformaldehyde
RAS	Rat-Sarcoma
RB	Retinoblastoma
RBC	Red Blood Cell
RCF	Relative Centrifugal Force
ROS	Reactive Oxygen Species

S-Phase	Synthesis Phase
TGF β	Transforming Growth Factor β
TME	Tumor Microenvironment
UV	Ultraviolet
V	Volt
VEGF	Vascular Epidermal Growth Factor Receptor
WBC	White Blood Cell
WGA	Whole Genome Amplification

1 Working hypothesis

Cancerous diseases and especially tumor metastasis are the fundamental cause for approximately 25% of death cases in Germany. Cancerous spread into distant tissues is caused by circulating tumor cells (CTCs) that achieved the separation from their former cancer tissue and reached the vascular system. If surviving the hostile conditions in the blood stream, they can extravasate and form secondary tumor masses.

These CTCs can be taken advantage of by enriching them from the blood for further analysis with a so-called liquid biopsy. As cancer cells are extremely rare in the blood, a CTC enrichment is necessary to enable subsequent CTC counting, further molecular analysis, or even CTC cultures. Different techniques have been established to achieve the separation of CTCs from surrounding blood cells. As CTC numbers in the blood can be low, especially in early cancer stages, increasing the sample volumes and therefore the extractable CTC numbers might enhance the diagnostic potential of a liquid biopsy. Most enrichment techniques currently used struggle when confronted with higher blood volumes with limitations in prolonged processing times or clogging of the device. Furthermore, many enrichment devices do not enable the collection of viable CTCs. The establishment of CTC cultures is a promising perspective in liquid biopsy research. Because tumor cells circulating in the blood represent a heterogeneity of cancer cells from the primary tumor as well as from metastases, CTC cultures could provide a platform for personalized cancer diagnostics and therapy. However, the chances to achieve successful CTC culture also depends on the number of CTCs in a blood sample.

Therefore, this research focuses on the slanted spiral microfluidic device, an enrichment technique that is capable of processing large sample volumes with a high throughput in short time. In this work, a protocol for its optimal application will be established and the spiral's effectivity compared to the current FDA approved CellSearch® device. Furthermore, a new, microwell-based culture technique should be tested to enable culture even from small CTC quantities in the blood. Combining these two innovative techniques may pave the way for standardized CTC cultures also from patients with low CTC blood counts and help to deepen the understanding of CTC behavior in cell culture.

1 Introduction

In Germany in 2015, around 500 000 people were diagnosed with cancer and around 125 000 people died from a cancerous disease. The lifetime risk of developing cancer lies at 42.6% for a German woman and 47.5% for a German man and the risk of cancer related death at 20.7% or 25.6%, respectively (Robert Koch-Institut (Hrsg) und die Gesellschaft der epidemiologischen Krebsregister in Deutschland e.V. (Hrsg), 2019). This marks cancer as one of the most common causes of death, being responsible for one out of four deaths in Germany (Statistisches Bundesamt, 2021). The importance of gaining a better understanding of this deadly disease enabling earlier diagnosis and implementing reliable treatment options is evident. The following paragraphs provide an inside into the fundamentals of cancer development, the formation of metastasis and the role that circulating tumor cells (CTCs) might play in the dissemination, but also the detection and therapy of cancer.

2.1 Cancer and Carcinogenesis

2.1.1 Genetic mutations - the basis of tumor development

Tumors derive from normal cells that acquire the capability of uncontrolled cell growth. To do so, cells need to achieve the ability to proliferate continuously. Some tumors unable of invading adjoining tissues and lacking the capability to metastasize, can be classified as benign. Those formations can also affect the patient, e.g. by compressing surrounding organs and thereby leading to their malfunction, or by intervening into hormonal releases. Furthermore, over time, some benign cellular formations can transform into invasive cancers. Malignant tumors, on the other hand, can invade and destroy their healthy surroundings in this manner. They can furthermore access blood and lymphatic vessels, enabling them to settle in distant tissues and form metastatic lesions (Boutry et al., 2022).

The basis of all changes a cancer cell undergoes during its evolution are genetic mutations and/or epigenetic modifications. A difference must be made between germline mutations and somatic mutations, where the former are inherited or newly acquired alterations in the genome of the zygote (Pon and Marra, 2015; Stratton et al., 2009). A common example for germline mutations are alterations in the Breast Cancer 1 gene (BRCA1) responsible for repairing the DNA double-helix. In affected patients, such mutations can lead to impaired functionality of the gene products. Without these DNA repairing mechanisms, individuals are exposed to accumulation of DNA-damage and are therefore more likely to develop a broad range of potentially oncogenic mutations. Women bearing these genomic alterations

have an increased risk of suffering from different cancers, with a lifetime risk of 85% for being diagnosed with breast cancer and 40-50% for ovarian cancer, respectively (Varol et al., 2018).

Somatic mutations, on the other hand, happen through DNA damage acquired over time. Found in 90% of all tumors, they induce cancer formation more frequently (Pon and Marra, 2015). Different causes lead to the accumulation of these alterations, but as they develop over time, age is considered the biggest risk factors for cancer development (Wu et al., 2018a).

2.1.2 Cancer risk factors

As described above, cancers arise from DNA mutations. The underlying mechanisms for these mutations constitute the risk factors for cancer development.

Intrinsic risk factors derive from random DNA damages during mitosis. It is estimated that these coincidental mutations are causative in 10-30% of all cancer cases (Wu et al., 2018b). It is presumed that tissues with high division rates, e.g. epithelial tissues, are generally at higher risk for developing cancers. This process is considered a basic risk for cancer occurrence that is carried by every individual (Tomasetti and Vogelstein, 2015; Wu et al., 2018a).

Exposure to external influences with carcinogenic potential constitutes the main preventable source for cancer development. The most common oncogenic mechanism of these influences is genotoxicity, which leads to DNA damages and gene mutations. Established agents with an oncogenic potential are diverse. Lifestyle choices as the consumption of tobacco, processed meat, or alcohol, but also the exposure to ultraviolet, solar, X- and gamma radiation are shown to be carcinogenic. Furthermore, also chemical substances as arsenic, asbestos, or even wood dust can be rated among these. There are also pharmaceuticals with an oncogenic potential, e.g. Ciclosporin or Azathioprin (Krewski et al., 2019). Gaining more importance over the past years are viral or bacterial diseases with potential to cause cancer (Birkett et al., 2019). For example, chronic *Helicobacter pylori* infections can lead to gastric cancer and human papilloma virus infections can cause cancer of the cervix, vulva, penis, or anus (Centre international de recherche sur le cancer, 2012).

However, there are also endogenous factors leading to DNA alterations. As already mentioned, age constitutes the biggest risk factor for cancer development. Furthermore, there is also a noticeable inherited risk to develop cancer. Tissue inflammation also enhances the formation of cancer and individual endocrine factors must be considered (Wu et al., 2018a).

In breast cancer for example, the amount of estrogen a woman is exposed to during her lifetime is increasing the risk of breast cancer. Therefore, early menarche and late menopause but also obesity, which is associated with higher estrogen levels, increase the lifetime risk. A high number of carried children on the other hand reduces breast cancer occurrence (Samavat and Kurzer, 2015).

2.1.3 Passenger and driver mutations

Of course, not all changes in the DNA lead directly to cancer. Through its lifetime, a cell's DNA is affected by a wide range of alterations most of which do not have oncogenic potential. In a cancer genome, these so called "passenger mutations" form a major part of detectable DNA-changes. But there also exists a small percentage of mutations that deliver advantages in terms of proliferative growth and clonal expansion. These are called "driver mutations" and can roughly be separated in two groups: oncogenes and tumor suppressor genes. Oncogenes are genes that, when affected by mutations, enhance new capabilities in the cell, whereas tumor suppressor genes become inoperable by driver mutations. It can be assumed that around 5 to 8 driver mutations are needed in the course of cancer formation (Martincorena and Campbell, 2015; Pon and Marra, 2015).

It is apparent that tumors profit from the accumulation of mutations also in a way that makes them more predisposed for further genomic changes. As described above, common mutations affect mechanisms that are responsible for detection or repair of damaged DNA. In this way tumors become more vulnerable and enter a state of "genomic instability" (Hanahan and Weinberg, 2011).

DNA alterations can range from deletion, insertion or exchange of single bases or longer DNA sections (Stratton et al., 2009) up to translocation and fusion of whole chromosome arms as in the formation of the Philadelphia Chromosome (Kang et al., 2016). Copy number alterations (CNAs), meaning amplification of one or more genes, but also losses of entire DNA sections, are also characteristic for cancer DNA (Stratton et al., 2009). By sequencing a tumor's DNA, these CNAs can be used to classify cancer cells, as a specific pattern of alterations can be assigned to a particular type of tumor (Hanahan and Weinberg, 2011).

The most common affected genes are *TP53* with mutations existing in 36.1% of all cancer cases and *PIK3CA* and *BRAF*, being present in 14.3% and 10% of tumors, respectively (Martincorena and Campbell, 2015).

2.1.4 Epigenetic modifications

Besides genomic changes, there are also non-genetic alterations contributing to cancer development. In the human genome, the nucleic acids forming the DNA double helix are wrapped around protective proteins called histones. This complex is referred to as a nucleosome and, in an inactive state, the nucleosomes arrange in dense formations termed chromatin. By unraveling these compact structures, transcription factors can access a coding region and induce mRNA synthesis. Furthermore, the reading of the genome is regulated by specific DNA sequences that are located before (promoter) or after (enhancer) the respective gene. Depending on cell type and circumstances, different genes must be accessible for transcription. Hence, the chromatin must be adaptable and be able to switch between an active and inactive conformation. The machinery responsible for chromatin organization and gene transcription is part of the epigenome. Changes in the chromatin complex or in its regulatory units can lead to altered gene expressions (Flavahan et al., 2017; Valencia and Kadoch, 2019).

Half of all cancers show mutations in genes responsible for chromatin architecture and regulation (Valencia and Kadoch, 2019). But apart from genetic alterations, also non-genetic mechanisms can lead to a modification of the epigenome. For example, alterations in histone proteins can lead to chromatin remodeling. Tumors can show suppression of Histone-1 proteins stabilizing the DNA and linking the individual nucleosomes. Cancer cells with these epigenomic modifications express a more stem cell-like phenotype (Hanahan, 2022).

Another epigenetic mechanism is the methylation status of gene promoters. In a tumor cell, methyl groups can be erroneously transferred to CpG dinucleotides, which are all cytosine nucleotides followed by a guanine. These methylations lead to the inactivation of the associated gene sequence. In many cancers, genes coding for tumor suppressors or DNA repair genes are hypermethylated. One example is the methylation and inactivation of a promoter associated to the MGMT DNA repair factor. Once this gene is inactivated, countless genetic mutations can follow without being repaired. Besides hypermethylation, a global hypomethylation can be observed in cancer, leading to chromosomal instability. Hypermethylation might be independent of genetic mutations as it can also occur due to chronic inflammation, hypoxia, or cell ageing (Flavahan et al., 2017).

Epigenetic modifications seem to contribute to a wide range of key features a cancer cell must acquire during its development. They should therefore be part of future investigations and cancer therapy research (Flavahan et al., 2017; Valencia and Kadoch, 2019).

2.1.5 The achievement of unlimited cell growth

There are several pathomechanisms leading to the development of malignant cell growth called the “hallmarks of cancer” (Hanahan, 2022; Hanahan and Weinberg, 2011).

The crucial accomplishment distinguishing cancer cells from healthy cells is the acquisition of clonal expansion. There are different signaling pathways initiating cell proliferation. Growth factors (GF) function as a ligand and bind to receptors as the “epidermal growth factor receptor” (EGFR) or the “human epidermal growth factor receptor 2” (HER2), which are typically provided with a tyrosine kinase domain. When activated they trigger intracellular signal transduction pathways mostly resulting in surviving signals, induction of mitosis or cell size expansion. There is a broad range of possibilities to enhance the proliferative cascade. Tumor cells can upregulate their receptor density to increase stimulatory activity. Furthermore, mutations in the receptors themselves can cause a continuous activation leading to constant growth signals. Besides the previous listed “upstream mechanisms”, there is also the opportunity to alter intracellular so-called “downstream” parts of the cascade. A common example is the rat-sarcoma (RAS) signal transducer which is located under the surface of the cellular membrane and is triggered by signals forwarded from the activated receptors on the cell surface (Hanahan and Weinberg, 2011; Stratton et al., 2009). When stimulated, GDP is exchanged for GTP which functions as a “turn-on switch” for the RAS protein and leads to downstream signaling for cell growth and proliferation. There are three different RAS-genes: K-RAS, H-RAS and N-RAS and all can assemble oncogenic mutations leading to continuous activation of the protein (Prior et al., 2020).

These signaling pathways are also in the focus for new therapy concepts. Besides the initial three pillars of cancer therapy, surgery, radiation, and chemotherapy (Hunter, 2017), targeted therapy gains more and more importance. Small molecules, e.g. tyrosine kinase inhibitors, can pass through the cell membrane. Erlotinib or Gefitinib block the tyrosine kinase domain of the EGFR. Therapeutic monoclonal antibodies target extracellular structures as transmembrane receptors and either inhibit their function or activate immune cells to attack the cancer cell (Lee et al., 2018). A notable example is Cetuximab, a monoclonal antibody that inhibits the EGFR pathway (Castelli et al., 2019).

2.1.6 Overcoming defensive mechanisms

Even if a cancer cell has managed to establish continuous cell growth and proliferation, there are still mechanisms provided by healthy cells to prevent clonal expansion. These are commonly regulated by gene products of tumor suppressor genes. The two most frequent examples are the retinoblastoma (RB) protein and the p53 protein (Hanahan and Weinberg, 2011). The RB-protein controls the cell cycle by inhibiting the transition into the Synthesis-Phase (S-Phase) and therefore navigates cell growth and proliferation. Mutations can affect the RB-gene itself or influence its function by altering upstream proteins which regulate RB-function as, e.g. cyclin dependent kinase (CDK) 4 and 6. When affected by a mutation this cell cycle checkpoint is missing and cells can achieve the capability of uncontrolled reproduction (Dick and Rubin, 2013). The CDK4 and 6 are also a target of molecular therapy, e.g. by Palbociclib, which can be used in the treatment of metastatic breast cancer (Lee et al., 2018)

The p53 protein on the other hand, functions as an initiator of apoptosis. If there are concerning signals like cellular stress or genetic alterations, this protein can lead to cell cycle arrest or programmed cell death. Mutations in this gene, which are present in 36.1% of all cancers, are leading to its dysfunction and thereby permit the survival and further development of altered cells (Bykov et al., 2018; Martincorena and Campbell, 2015).

There are also other mechanisms preventing immortality of human cells. In a healthy cell, telomeres protect the chromosomes. They consist of a few hundred non-coding base pairs located at the end of each chromosome arm and protect the DNA from merging at the edges. This would lead to its entanglement and consequently to cellular destruction. With each cell cycle these telomeres shrink in length resulting in a limited number of reproduction cycles every cell can undergo. When this limit is reached cells switch into a senescence state or undergo apoptosis. Cancer cells, on the other hand, have required the ability of continuous proliferation. Therefore, they establish mechanisms to preserve their telomeres, for example by upregulating the activity of telomerases, enzymes that elongate telomeric ends (Hanahan and Weinberg, 2011).

2.1.7 The role of the immune system

Once tumor cells have managed to acquire the ability of unlimited growth and immortality there are other obstacles they need to overcome. One big challenge is to escape the immune system which can eliminate tumor cells based on the antigens presented on their cell surface.

Successful cancer cells evade this eradication by establishing different characteristics. For example, they can use the immunosuppressive activity of regulatory T cells by inducing their migration or transformation. Furthermore, they can gain the ability to downregulate their major histocompatibility complex I (MHC I) which would normally represent tumor antigens. Consequently, cytotoxic T cells fail to detect the affected cells as threatening. Another mechanism tumors can establish to escape immune response, is by releasing immunosuppressive cytokines (Vinay et al., 2015).

However, the immune system also plays a supportive role in tumor development. Cancer tissue is usually infiltrated by a variety of immune cells. Studies have shown that these cells can also provide substrates that are important for tumor development as e.g. growth or - survival factors. Furthermore, the inflammation in cancer tissues leads to the formation of reactive oxygen species (ROS) which once again have a mutagenic effect (Hanahan and Weinberg, 2011).

2.1.8 Angiogenesis and tumor metabolism

When cancer cells are expanding, they will reach a point at which they will no longer be able to nourish themselves in the existing conditions. One big factor is the vascular system which was originally not predetermined to provide for this extra tissue. When reaching about one millimeter in size, tumors need to induce an expansion of the preexisting blood vessels in order to be supplied with a sufficient amount of oxygen and nutrition. This so-called angiogenesis is a crucial step in tumor development. If tumors fail to induce vascular expansion, they will lack the capability of further growth or invasion.

As the achievement of tumor metastasis relies on the invasion of cancer cells into the blood vessels, a sufficient angiogenesis in the tissue is crucial. When cancer cells proliferate, they will become hypoxic to a point, where the existing vascular system can no longer supply for their need of oxygen. As a result of hypoxia, but also due to mutations in associated genes, they release angiogenic factors as e.g. the vascular endothelial growth factor protein (VEGF). The newly formed blood vessels are not as accurately built as in healthy tissues resulting in a deficient, chaotic architecture with leaky endothelium (Al-Ostoot et al., 2021). This constitutes a favorable factor for invasion of the endothelium by cancer cells and therefore enhances the process of metastasis (Sobierajska et al., 2020). Furthermore, these vessels might not always be able to guarantee sufficient oxygen supply, so that environmental conditions in cancer cells might fluctuate between hypoxia and normoxia (Hanahan and Weinberg, 2011). VEGF also plays a major role in targeted therapy as it can

be inactivated by different small molecules as Sunitinib or Sorafenib but also by monoclonal antibodies as Bevacizumab (Castelli et al., 2019; Lee et al., 2018).

Cancer cells have a high requirement of energy and essential cell cycle components, due to their increased division rate. Therefore, tumor cells can establish altered energy metabolisms. The so-called Warburg-effect has already been discovered around a hundred years ago (Schiliro and Firestein, 2021; Warburg, 1925). It describes the use of glycolysis by the tumor to create adenosine triphosphate (ATP), the main energy carrier of the human organism, even under aerobic conditions. Instead of 36 ATP molecules that can be generated by oxidative phosphorylation, glycolysis only offers 2 ATP molecules. But cancer cells still profit from this approach. On the one hand, aerobic glycolysis can proceed more rapidly than oxidative phosphorylation. On the other hand, it offers intermediates necessary for cell divisions as nucleosides or amino acids. In tumor tissues there can also be a coexistence of cells performing aerobic glycolysis with lactate as the final product and other cells that profit from the lactate by using it as source for oxidative phosphorylation (Schiliro and Firestein, 2021).

2.1.9 Individual tumor characteristics

Every tumor has its own different characteristics and uncovering these attributes plays a crucial role in treatment strategies.

Nowadays it is well established to perform molecular analyses on a patient's tumor tissue searching for common genetic alterations that are linked to these types of tumors (Allison et al., 2020; Kalemkerian et al., 2018; Sepulveda et al., 2017).

In breast cancer for example, these evaluations are the basis for further classification into different subtypes fundamental for the choice of therapy regimen. Clinical guidelines recommend a distinction based on expression of the steroid receptors "estrogen receptor" (ER) and "progesterone receptor" (PR) or upregulation of the "human epidermal growth factor receptor 2" (HER2). The luminal-like subtypes are cancers tested positive for hormonal receptors. They can further be divided into Luminal A type that is less progressive and shows a low proliferation index and better prognosis or Luminal B type that is high proliferative and may also be HER2 positive. Then, there is the so-called HER-2 positive subtype, that is positive for HER2 but negative for ER or PR, and finally the triple negative breast cancer, that does not express any of the stated receptors and shows the worst prognosis of all subtypes (Burstein et al., 2021; Łukasiewicz et al., 2021).

These tumor characteristics are also used for therapy regimens. As estrogen binds to its intracellular steroid receptor, it triggers a cascade resulting in cell proliferation and growth (Siersbæk et al., 2018). This knowledge led to the development of endocrine therapies that deprive the receptor from its continuous stimulation by hormones. The first developed substance was the selective estrogen receptor modulator (SERM) tamoxifen, which binds the ER and prevents its activation. This drug is used mainly in premenopausal women. Another approach is the inhibition of aromatase, the enzyme that plays the central role in estrogen synthesis, with substances like anastrozole or letrozole that are established in therapy of postmenopausal women. Therapies also target HER2, a tyrosine kinase receptor, as for example the anti-HER2 humanized monoclonal antibody Trastuzumab (Kharb et al., 2020; Nagini, 2017).

The concept of choosing a therapy regimen based on molecular characteristics of a tumor is implemented also for other cancers. For example, lung and colon cancer can express EGFR (Kalemkerian et al., 2018; Sepulveda et al., 2017), which can also be targeted with monoclonal antibodies (Castelli et al., 2019).

2.1.10 Cell types within the cancer microenvironment

Molecular characteristics of the tumors do not only differ between patients (inter-tumor heterogeneity), but also between cells composing one and the same tumor tissue (intra-tumor heterogeneity). Thus, the cancer tissue is not built from an identical group of cancer cells, but rather consisting of different subpopulations that show individual genetic traits and also vary in susceptibility to anti-cancer therapy. One theory explains this heterogeneity as a result of natural selection, where cell clones with special capabilities can outgrow other cells lacking these achievements. Different subclones can form within a tumor, as, depending on location, disparate characteristics offer a growth advantage. Another theory justifies this clonal diversity on the existence of cancer stem cells (CSC). CSCs are cancer cells that express stem cell-like markers, show the ability of self-renewal and serve as progenitor cells for differentiated cancer cells. Whereas some CSCs derive from actual tissue stem cells, it is also proven that normal cancer cells are able to dedifferentiate into a CSC-like state. These cancer stem cells constitute a major challenge for cancer research and therapy. As they do not express one consistent marker, it is challenging to establish reliable methods to detect these cells. Furthermore, CSCs seem to be more resistant to cancer therapy and can serve as initiators of cancer relapse (Prasetyanti and Medema, 2017).

Contrary to previous assumptions the tumor-surrounding cells are not only associated to the cancer but also participate in its formation and development. As illustrated in Figure 1 by Hanahan and Weinberg in 2011, the tumor microenvironment (TME) harbors a diverse collection of different cell types.

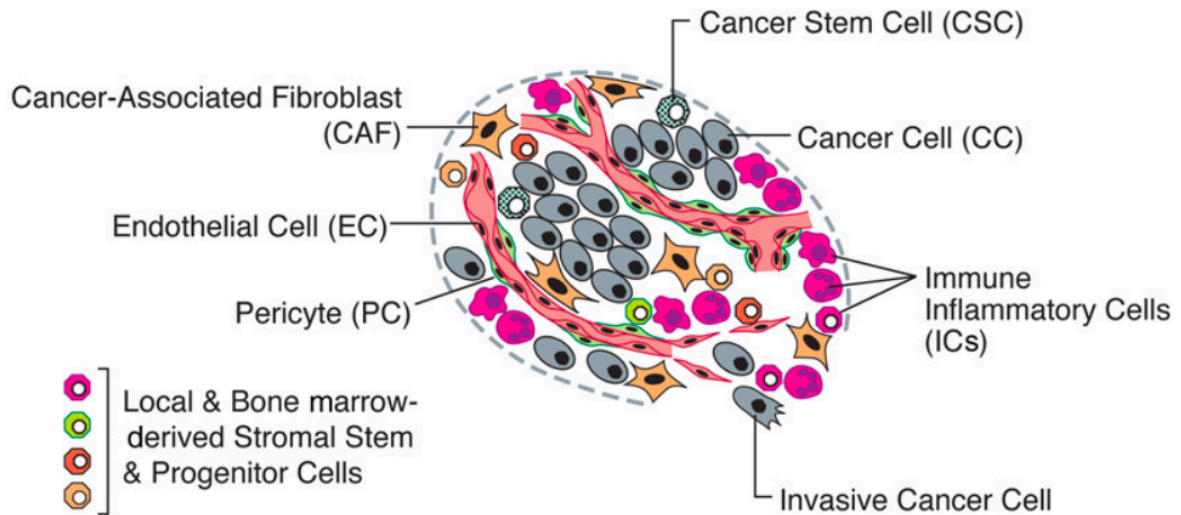


Figure 1 The Cells of the Tumor Microenvironment

Illustrated here by Hanahan and Weinberg are the different cell types that are involved in the formation of the tumor microenvironment. Besides the different types of cancer cells including cancer stem cells and invasive cancer cells, also other cell species are part of the tissue. Illustrated are immune cells, endothelial cells, cancer-associated fibroblasts, and various stromal cells.

(Hanahan and Weinberg, 2011)

The role of immune cells in tumor suppression but also in promotion of cancer growth has been described earlier. As also stated previously, tumor associated endothelial cells result from angiogenesis induced by the tumor. Pericytes are associated to the blood vessels and stabilize the endothelium wall. In cancer vessels, pericytes are often distributed more loosely which may further facilitate tumor cell invasion (Hanahan and Weinberg, 2011).

Cancer associated fibroblasts (CAFs) play an important role in carcinogenesis. They support the cancer tissue in a variety of functions. First, they organize the extracellular matrix (ECM) and can, on the other hand, create pathways for tumor cell invasion. However, the CAFs also induce the formation of a tighter and less flexible tumor tissue (Sahai et al., 2020). As a result, the ECM itself can promote tumor development. The mechanical tensions are detected by the cancer cells and provoke further shifts in terms of cell shape, growth or metastasis (Prasetyanti and Medema, 2017). But despite the organization of the ECM, CAFs promote

carcinogenesis in various other ways. They are significantly responsible for the secretion of factors that induce tumor growth, as for example transforming growth factor β (TGF β) or fibroblast growth factor 5 (FGF5) (Sahai et al., 2020), but also VEGF to promote tumor angiogenesis (Hanahan and Coussens, 2012; Nurmik et al., 2020). Furthermore, cancer associated fibroblasts have the ability to communicate with the immune system and mainly induce an immunosuppressive environment (Sahai et al., 2020).

There are further stromal cells to be found in the TME, as for example local cells can provide for the tumor stroma by initiating proliferation and expansion. But it is also known that mesenchymal stem cells can immigrate from the bone marrow and develop into different stromal cell types (Hanahan and Weinberg, 2011).

Taken together, it is now evident that a cancer tissue is not only an accumulation of proliferating cancer cells, but rather a network of a variety of cancer, immune, endothelial and stromal cells that, together, orchestrate the development, expansion, invasion and metastasis of cancer.

2.2 Metastasis and the role of circulating tumor cells

Metastases occur due to the spread of single or clusters of tumor cells through the vascular or lymphatic system. When these cells manage to extravasate into distant tissues, survive in these new conditions and furthermore accomplish to grow and proliferate, new metastatic lesions occur (Joosse et al., 2015) (Fig. 2).

Currently, metastasis is responsible for two thirds of tumor related deaths in cancer patients (Dillekås et al., 2019) Therefore, the development from limited to systemic disease is a prognostic turning point in a patient's disease. It is hence crucial to understand the molecular biology of metastatic dissemination to improve cancer diagnostic and treatment.

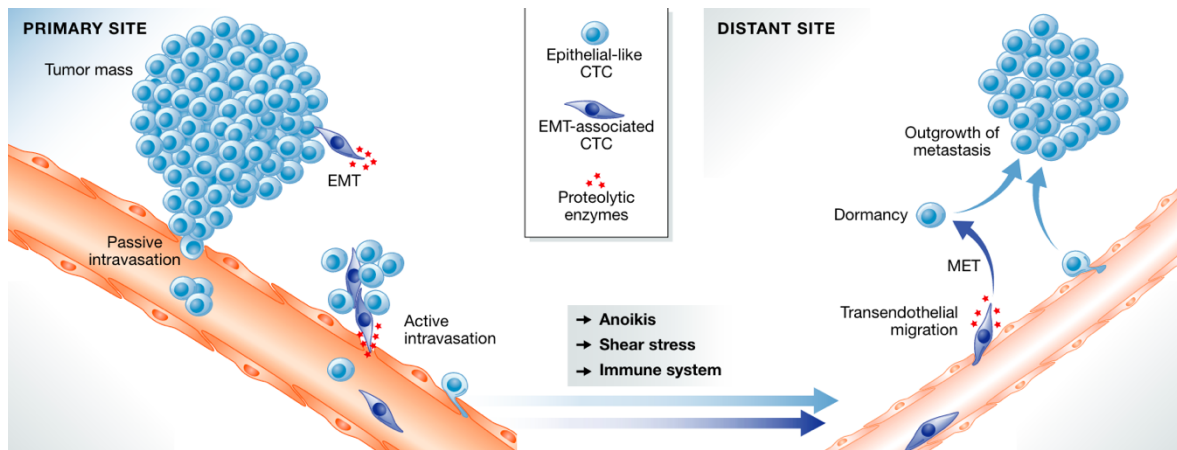


Figure 2 The Metastatic Cascade

Depicted is an overview of the steps a cancer cell undergoes on the journey to the formation of distant metastases. Cells are either passively or actively intravasating the vascular system. Some of these actively moving cells perform an epithelial-to-mesenchymal-transition (EMT). Those circulating tumor cells (CTCs) surviving the intravascular stress of shear forces and the attack by immune cells can extravasate in distant tissues. EMT can be reverted by mesenchymal-to-epithelial-transition (MET) and, depending on the adaptation to the new tissue, the cancer cells can either enter a dormant state or form new tumors in distant organs. (Joosse et al., 2015)

2.2.1 Migration and intravasation

If a cancer develops from a localized tumor into a metastatic disease, the cells must accomplish the detachment from the primary tumor. This can either occur during passive separation or actively, when cells acquire the capability of segregation from the primary tumor and migrate through the surrounding tissue (Joosse et al., 2015).

Not much information exists on the passive movement of cancer cells over the course of metastasis. When tumors expand rapidly, they simply shed their edging cells into the blood stream by pressing them through the leaky cancer vessels (Bockhorn et al., 2007; Joosse et al., 2015). This might also happen during surgical procedures as cancer biopsy (Joosse et al., 2020).

More research exists on the process of active cancer cell migration. As all other tissue cells, also cancer cells express adhesion proteins as cadherins that attach them to their surrounding cells. Invasive cancers achieve the downregulation of E-cadherin enabling their segregation from the original tumor mass. On the other hand, molecules as N-cadherin that enable

cellular migration, e.g. during embryogenesis, can be upregulated in these cancers (Hanahan and Weinberg, 2011).

A very important role in active cancer cell migration is played by the epithelial-to-mesenchymal-transition (EMT), which, in healthy individuals, has its principal function during embryogenesis or wound closure. As epithelial cancers have phenotypes that still resemble their cells of origin, they are equipped with features to ensure strong cell-to-cell adhesions. One opportunity for them to escape these contacts, is the transformation into a more mesenchymal state in which they lose their adhesion proteins, gain the ability to migrate to the next blood or lymphatic vessel, and actively infiltrate the endothelium. Cells can migrate solitarily but also in clusters. Here, initiating cells acquire mesenchymal features and guide the following epithelial-like cancer cells (Hanahan and Weinberg, 2011; Joosse et al., 2015).

2.2.2 Circulating Tumor Cells

As cells enter the blood stream they are traveling through the human body as circulating tumor cells (CTCs). Advanced tumors secrete thousands of CTCs per day but apparently the vast majority of these cells do not end up as metastasis initiating cells in distant tissues. This is due to the fact that only a fraction of CTCs survive the new conditions and stressors they are exposed to in this new environment (Joosse et al., 2015; Strilic and Offermanns, 2017). One limiting factor is given by the elimination of CTCs by the immune system. As they enter new territories, they lose the protection of their immune suppressive environment and may, once again, fall victim to the attack of immune cell, mainly natural killer cells. Other CTCs may simply be eliminated by the shear forces in the arterial high-pressure system, mechanical pressure in small capillaries or collisions with normal blood cells. A strategy to escape these threats seems to consist in the accumulation of a protective wall of platelets that shield the CTCs from immune cells and physical forces (Joosse et al., 2015; Strilic and Offermanns, 2017). CTCs that travel in clusters seem to be less vulnerable to elimination by natural killer cells (Pereira-Veiga et al., 2022).

Furthermore, epithelial cells receive survival signals through cell-to-cell contacts from their surrounding stroma. Once they have lost these contacts, they enter an apoptotic state called anoikis. CTCs bearing mutations that hinder this sort of cell death or that provide very strong survival signals can endure in this new state of solitariness.

Generally, CTCs travelling in clusters seem to have better chances in surviving the new conditions they are confronted with in the blood circulation and have also increased chances

to form metastasis (Aceto et al., 2014; Gkoutela et al., 2019; Joosse et al., 2015; Strilic and Offermanns, 2017). These cluster formation not only happen through aggregation with other tumor cells but CTCs can also form heterotypic clusters with fibroblasts, platelets or white blood cells (WBC) (Pereira-Veiga et al., 2022).

CTCs also have prognostic importance as their presence has a negative predictive value on the disease's outcome. The presence of even a single CTC in a 7.5 ml blood sample in breast cancer patients is associated with a decreased progression-free survival, a higher risk of recurrence, and a shorter overall survival (Alba-Bernal, 2020). Also in other entities as prostate or colon cancer (Cohen et al., 2008; de Bono et al., 2008), CTC counts can be associated with disease prognosis. Additionally, the detection of CTC clusters indicates an even worse prognosis and predict a higher risk of metastatic formations (Pereira-Veiga et al., 2022). Besides their prognostic significance, the quantification and analysis of CTCs as a so called "Liquid Biopsy", can serve as a marker for early cancer diagnostics, patient stratification for treatment, risk estimation for relapse, and real-time treatment monitoring (Heidrich et al., 2021).

2.2.3 Extravasation and Colonization

The CTCs that have survived the hostile conditions in the blood circulation also have to master the process of extravasation. There are different strategies applied by the cells. One opportunity is the arrest in the capillaries simply due to their larger cell diameter. Especially cell clusters can easily be trapped in small vessels, where they start proliferating and, at some point, break through the endothelial wall. But CTCs are also believed to actively attach to and pass through the endothelium as a result of ligand-receptor communications. Two mechanisms are described: cells can either slip through the gap between two endothelial cells or perform a "transcellular migration". Also in this situation the escorting blood cells can be of help to the tumor cells. Namely, neutrophils are capable of passing through the endothelial wall in the course of inflammation. When they form clusters with tumor cells, they can enable the CTCs to follow them (Pereira-Veiga et al., 2022; Strilic and Offermanns, 2017). Platelets can promote mesenchymal characteristics in the cancer cells via stimulation with TGF β , which enhances extravasative capacities in the cells (Strilic and Offermanns, 2017).

Once a CTC has overcome all obstacles to finally settle in a distant tissue, it still might not have the prerequisites to survive in this new environment or to even initiate proliferative growth into a metastasis. Especially CTCs that have undergone EMT to achieve invasion,

intra- and extravasation might not possess the optimal qualities to achieve clonal expansion in this new tissue. Therefore, when no longer receiving EMT-activating signals, CTCs can reverse their previous conversion by performing a mesenchymal-to-epithelial transformation (MET). Once settled in the unfamiliar tissue, it may take some time until the disseminated tumor cells (DTCs) have sufficiently adapted to the conditions of their new habitat (Hanahan and Weinberg, 2011; Joosse et al., 2015). Nevertheless, only one out of 40 disseminated cells manages to develop into a micrometastasis and only one percent of cells progress into a macroscopic visible metastasis (Phan and Croucher, 2020).

A fraction of the DTCs also initially enter a non-proliferative, termed “dormant”, state. If confronted with overly hostile conditions, as e.g. hypoxia, or a surrounding stroma that is providing dormancy signals, the cancer cells can switch into a G0-G1 cycle arrest. In this state they are also able to elude cytotoxic anti-cancer drugs as those mainly target highly proliferative cells. When the surrounding conditions change, dormant cells can reenter a proliferative state. In a patient, this switch manifests in a disease relapse, with new metastasis that might even appear years after initially successful treatment (Phan and Croucher, 2020).

2.3 Liquid biopsy

The analysis of cancer-derived material in a patient’s blood stream as a so called “liquid biopsy” holds great promises. It can serve as a marker for early cancer diagnostics, patient stratification for treatment, risk estimation for relapse, and real-time treatment monitoring (Heidrich et al., 2021; Mader and Pantel, 2017).

There are different analytes that can be examined, including CTCs, ctDNA and cancer-derived exosomes (Yu et al., 2021). The initial concept consisted in the detection of circulating tumor cells in a cancer patient’s blood sample. Circulating tumor cells are not only shed by the primary tumor but also from its metastases and can provide valuable information on its characteristics (Mader and Pantel, 2017). Besides these intact circulating cells also other cellular components can be detected in a liquid biopsy. As cancer cells become apoptotic or necrotic, their fragmented DNA can be found in the blood stream. However, a fraction of this circulating tumor-derived DNA (ctDNA) might also be actively secreted by the tumor (Heidrich et al., 2021). Furthermore, exosomes and other vesicles secreted by cancer cells can be detected in a liquid biopsy. They carry valuable information in form of DNA, RNA or nutrients and metabolites (Yu et al., 2021). In the following text, the focus will lie on CTCs and their potential when extracted from a patient’s blood stream, as well as on the current challenges regarding the clinical implementation of liquid biopsies.

Compared to the conventional needle biopsy, a liquid biopsy offers several advantages. Original tissue biopsies must be considered as small surgical procedures, so they also bear potential pain and health risks for the patient. Depending on organ and tumor location, a needle biopsy might even be unfeasible. Furthermore, it represents a temporal expenditure for patient and physician and high costs for the health care system. A liquid biopsy on the other hand, only requires blood sampling from a peripheral vein and is therefore minimally invasive with low risks for the patient and carried out in a short period of time at lower costs (Alba-Bernal, 2020; Mader and Pantel, 2017; Yu et al., 2021).

Besides these methodical advantages, also the quality of the material obtained by liquid biopsy might be exceeding the conventional tissue biopsies. The latter are most often performed on the primary cancer site and contain only a small fraction of the tumor. Since cancers are heterogeneous and develop over time, one-time molecular analyses of a biopsied cancer tissue might only reflect individual subclones at one specific time. Furthermore, in advanced patients, distant metastases may have developed a divergent genome compared to the primary tumor and are often present in multiple different locations. A liquid biopsy can be performed repeatedly and display the characteristics of all cancer sites. Furthermore, the cells detected in the bloodstream, are the subclones that have potentially already achieved the first steps of the metastatic cascade which makes them an interesting target for research and cancer treatment. Liquid biopsies may therefore permit a real-time monitor of a cancerous disease and build a foundation for individual cancer therapies (Alba-Bernal et al., 2020; Heidrich et al., 2021; Mader and Pantel, 2017).

Circulating tumor cells also have a prognostic value as the presence of even a single CTC in 7.5 ml blood in breast cancer patients is associated with a decreased progression-free survival, a higher risk of recurrence, and a shorter overall survival (Alba-Bernal, 2020). Nevertheless, so far, CTC enumeration lacks sensitivity as a diagnostic marker (Alix-Panabières and Pantel, 2016). One big hindering aspect is the rarity of cancer cells in the blood with only one CTC among 10^6 - 10^7 normal peripheral mononuclear blood cells (PBMCs) (Joosse et al., 2015). One way to decrease this impact is by increasing the analyzed volume. In a patient with an average of one CTC per 7.5 ml of blood, the probability of detecting this one CTC in a 7.5 ml tube is only 63%. But this rate can be increased to 86, 95, and 98% by collecting 2, 3, or 4 tubes of blood, respectively (Tibbe et al., 2007) (Fig. 3).

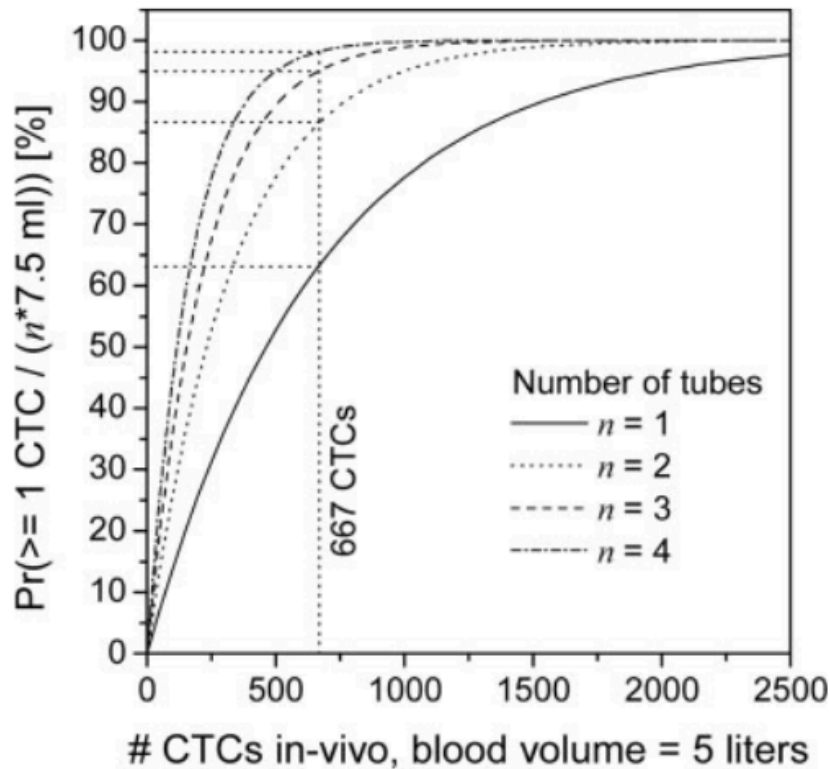


Figure 3 CTC detection rates depending on analyzed blood volume

This figure published by Tibbe et al. shows the dependency of CTC detection rates from the amount of analyzed blood volume. The x-axis demonstrates the probability of detecting at least one CTC in the blood sample, the y-axis shows its dependency on quantity of CTCs present in a patient's blood. At 667 CTCs per 5 liters of blood representing one CTC per 7.5 ml of blood, the probability to detect this one CTC is 63% if one 7.5 ml tube is taken and 86%, 95%, and 98% when collecting 2, 3, or 4 tubes of blood, respectively.

(Tibbe et al., 2007)

Therefore, using current standards, patients can easily be misidentified as CTC negative, especially when only small numbers of cancer cells are present in the blood circulation. Another strategy to increase the likelihood of detecting CTCs at low concentrations is diagnostic leukapheresis (DLA). This procedure can drastically increase the number of detectable tumor cells per patient. However, it is associated with long sample times of up to 1.5 hours and currently unmanageable high amounts of white blood cells (Fischer et al., 2013, Andree et al., 2018).

Another obstacle for the implementation of liquid biopsies into practice is given by the CTC enrichment methods that, so far, do not perform accurately enough to detect all cancer cells present in the sample (see 2.4).

2.4 CTC enrichment methods

Blood is composed from red blood cells, platelets and white blood cells circulating in a liquid called plasma (Castillo et al., 2019). As one CTC is present in front of a background of 10^6 - 10^7 PBMCs, techniques need to be implemented that separate the cancer cells from the remaining blood cells. A variety of these enrichment methods have been developed that can broadly be divided into label-dependent and label-independent methods (Joosse et al., 2015). Label-dependent methods rely on the distinction of different cell types based on their expression of certain cell surface markers. Common proteins expressed by epithelial cells, and therefore also by many carcinomas, are the epithelial cell adhesion molecule (EpCAM) (Rushton et al., 2021) or intermediate filaments called keratins (Toivola et al., 2015). Many enrichment methods use these markers to perform a positive selection by e.g. identifying EpCAM positive cells through binding of specific antibodies. The most common instrument is the CellSearch® System which, up to date, is also the only Food and Drug Administration (FDA) cleared device for tumor cell enrichment (Joosse et al., 2015; Rushton et al., 2021). This semi-automated device is using antibody coated ferrofluids that bind to EpCAM-expressing cells and can be collected from the blood through magnetic separation. In a following step the cells can be stained with fluorescent antibodies and examined by an expert. But the device is only designed to process blood samples of 8-10 ml (Swennenhuis et al., 2016) and cells lose their viability during prefixation (Habli et al., 2020). Besides immunomagnetic approaches, there are also microfluidic devices as e.g. the CTC-Chip, where blood is processed through EpCAM-coated micropillars. In this approach, cells maintain viability but it is also not adaptable to larger volumes (Rushton et al., 2021).

The downside of label-dependent methods is their reliability on specific cell-surface markers. Patients with non-epithelial cancers as, for example, sarcomas cannot be analyzed for CTCs by these devices. Moreover, this can also present a problem in the detection of carcinoma cells, as cancer cells that undergo EMT also downregulate typical epithelial markers as keratins or EpCAM and might be not captured during the enrichment. Consequently, enrichment methods relying on these proteins might miss a fraction of cells and therefore give imprecise CTC rates. Furthermore, the cells that achieved EMT are particularly invasive and therefore of highest interest for a patient's prognosis and further analysis (Joosse et al., 2015; Rushton et al., 2021).

Some developers have therefore emphasized the concept of negative depletion, where leukocytes are extracted from the blood using anti-leukocyte antibodies as e.g. anti-cluster of differentiation 45 (CD45). This concept allows CTC-detection independent from cell

surface markers and therefore promises a more heterogeneous selection. Unfortunately, CTC-recovery rates in these methods are relatively low and cancer cells might accidentally be depleted together with the mass of leukocytes surrounding them (Rushton et al., 2021). Label-independent alternatives are therefore gaining popularity. There are different techniques that all take advantage of physical characteristics distinguishing CTCs from their surrounding cells. In density-based concepts, CTCs can be separated from other blood components due to their individual density by adding separation media and perform a centrifugation. Although they can be conducted in a short time period, the harvested liquid is still rich of PBMCs and not very convenient for further analysis (Ferreira et al., 2016; Rushton et al., 2021). As a result, these methods are often combined with other strategies. In the OncoQuick method, an additive filtering step should achieve further purification of the recovered cells. The RosetteSep™ CTC enrichment cocktail, on the other hand, adds antibodies that bind to the CTCs and increase their density. Nevertheless, these methods lack purity and are commonly used as a pre-enrichment procedure (Ferreira et al., 2016).

Another label-independent approach is the separation by cell size, as circulating tumor cells are usually larger than surrounding leukocytes (Ferreira et al., 2016). The Parsortix™ technology, for example, is based on a separation cassette that is comprised of gradually narrowing steps where large cancer cells get trapped (Miller et al., 2018). A different concept for size-based enrichment are microfiltration techniques. The blood is processed through a filter membrane with micropores that the smaller blood cells can pass through while the larger CTCs get trapped (Rushton et al., 2021). Both of these techniques enable the enrichment of viable cells (Bailey and Martin, 2019; Miller et al., 2018) but also have their own limitations. Filter based systems struggle with clogging, specifically when confronted with higher sample volumes (Rushton et al., 2021) and according to the user's manual, enriching 8 ml of blood with the Parsortix™ device takes 2 hours and separation cassettes are expensive.

Also in vivo enrichment techniques have been introduced. The CellCollector is a wire that can be placed in a patient's blood vessel. Its anti-EpCAM coated surface gives the opportunity to directly detect CTCs from the blood and thereby screen large volumes (Rushton et al., 2021). The same advantage is given by a second procedure called diagnostic leukapheresis. In an original leukapheresis, leukocytes are filtered from the blood based on their density by centrifugation. As CTCs have a similar density as leukocytes, they are also enriched by this technique. So far, there is no suitable method to further process the DLA product adequately. Most techniques struggle with the large volumes obtained from the

procedure and the extremely rich concentration of leukocytes. The CellSearch® system for example, is only capable of processing a small fraction of the whole product (Andree et al., 2018; Fehm et al., 2018).

With all the options existing on the market, there is still an urgent need for enrichment methods, that permit a high throughput of large blood volumes to increase the pool for potential CTCs. In order to establish personalized treatment concepts, the CTCs captured by those methods should also be enriched in a viable state (Pei et al., 2020).

The slanted spiral microfluidic device with a trapezoidal cross section designed by Warkiani et al. (Fig. 4) presents such an approach. Patient samples are processed through the loops of a spiral where internal forces as well as the drag-and-dean force have an influence on the position of the cells inside the loops. Larger and smaller cells drive to opposing walls of the loops and are consequently collected in different outlets. Samples can be continuously analyzed at a speed of 1.7 ml/minute and cell viability is preserved (Warkiani et al., 2014a). Existing studies evaluated recovery rates enriching donor blood spiked with cancer cell line cells. The original study by Warkiani et al. showed recovery rates from 80% to 87%, depending on the cell line, which has been confirmed by following research (Aya-Bonilla et al., 2017). Other studies showed more varying results. Müller Bark et al., for example, tested the recovery rates of five different glioblastoma cell lines and could show that the smallest analyzed cell line presents with rates of only 23-33% (Müller Bark et al., 2021).

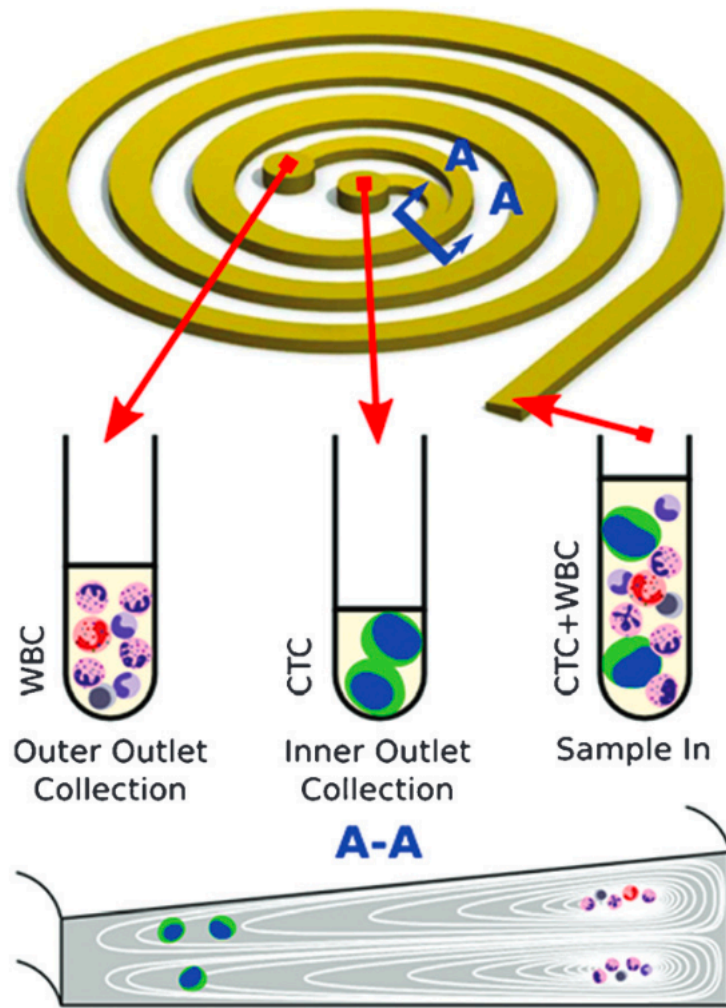


Figure 4 Illustration of the slanted spiral

This illustration of the slanted spiral as shown in the first publication is providing information on its operating principle. Samples comprising CTCs and white blood cells (WBCs) are loaded via an inlet tube and processed through the spiral. Inside of the spiral loops, a cell sorting is established due to internal forces combined with the drag-and-dean force. Larger cells, such as cancer cells, accumulate on the inner wall and are collected by the inner outlet, whereas smaller cells, as WBCs, circulate on the outer wall and are discarded by the outer outlet.

(Warkiani et al., 2014a)

2.5 CTC culture and its role in personalized medicine

A liquid biopsy permits the display of a heterogeneous population of CTCs, not only from the primary site but also from potential cancer metastases. It can be performed repeatedly over the course of a patients treatment to monitor therapy response and early detection of resistance (Alba-Bernal et al., 2020; Heidrich et al., 2021; Keller and Pantel, 2019; Mader

and Pantel, 2017). Furthermore, as CTCs represent the fraction of cancer cells that will eventually form metastasis in distant organs, cancer medicine particularly targeting those cells could have a major impact on a patient's course of disease (Smit et al., 2021).

Despite the simple quantification of CTCs in a patient's blood and their genomic analyzation to predict therapy response, an emerging approach to provide personalized cancer medicine is given by in-vitro or in-vivo drug testing on CTC cultures (Smit et al., 2021; Tellez-Gabriel et al., 2018). In recent years, various short- or long-term in-vitro CTC cultures could be established successfully by using different enrichment methods. A few studies also performed additional drug testing on the cultured CTCs including chemotherapy as well as endocrine therapy or targeted therapies (Smit et al., 2021).

Nevertheless, there is still no routine that allows reliable culture of patient derived CTCs. A major challenge remains the implementation of cell cultures in patients with low CTC burden. Most existing cultures were established from patients with high CTC counts where an initial CTC count of $>100/\text{ml}$ increases chances of success (Shimada et al., 2022).

In the existing literature, a distinction is made between short-term (<6 months) and long-term culture (>6 months). As cancer cells have high mutation rates, long-term cultivated cells are expected to have undergone a phenotypic change and no longer represent the original cancer. Short-term cultures might therefore be more suitable for drug-response testing (Shimada et al., 2022; Smit et al., 2021).

Original cell cultures from established and commercially available cell lines are usually performed in two-dimensional methods (2D), as e.g. in a petri dish (Shimada et al., 2022). In these conditions, cancer cells form an adhesive layer on the given surface. This is accompanied by a change in phenotype and altered cell-to-cell interactions. To perform drug testing on CTCs the cultivation method should aspire to be as close to in-vivo conditions as possible. As tumors are three-dimensional (3D) tissues that consist of heterogeneous subtypes of cancer cells as well as cells from the tumor microenvironment, 3D culture methods are on the rise (Tellez-Gabriel et al., 2018).

Tu et al. presented a rapid and cost-efficient option for the implementation of such cultures by using a microwell-based technique. Enriched CTCs can accumulate in the microwells, where they can develop cell-to-cell adhesions and form three-dimensional cell clusters. An advantage of this method compared to other models is given in the controllable size of the cancer cell spheroids, as sizes were only ranging from around 40 to 80 μm (Tu et al., 2014). As the circumference of the spheroids affect the drug distribution among the cultured cells (Nath and

Devi, 2016), the cultured spheroids should be of comparable sizes to ensure significant drug testing and develop evaluation standards.

The microwell technique has already successfully been used by Khoo et al. to perform drug testing on patient derived CTCs. Their team estimated that even one CTC per microwell might be enough to induce cancer cell growth, concluding that the technique might be suitable also for patients with low CTC counts (Khoo et al., 2016).

2.6 Study design

Low CTC rates in liquid biopsy samples hinder their promising perspectives in regard to disease monitoring and targeted therapy. Shimada et al. even described the CTC count as “the most important factor for the successful establishment of CTC cell lines” (Shimada et al., 2022). As illustrated by Tibbe et al., the screening of increased blood volumes would consequently increase CTC counts. Compared to conventional CTC enrichment methods that are not suitable for processing larger volumes, the slanted spiral microfluidic device with a trapezoidal cross section is capable of enriching enlarged samples in a short time by still maintaining cell viability. The aim of this study was to investigate optimal performing conditions of the slanted spiral microfluidic device for CTC enrichment from larger volumes. Three variables were examined: (1) The influence of increased PBMC concentrations on the spiral efficiency. (2) The optimal flowrate for maximum CTC recovery. (3) The utility of repetitive enrichments to reduce leukocyte contamination and its impact on CTC counts.

Once the optimal protocol was defined, patient samples were enriched and analyzed by the CellSearch® device and the slanted spiral to compare detection rates. Spiral enriched CTCs were stained with immunofluorescent antibodies and identified by microscopy. In a consecutive step, enriched CTCs were brought into culture. To verify tumor cell origin, molecular characterization using Next Generation Sequencing (NGS) was performed on CTCs captured by spiral enrichment. This research aims on establishing a new approach for CTC enrichment from large volumes and consecutive CTC culture. Furthermore, we expect to acquire new insights on the biology of CTCs, especially regarding their behavior in culture.

3 Material and Methods

3.1 Materials

Table 1 Consumable materials

Product	Catalog number	Provider
Adhesion microscope slides	02-0060/90	R. Langenbrinck GmbH
Cell Culture flask, 25 cm ²	38054	Stemcell Technologies
Cell Save preservative tubes	7900005	Menarini Silicon Biosystems
Centrifuge tube 50 ml, 15 ml	227261, 188261	Greiner Bio-One
CytoSep™ Funnel Chamber	11670601	Simport™ Scientific M966-8
Dako-Pen	S200230-2	Agilent Technologies
Flat Bottom Plate, 12 wells	38052	Stemcell
Injection Pipettes beveled (45°), OD 40 µm, straight, L: 55 mm	-	BioMedical Instruments
Micro tubes 2 ml, 1.5 ml, 0.5 ml	72.691, 72.690.01, 72.698	Sarstedt
Parafilm	13-374-13	Bemis Company Inc PM1000
Pipette tip 1000 µl, 200 µl, 10 µl	70.3050.205, 70.3030.205, 70.3010.205	Sarstedt
S-Monovette EDTA, 7,5 ml	01.1605.001	Sarstedt
Slide carrier	03-0060	R. Langenbrinck GmbH
Syringe 20 ml, 10 ml, 5 ml	300296, 309110, 309050	BD Medical Products
ViCell Sample Vials	5001041	Beckman Coulter

Table 2 Reagents

Product	Catalog number	Provider
AB-Serum	805135	Bio-Rad Laboratories
Dulbecco's Modified Eagle medium (DMEM)	P04-03600	PAN-Biotech
Dulbecco's phosphate-buffered saline (DPBS)	14190144	Gibco™
Fetal bovine serum (FBS)	F0804-500 ml	Sigma Aldrich
Ficoll-Paque™ Plus medium	17-1440-03	GE Healthcare
Human female DNA	G1521	Promega, Thermo Fisher Scientific
L-Glutamine	25030024	Gibco – Life Technologies
Paraformaldehyde (PFA)	K01629705	Merck
RBC Lysis Solution	158904	Qiagen
SeaKem® LE Agarose	50004	Lonza
Sodium hypochlorite	9062.1	Carl Roth
Trypsin/EDTA	25200072	Thermo Fisher Scientific

Table 3 Antibodies

Product	Catalog number	Provider
Anti-human CD45 antibody labeled with Alexa Fluor® 647	304018	Biolegend
DAPI (4',6-Diamidin-2-phenylindol, Dihydrochloride)	D1306	Invitrogen, Thermo Fisher Scientific
Pan-keratin monoclonal antibody clone AE1/AE3 labeled with Alexa Fluor® 488	53-9003-80	eBioscience™, Invitrogen, Thermo Fischer Scientific

Table 4 Kits

Kit	Catalog number	Provider
NucleoSpin® Gel and PCR Clean-Up	11992242	Macherey-Nagel GmbH & Co. KG
PicoPLEX® Single Cell WGA kit v3	R300722	Takara Bio USA
Qubit™ dsDNA BR Assay Kit	Q32853	Invitrogen, Thermo Fisher Scientific
Qubit™ dsDNA HS Assay Kit	Q33231	Invitrogen, Thermo Fisher Scientific

Table 5 Devices

Device	Provider
Axio Observer Fluorescence microscope	ZEISS
Biosafety cabinet Herasafe™	ThermoScientific
CFX96 Real-Time System, C1000 Touch	Bio-Rad
Heracell™ 150i CO2 Incubator	ThermoScientific
Heracell™ VIOS 160i CO2 Incubator	ThermoScientific
Megafuge 8	Thermo Heraeus
Multifuge 3 S-R	Thermo Heraeus
Pipetus ® 100-240 Volt	Hirschmann
Primovert microscope	ZEISS
Research® Plus mechanical pipettes	Eppendorf
Rotofix 32	Hettich Zentrifugen
Syringe pump	Kd. Scientific
ViCell™ XR	Beckman Coulter

Table 6 Software

Software	Source
BWA MEM2 v2.2.1	https://github.com/bwa-mem2/bwa-mem2
control-FREEC v11.6	http://boevalab.inf.ethz.ch/FREEC/tutorial.html
fastp v0.20.1	https://github.com/OpenGene/fastp
In-Silico Online	http://in-silico.online
Microsoft Excel	Microsoft
Microsoft PowerPoint	Microsoft
Microsoft Word	Microsoft
PubMed	https://pubmed.ncbi.nlm.nih.gov
R Foundation for Statistical Computing, version 4.1.0	https://www.r-project.org
Samtools v1.13	https://github.com/samtools/samtools
ZEISS Axio Vision 4.9.1 Software	Zeiss
Zotero	https://www.zotero.org

Table 7 External services

External Service	Provider
Next Generation Sequencing	BGI Genomics, Hongkong

3.2 Methods

3.2.1 Sample collection and processing

For optimizing the spiral protocol and testing the culture conditions, healthy donor blood samples were provided from the Department of Transfusion Medicine of the University Medical Centre Hamburg-Eppendorf. Furthermore, blood samples were taken from 12 metastatic breast cancer patients and 4 metastatic ovarian cancer patients treated in the Department of Gynecology at the University Medical Centre Hamburg-Eppendorf, after the patients gave written informed consent (ethical approval number: PV5329). Peripheral blood

was drawn into sterile 7.5 ml ethylene diamine tetraacetic acid (EDTA) containing tubes and sample processing was initiated within one hour.

PBMC and CTC isolation was achieved by density-based separation with a Ficoll-Paque™ Plus medium. The blood samples were diluted in DPBS (1:1 - 1:3) and pipetted onto a 20 ml Ficoll layer into a 50 ml tube. After a first centrifugation of 30 mins at a relative centrifugal force (RCF) of 400 x g the supernatant consisting of the patient plasma and a buffy coat was transferred into another 50 ml tube and centrifuged a second time for 10 minutes at a RCF of 400 x g. To clear the sample from remaining erythrocytes, the pellet was resuspended in 10 ml of RBC Lysis solution incubated at room temperature for 5 minutes and centrifuged at a RCF of 1000 x g for 5 minutes. Cells were then washed with DPBS and the PBMC concentration was calculated using the ViCell™ XR. Cell isolation of the samples from the ovarian cancer patients was only performed with 3 cycles of RBC lysis.

3.2.2 Enrichment with the slanted spiral microfluidic device

Tumor cell enrichment was performed with a slanted spiral microfluidic device with a trapezoidal cross section (Warkiani et al., 2014a). Prior to processing, samples were diluted in DPBS to a PBMC concentration of up to 6×10^6 PBMCs/ml, if not indicated differently. A 20 ml syringe pump was utilized to process the samples through the spiral at a flowrate of 1.7 ml/minute unless noted otherwise. The enrichment was performed under sterile conditions. Before usage, the spiral was cleaned with 10 ml Sodium hypochlorite (5%) (NaClO), followed by 10 ml distilled H₂O and 10 ml DPBS, each at a flowrate of 1 ml/minute. Samples were loaded into 20 ml syringes, processed through the spiral and volumes from the inner and outer outlet were separately collected in 15 ml tubes. In a final step, remaining cells were eluted by processing 1 ml of DPBS through the spiral. In case of a high post-enrichment volume, another centrifugation at a RCF of 1000 x g for 5 minutes was performed and the pellet was resuspended in a smaller volume of DPBS. After enrichment the device was cleaned with NaClO (5%) and H₂O as described above.

The spiral enriched cells from metastatic breast cancer patients were divided into two fractions. One fraction was used for CTC enumeration and method comparison, the other for CTC culture. The samples from the ovarian cancer patients were directly transferred into culture.

3.2.3 CellSearch® analysis

For method comparison, 7.5 ml of the blood drawn from the patients was also screened for cancer cells by the FDA cleared CellSearch® System. Samples were transferred to CellSave preservative tubes within 1 hour after withdrawal and processed within the next 96 hours as recommended by Menarini Silicon Biosystems. The operator did not have access to the spiral enrichment data and was therefore blinded to the results.

3.2.4 Culture of MCF7 cell line cells

MCF7 breast cancer cells (ATCC) were cultured in DMEM media complemented with 10% fetal bovine serum (FBS), 1% L-Glutamine and 1% Penicillin/Streptomycin in 25 cm² flasks. Flasks were incubated at 37°C with a 10% carbon dioxide (CO₂) concentration. When split, cells were harvested with trypsin/EDTA and washed with DPBS.

3.2.5 CTC immunofluorescence detection

For cancer cell detection and enumeration, the volume of interest was transferred into an 8 ml CytoSep™ Funnel Chamber connected to a microscope slide held by a slide carrier. After centrifugation at a RCF of 190 x g for 5 minutes and overnight drying, cells were fixed with 0.5% paraformaldehyde (PFA) (Merck) in DPBS for 10 minutes, washed with DPBS 3 times and incubated in 10% AB-Serum (blood group A and B) at room temperature for 45 minutes. Immunofluorescence staining was performed with the nuclear stain DAPI (4',6-Diamidin-2-phenylindol, Dihydrochloride) (1:700), Pan-keratin monoclonal antibody clone AE1/AE3 labeled with Alexa Fluor® 488 (1:500) and anti-human CD45 antibody labeled with Alexa Fluor® 647 (1:700) overnight at 4°C. Under a fluorescence microscope, DAPI+, Keratin+ (K+) and CD45- cells were picked and stored under -80°C until further processing.

3.2.6 Culture of spiral-enriched cancer cells

To culture CTCs from patient samples, a microwell-based technique presented by Tu et al. was used with some adjustments (Tu et al., 2014). Enriched cells accumulate in the microwells, where they maintain close cell-to-cell contact and form three-dimensional cell clusters. In this study, Polydimethylsiloxan (PDMS) master molds (diameter: 13mm, height: 3.5 mm) (Fig. 5A) were used as a template to produce agar chips with imprinted microwells.

The PDMS molds were placed onto microscope slides fixated with funnel chambers in slide carriers (Fig. 5B). Under sterile conditions, a 2% agarose gel was prepared from 0.3 g SeaKem® LE Agarose and 15 ml distilled H₂O. 800 µl of the heated gel was pipetted on top of the molds and in the circular space between molds and funnel wall until fully covered. The funnel chamber was covered with Parafilm and centrifuged for 4 minutes at 190 x g. Subsequently, each agar chip (Fig. 5C) was transferred into one chamber of a 12-well cell-culture plate. As a final step, the agar chips were sterilized under ultraviolet (UV) light for 10 minutes.



Figure 5 Production of the microwell agar chips

PDMS molds (A) were used as a template and placed onto a microscope slide with funnel chambers into a slide carrier (B). Heated liquid agarose was transferred onto the molds, centrifuged and cooled down. In sterile conditions, the mold was removed resulting in an agar chip (C) with a microwell-imprinted surface and a surrounding wall to contain liquids on the chip.

The sample volume intended for culture was immediately transferred into microwells after enrichment with the slanted spiral. 200 µl of the cancer cell enriched volume were pipetted into the inside of each agar chip. When the cells had settled into the microwells, 2 ml of DMEM medium (complemented as described above) was slowly added in the circular space around the agar chip until overflowing into the microwells. Medium was exchanged the day after enrichment and then periodically every fifth day. Cultured cells were examined under a bright light microscope and pictures were taken with the ZEISS AxioVision 4.9.1 Software. Cells from the breast cancer patients were cultivated at a 1% oxygen and a 10% CO₂ level for 10 to 21 days. The culture of the cells deriving from ovarian cancer patients was performed under normoxic conditions (21% oxygen) at a 5% CO₂ concentration and maintained for up to 90 days. At the end of the culture period harvesting from the wells was achieved by repetitive pipetting, after washing with DPBS. Cells were then transferred into funnel chambers and centrifuged as described above.

3.2.7 Whole Genome Amplification (WGA)

Single cell DNA amplification was performed with the PicoPLEX® Single Cell WGA kit v3). After amplification, a polymerase chain reaction (PCR) clean-up was completed with the NucleoSpin® Gel and PCR Clean-Up. Next, DNA concentrations were measured with Qubit™ dsDNA BR and HS Assay Kit. All steps were performed according to the manufacturer's manual.

To evaluate the quality of the amplified product a Glycerinaldehyd-3-phosphat-Dehydrogenase (GAPDH) multiplex PCR was conducted. A positive control was created from human female DNA and a negative control without any added DNA. Four primer sets were used, creating 100, 200, 300 and 400 bp fragments from the GAPDH gene. A loading dye was added to the samples. An electrophoresis gel was prepared from 2% SeaKem® LE Agarose TAE gel, loaded with the samples and the electrophoresis performed at 100V. Samples that showed three or four bands, indicating high DNA-quality, were classified as suitable for next generation sequencing analyses.

3.2.8 Next generation sequencing

DNA amplification products were analyzed by whole genome re-sequencing on a DNBseq (BGI, Denmark). Fastq files were processed by fastp v0.20.1 (Chen et al., 2018) to remove PicoPlex adapters and low quality reads, followed by aligning to the human genome hg38 using BWA MEM2 v2.2.1 (Md et al., 2019). Finally, Samtools v1.13 (Danecek et al., 2021) was used for converting tocBAM file, fix mate coordinates, sort, mark duplicates, and produce an index file. Copy number alterations were detected using control-FREEC v11.6 (Boeva et al., 2012).

3.2.9 Statistical Analyses

Statistical analyses were performed using R (R Foundation for Statistical Computing, version 4.1.0) and In-Silico Online, version 2.3.1 ("In-Silico Online," 2006). ANOVA was applied to determine whether the mean difference between more than 2 groups of measurements was statistically significant ($p < 0.05$).

4 Results

4.1 Development of the slanted spiral enrichment protocol

To establish a protocol with optimal conditions for cancer cell enrichment from larger volumes, influencing parameters on the spiral performance were investigated.

First, the influence of PBMC concentrations and spiral flowrate on the purity and CTC recovery of the enriched product were examined. In a second experiment, the spiral recovery rate of breast cancer cell line cells (MCF7) was evaluated. Furthermore, the effectiveness of repetitive enrichment cycles for reduction of leukocyte contamination and its impact on CTC counts were examined.

4.1.1 PBMC removal efficiency depending on cell concentrations and flowrate

There is a need for CTC enrichment methods that are capable of handling larger blood volumes. Furthermore, with the diagnostic leukapheresis there is a new concept that might enable the screening of large patient blood volumes but comes with an enormous background of PBMCs. Consequently, it is crucial to know which PBMC concentrations the spiral can process while still maintaining sufficient purity of the enriched product.

To investigate the slanted spiral's efficiency on PBMC removal, blood from healthy donors was collected in EDTA tubes. PBMCs were isolated as described before and their concentrations counted with the ViCell™ XR. In a following step, the donor PBMCs were diluted in DPBS to achieve a spectrum of concentrations ranging from 1×10^6 to 25×10^6 /ml DPBS. Duplicate samples were processed through the slanted spiral at a flowrate of 1.7 ml/minute and cell concentrations from both outlets were determined by counting with the ViCell™ XR.

The fraction of removed PBMCs in percent was calculated as follows:

$$removal (\%) = \frac{\text{ViCell-counted PBMCs from outer outlet}}{\text{ViCell-counted PBMCs from inner + outer outlet}} \times 100$$

The PBMC removal efficiency for samples with a concentration from 1 to 6×10^6 PBMCs/ml was ranging between 94.75% and 97.35%. By further increase of concentration, a decrease in enrichment efficiency was observed. For a concentration of 10×10^6 PBMCs/ml only 91.48% of PMCs could be removed and for concentrations of 15, 20 and 25×10^6 PBMCs/ml only 91.18%, 89.24% and 85.44 %, respectively (Fig. 6).

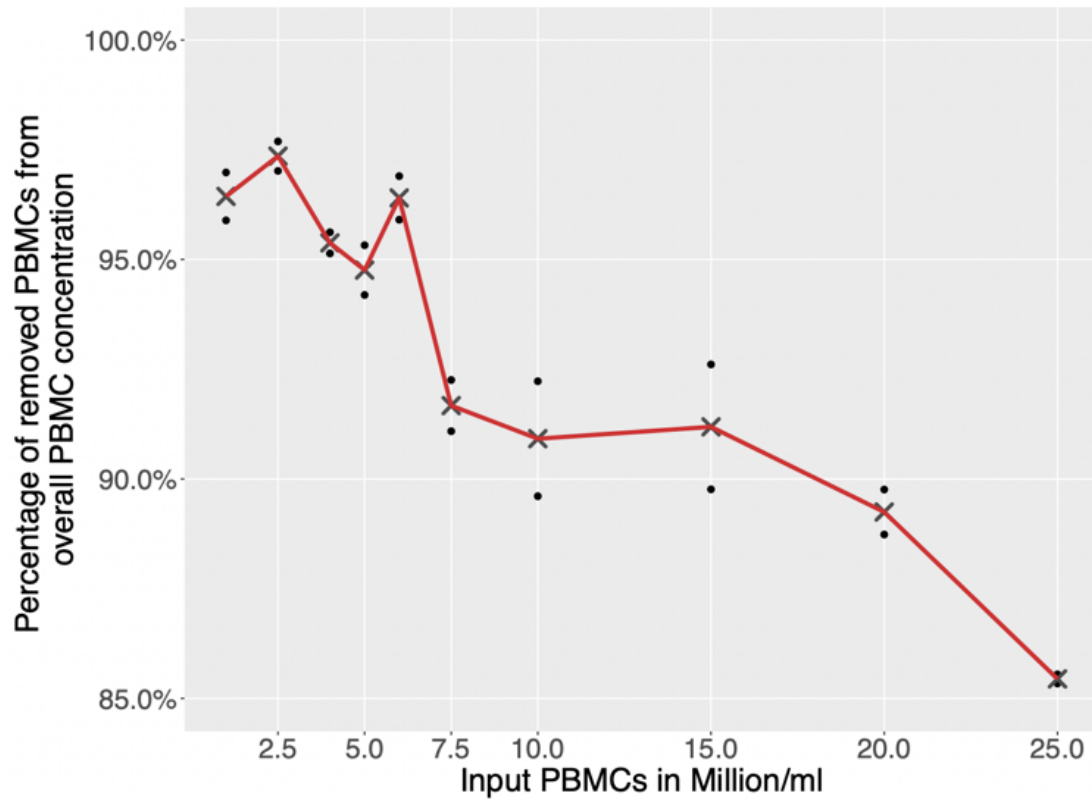


Figure 6 Influence of PBMC concentration on the spiral's PBMC removal efficiency

PBMCs from healthy donor samples were diluted to different concentrations and processed through the slanted spiral. The x-axis shows the PBMC concentrations in million/ml and the y-axis the percentage of PBMCs that could be removed from the overall concentration ranging from 85-100%. For each concentration, enrichment was performed on two samples (dots) and the means were calculated (crosses).

Additionally, the influence of the processing speed was taken into account. A faster flowrate permits higher throughput which is advantageous when processing large volumes. As the authors of the original paper introducing the spiral (Warkiani et al., 2014a) are recommending a processing speed of 1.7 ml/min, we wanted to investigate if increased flowrates have an impact on the purity of the enriched fraction.

Therefore, PBMCs were isolated from healthy donor samples and brought to concentrations of 1, 5, and 10x10⁶ PBMCs/ml as described before. Duplicate samples were then processed at flowrates of 1.7, 1.9 and 2.1 ml/minute and PBMC concentrations from both outlets were counted with the ViCell™ XR. Subsequently, the PBMC removal efficiency was calculated for each flowrate. For all PBMC concentrations a flowrate of 1.7 ml/minute resulted in the best removal. The most prominent discrepancy between flowrates was observed at a PBMC concentration of 5x10⁶ PBMCs/ml (Fig. 7).

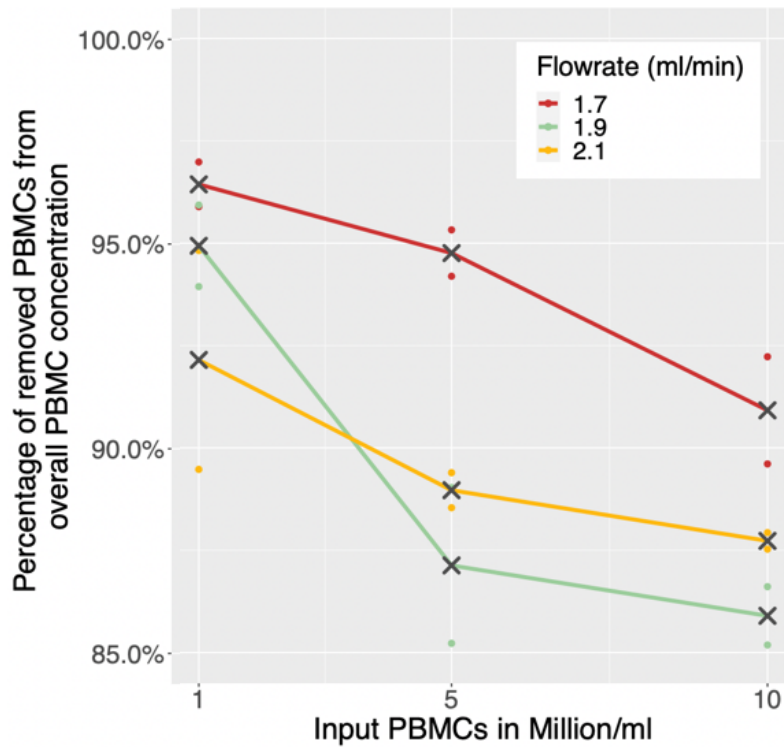


Figure 7 PBMC removal efficiency of the slanted spiral depending on cell concentration and flowrate

PBMCs from healthy donor samples were diluted to different concentrations and processed through the slanted spiral at flowrates of 1.7 (–), 1.9 (–) and 2.1 ml/min (–). The x-axis shows the PBMC concentration in million/ml and the y-axis the percentage of PBMCs that could be removed from the overall concentration ranging from 85-100%. For each concentration, enrichment was performed on two samples (dots) and the means were calculated (crosses).

An analysis of variance (ANOVA) showed a significant difference in mean clearance of PBMCs based on flowrate ($p=0.0080$) and initial cell concentration ($p=0.0007$). No interaction effect was found between flowrate and cell concentration ($p=0.7$).

Therefore, a flowrate of 1.7 ml/minute and a cell concentration of 6×10^6 /ml were used for subsequent experiments.

4.1.2 Tumor cell line (MCF7) recovery rate of the slanted spiral

Previous research has shown that the average recovery of cell line cells using the slanted spiral is dependent on cell size and ranges from 23% to 90% (Table 8).

Table 8 Tumor cell recovery rates from existing publications

Publications on recovery rates from cancer cell line cells together with cell diameter. In all experiments, healthy donor blood was pre-processed with an erythrocyte lysis buffer and subsequently spiked with cancer cell line cells.

For the study of Warkiani et al. diameters have been adopted from a subsequent publication of the group (*Warkiani et al., 2014b*). No data was available on the diameter of the MDA-MB231 cell line. Data on the cancer type in the publication of Kulasinghe et al. were taken from manufacture sources. For Aya-Bonilla and Müller Bark et al. diameters have been read of the associated figures in the studies.

Author	Cell-Line	Cancer Type	Approximate Diameter (μm)	Average recovery (%)
Warkiani et al., 2014a	T24	Bladder	30	80
	MCF7	Breast	20	85
	MDA-MB-231	Breast	N/A	87
Aya-Bonilla et al., 2017	A2058	Melanoma	~ 14	83
	Skme15	Melanoma	~ 18	
Kulasinghe et al., 2017	FaDu	Hypopharyngeal	23	60-70 (100-150 spiked cells) 40-60 (<100 spiked cells)
	CAL27	Tongue	17	
	RPMI2650	Nasal	26	
	MDA-MB-468	Breast	22.5	
Müller Bark et al., 2021	U251MG	Glioblastoma	~ 16	70-90
	U87MG		~ 16	70-80
	BAH1		~ 15	56-71
	MN1		~ 20	90
	PB1		~ 12	23-33

Recovery rates seem to be depending on cell size (Müller Bark et al., 2021), but also on other parameters as amount of spiked cells (Kulasinghe et al., 2017). Other factors as concentration of PBMCs or individual characteristics of each cell line might have an influence as well. Therefore, we evaluated the spiral's recovery rate of MCF-7 cell line cells under the optimal conditions examined beforehand (3.1.1).

The focus of this work lies on successful CTC enrichment also from patients with few numbers of circulating cancer cells. Therefore, one ml of DPBS with healthy donor PBMCs (concentration 6×10^6) was spiked with only 100 MCF7 cells. The experiment was performed in quadruplicate and the enriched fraction as well as the discarded fraction was spun down and stained as described before. Under a fluorescence microscope cells per slide were counted manually and the recovery was calculated as follows:

$$recovery = \frac{K+/DAPI+/CD45- \text{ cells from inner outlet}}{K+/DAPI+/CD45- \text{ cells from inner + outer outlet}}$$

Not all recovered keratin positive (K+) cells appeared to have an intact phenotype (Fig. 8A), with some cells showing a torn cell membrane, non-circular shape, and diffuse keratin signal (Fig. 8B).

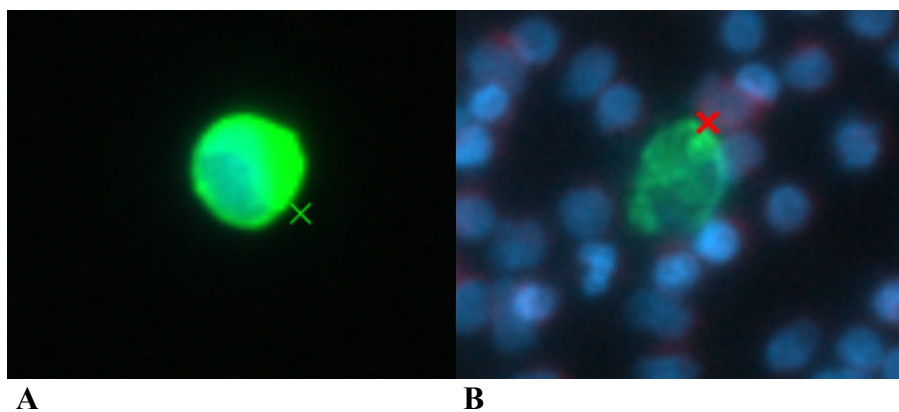


Figure 8 Exemplary pictures of cells categorized as “intact” and “torn”
 During microscopic examination some MCF7 cells were revealed as phenotypically damaged. Pictured above is an example of an intact MCF7 cell (A) and a cell counted as not intact (B).

Therefore, two different recovery rates were calculated, resulting in a recovery of 63.4% counting all keratin positive cells regardless their integrity and an even higher rate of 70.9% counting only cells with an intact looking membrane and nucleus (Fig. 9).

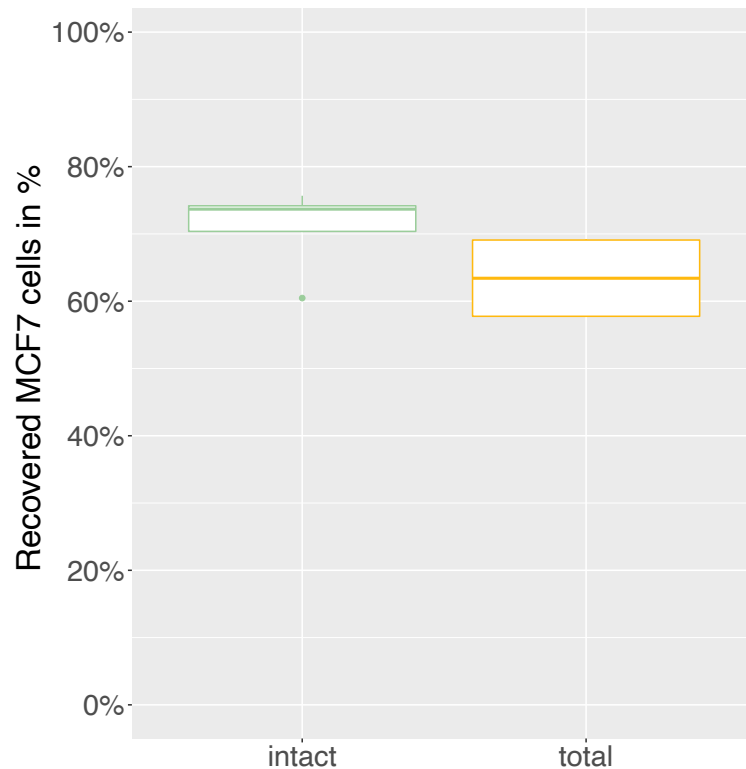


Figure 9 Tumor cell line (MCF7) recovery of the slanted spiral

PBMC solutions spiked with MCF7 cells were processed through the slanted spiral and recovery rates calculated by analyzing the enriched fractions under a fluorescence microscope. The y-axis is showing MCF7-recovery in percentage. A difference was made between cells with an intact looking cell membrane (intact) and the overall K⁺ positive cell counts (total). Results indicate an overall recovery rate of 63.4% and 70.9% counting only intact looking cells.

4.1.3 The influence of repetitive enrichment cycles on sample volume, CTC recovery and PBMC clearance

The slanted spiral processes samples at a speed of 1.7 ml/min and therefore enables a high throughput. This gives the opportunity of repetitive enrichment cycles with the goal to further decrease PBMC contamination and volume of the enriched fraction. On the other hand, this might come along with a loss of CTCs during the additional enrichments.

The group of Guglielmi et al. showed that spiral devices can offer a big opportunity also regarding the enrichment of DLA samples. In their study, mimicked DLA product was processed through a so-called *DLA biochip* that is based on a spiral with a trapezoidal cross section. In their study the group performed two enrichment cycles. They only achieved an average recovery rate of 47% for all their cell lines (Table 9), which is below the average recovery of other studies (Table 8).

Table 9 Tumor cell recovery rates after a secondary enrichment

The group of Guglielmi et al. performed a study mimicking DLA product by isolating WBCs from healthy donor samples with Ficoll-Paque or Ficoll-Paque PREMIUM. 50, 200 and 400x10⁶ WBCs/20 ml were spiked with 1 000, 4 000 and 8 000 cell line cells, respectively. Their spiral, called DLA biochip, was used with a flowrate of 2.1 ml/min and the enriched fraction was processed through the spiral a second time.

Author	Cell-Line	Cancer Type	Approximate Diameter (µm)	Average recovery (%)
Guglielmi et al., 2020	Hup-T4	Pancreas	15.1	48
	Sk-BR-3	Breast	13.7	
	LNCaP	Prostate	15.9	

Due to the use of a different spiral device, the results might not be comparable to the original slanted spiral device. Nevertheless, repetitive enrichment cycles might prove useful when handling larger sample volumes. We therefore decided to investigate the effect of two additional enrichment cycles on the cancer cell recovery rate, the amount of the enriched volume and the PBMC removal efficiency. We furthermore examined if an additional processing of the normally discarded volume can further increase CTC counts.

Healthy donor PBMCs spiked with MCF7 cells were diluted in 20 ml of DPBS (concentration of 4x10⁶ PBMCs/ml). The experiment was conducted in duplicate once with 5 000 and once with 10 000 spiked cancer cells. The solution was processed through the spiral, the enriched volume collected, retransferred into a syringe, and enriched a second time. After the second repetition the enriched volume was processed a third time.

Volumes were measured after each cycle to determine the effect of repetitive enrichments on quantity reduction. The volume recovered from the first cycle amounted to 7 ml and could be decreased to 2.63 ml and 0.96 ml, with the second and third enrichment, respectively.

After each enrichment, 5% of the volume obtained from the first and second cycle and 5.7% of the volume gained from the third cycle were transferred onto a slide for microscopic investigation. The slides were stained and CTC numbers as well as PBMC numbers were counted under the fluorescence microscope. The numbers were then extrapolated to the whole processed product and PBMC removal and CTC recovery calculated.

PBMC counts in the enriched fractions could be reduced by a further 98% with the second enrichment cycle, but only by another 1.2% after the third enrichment cycle compared to the clearance of the first enrichment cycle.

For CTC counts, an average decrease in countable cells of 9.5% after second enrichment and 36.7% after third enrichment was observed, compared to recovery rates after primary enrichment (Fig. 10).

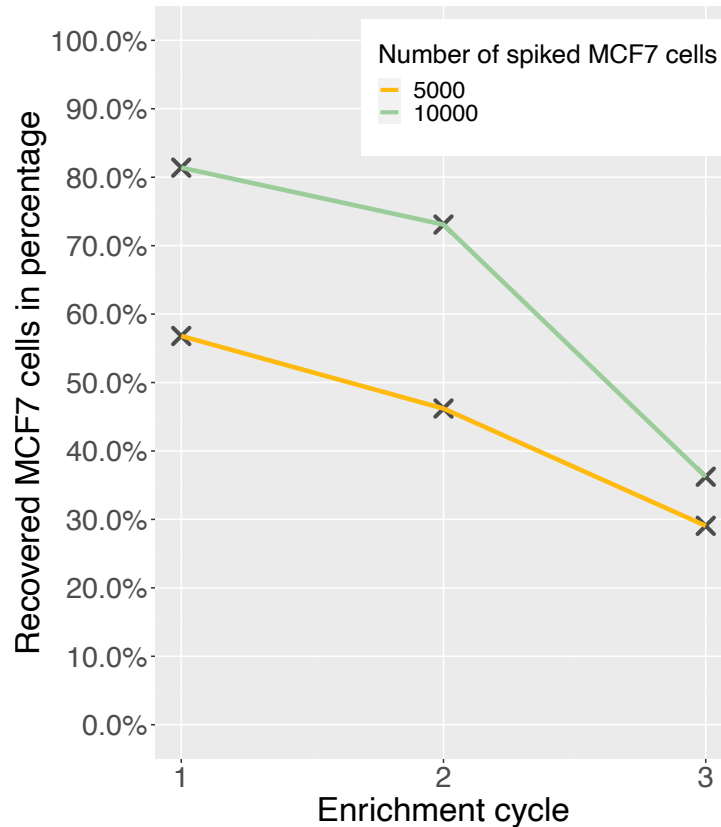


Figure 10 Effects of multiple enrichment cycles on CTC recovery rate

PBMC solutions spiked with precultured MCF7 cells were processed through the slanted spiral and recovery rates calculated by analyzing 5% of the enriched fractions after first and second and 5.7% percent after the third enrichment under a fluorescence microscope. The x-axis represents the three enrichments, whereas the y-axis shows the MCF7 recovery in percent.

To investigate whether an additional enrichment of the normally discarded fraction has a positive effect on CTC recovery, the waste fraction from the first enrichment was re-enriched through the spiral. The entire gained volume from this additional cycle was transferred to a slide and examined under the fluorescence microscope as well. From the enrichment of the discarded fraction, an additional average of 2.7% of CTCs could be recovered (Fig. 11).

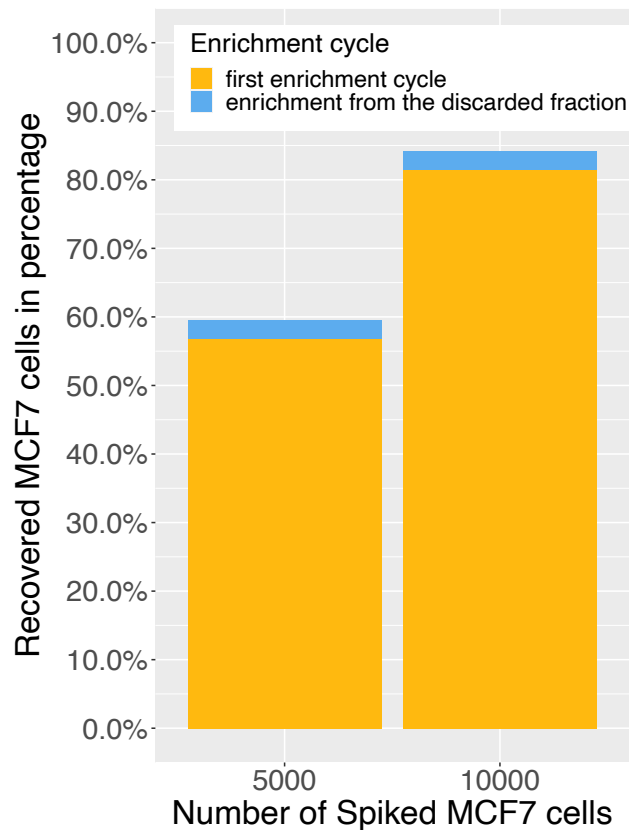


Figure 11 Increase of CTC recovery after enrichment of the discarded fraction

PBMC solutions spiked with precultured MCF7 cells were processed through the slanted spiral and the normally discarded fraction was additionally enriched. 5% of the volume from the first enrichment (yellow) and all volume from the additional waste enrichment (blue) were analyzed under the microscope for MCF7 cells. The x-axis shows the number of previously spiked MCF7 cells, whereas the y-axis represents the MCF7 recovery in percent.

Taken together, the enriched volume could be decreased by ~63% with every enrichment cycle and PBMC background was reduced from first to second enrichment, but not relevantly further with the third cycle. However, multiple enrichments also negatively affected the recovery rate of detectable tumor cells in the enriched fraction reducing them further by 9.5% after second enrichment and 36.7% after third enrichment. An additional enrichment of the discarded fraction elevated CTC recovery rates only by 2.7%.

4.2 Viability of MCF7 cells after spiral enrichment and suitability of the culture conditions in microwells

One aim of this study was the implementation of successful CTC culture from the spiral enriched product. Therefore, after establishing an optimal protocol for the slanted spiral, we wanted to investigate cell viability after enrichment and show the suitability of CTC culture

in microwells. For this, living MCF7 cell line cells were enriched through the spiral and subsequently cultured on the agar-chips.

PBMCs from healthy donors were isolated and resuspended into 20 ml DPBS to a final concentration of 3.79×10^6 PBMC/ml. Subsequently, the solution was spiked with 1 000 MCF7 cells. The sample was transferred into a syringe and processed through the slanted spiral. The cells from the enriched fraction were transferred onto 12 agar chips as described before and cultured under normoxic conditions (21% oxygen). Cell culture medium was replaced and cell growth examined under a bright light microscope every second day.

On day one of culture, solitary single cells of a larger size could be observed in the microwells surrounded by small cells and cell debris (Fig. 12A). After incubation under hypoxic conditions (1% oxygen) for 2 weeks, those single MCF7 cells were proliferating and forming dense three-dimensional clusters while keeping their round phenotype (Fig. 12B).

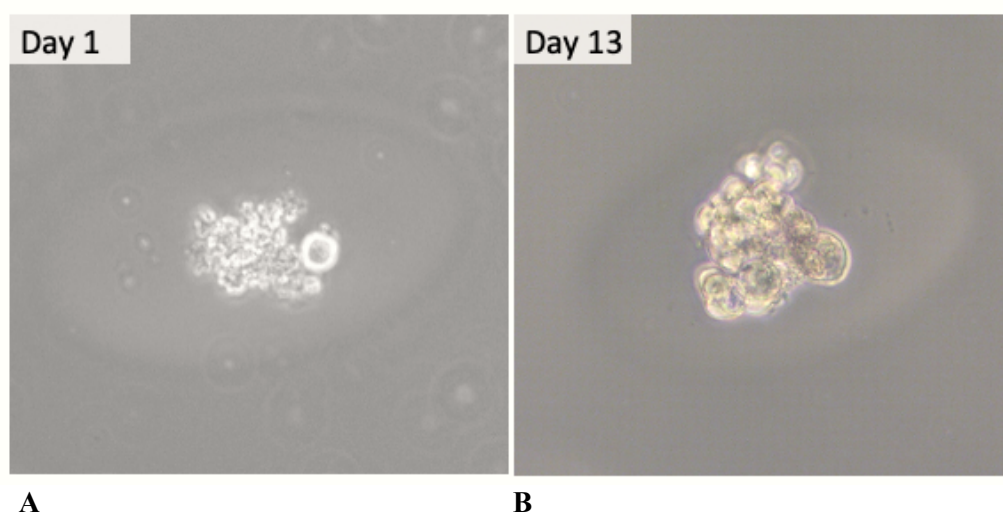


Figure 12 Development of the spiral enriched MCF7 cells in microwells

MCF7 cells were enriched by the slanted spiral and transferred onto agar-chips with imprinted microwells. These pictures show one of these microwells with one MCF7 cell on day 1 surrounded by small cells and cell debris (A) and a cluster formation of the cells on day 13 of culture (B).

On day 14 cells from 6 of the 12 agar chips were transferred into 96-well plate chambers. Cells from the remaining 6 chips were spun down on a microscope slide and investigated under the fluorescence microscope, where compact clusters of keratin positive cells could be identified (Fig. 13A). The cells remaining in culture started to grow adherently on the surface of the well plates and further proliferated into circular complexes (Fig. 13B).

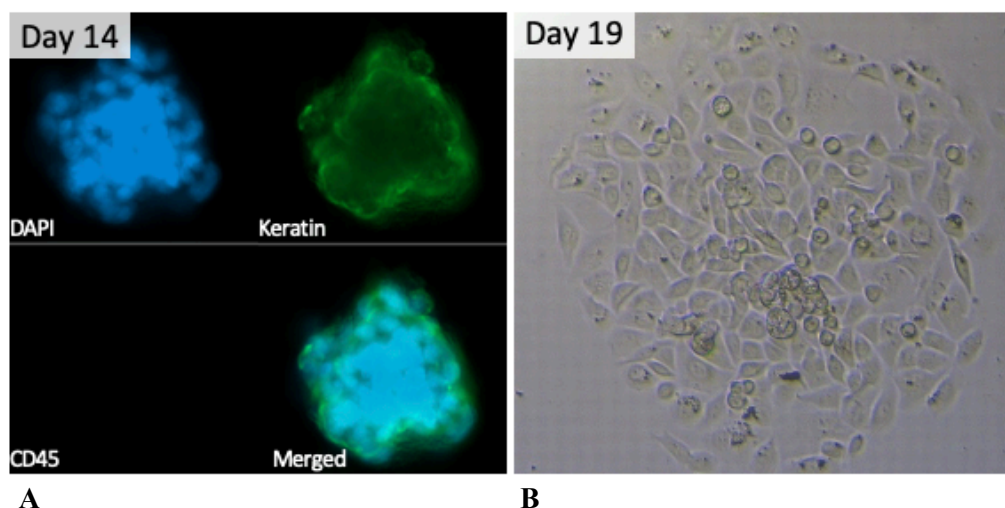


Figure 13 Development of MCF7 cells in culture after spiral enrichment

On day 14 cells from 6 of the 12 agar chips were removed from culture and analyzed under the fluorescence microscope. In each agar chip cluster formation could be shown with cells being DAPI+, Keratin+ and CD45- (A). Remaining cells were transferred into a regular 96 well plate where proliferation proceeded (B).

When reaching the size of the chamber, the growing MCF7 cells could be further transferred into a 48 well plate chamber and further into a 6 well plate chamber.

On day 36, cells were removed from culture and counted, resulting in a final cell count of 1.18×10^6 cells. Consequently, the spiked MCF7 cells proliferated a thousand-fold proving cell viability after spiral enrichment as well as the suitability of our culture method.

4.3 CTC enrichment and microwell culture from patient samples

After establishing optimal spiral conditions and proving the viability of cells after spiral enrichment as well as the suitability of the microwell culture method, the method was applied to patient samples. To evaluate the efficiency of CTC recovery, patient samples were simultaneously analyzed by the CellSearch® System and enriched with the slanted spiral. In a second step, spiral enriched cells were transferred into microwells to investigate the success of CTC culture with the established protocol. Blood was obtained from 12 metastatic breast cancer patients (Table 10). As this study was aiming to implement a method for enrichment of enlarged sample volumes, higher volumes than the usual 7.5 ml blood tube were aspirated. Blood volumes ranging from 10 ml to 51 ml with a mean volume of 27.88 ml were obtained, depending on the vein status and physical conditions of the patients assessed by the responsible physician. An additional 7.5 ml were provided for CellSearch® analysis.

Table 10 Breast cancer patient cohort

This table gives more information on the 12 breast cancer patients regarding age, sex, hormone and HER2 receptor status as well as UICC stage.

n (patients)	12
Age (years)	
Mean Age	62
Range	45-97
Sex	
female	12
male	0
ER	
positive	9
negative	3
PR	
positive	5
negative	7
HER2	
positive	7
negative	5
UICC Stage	
IV	12

4.3.1 CTC categorization after sample enrichment with the slanted spiral depending on fluorescence appearance

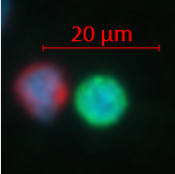
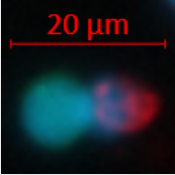
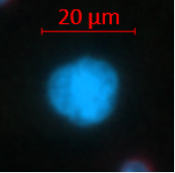
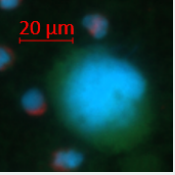
For CTC enrichment from patient samples with the slanted spiral microfluidic device, the samples were subsequently pre-enriched with the Ficoll-PaqueTM Plus medium and an RBC lysis buffer solution as described before. PBMC concentrations were assessed with the ViCELLTM XR and samples diluted in DPBS to a PBMC concentration of up to 6×10^6 PBMCs/ml. The samples were then loaded into a syringe and processed through the spiral and the enriched fraction centrifuged onto a microscope slide and stained as indicated.

By fluorescence microscopy four different types of cells were distinguished, that could potentially emerge as CTCs. The cells classified as Type A were positive for DAPI, negative for CD45 and expressing a very strong keratin signal. Type B cells were also showing DAPI-

positive and CD45-negative signals but were only weakly positive for keratins. Additionally, also cells were identified that neither expressed keratins nor CD45 which were categorized as type C. Furthermore, some cells were positive for DAPI, keratin and CD45. These cells, which were much larger than the detected other cell types and were classified as Type D (Table 11).

Table 11 Different cell types detected in the patient samples by fluorescence microscopy after slanted spiral enrichment

After spiral enrichment, CTC candidate cells were categorized into four different subclasses.

Cell Type	Microscopic picture of the cell with merged signals	Marker
A		DAPI+/keratin+/CD45-
B		DAPI+/keratin(+)/CD45-
C		DAPI+/keratin-/CD45-
D		DAPI+/keratin+/CD45+

4.3.2 CTC enumeration from patient samples after spiral enrichment

After establishment of the four different categories, samples of all patients were examined under the fluorescence microscope for classification into the outlined characteristics. Those cells were counted resulting in a distribution pictured in table 12.

In total, we could detect DAPI+/keratin+/CD45- cells in 7/12 patients after spiral enrichment by fluorescence microscopy. From these seven patients, four were positive for type A CTCs and five for type B CTCs. Two of these patients were expressing CTCs from both categories.

In the blood of all seven patients, single cells were detected. Additionally, two clusters of CTCs were found in the blood of two patients. In three cases a high number of CTCs with a faint keratin signal (cell type B) was identified.

Cells from Category C were observed in seven patients, two of whom also expressed Type A and two Type B cells, respectively. Four of the patients positive for Category C cells did not show any keratin+ and CD45- cells.

Discovered cells classified as category D were found in 4/12 patients. In all of these patients cells from Type C were found, but only one showed positivity for type A cells.

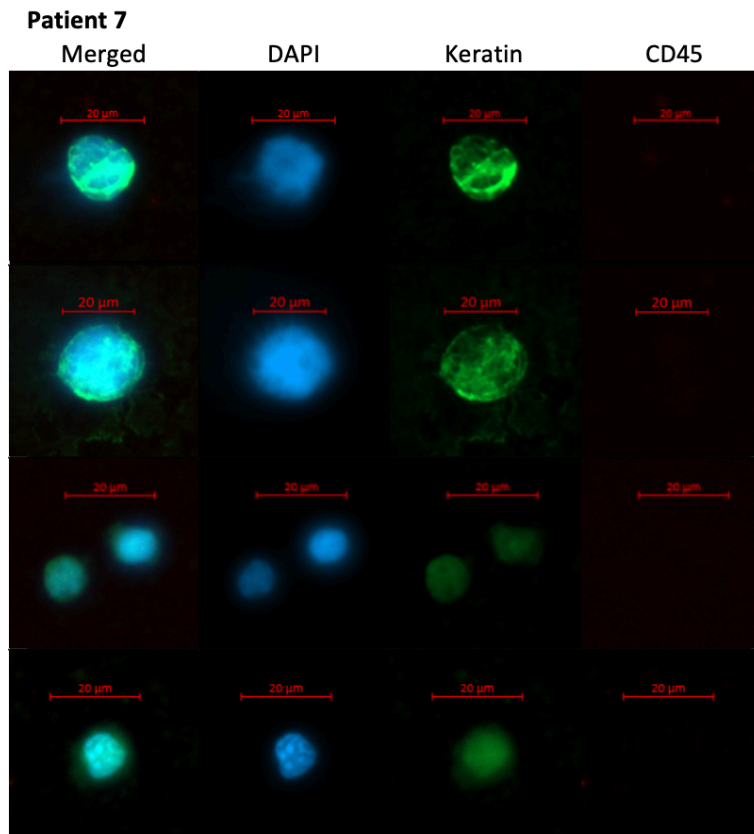
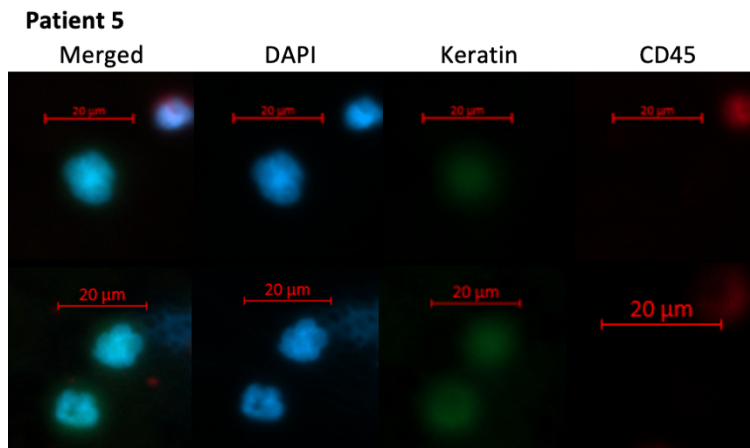
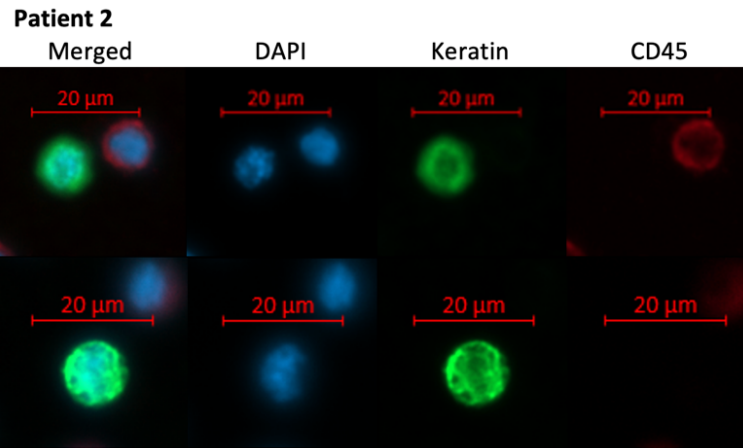
In general, CTC size varied between patients, but was also heterogenous in individual samples.

Table 12 Classification of cells enriched by slanted spiral from patient samples

This table gives an overview of the CTC counts after spiral enrichment in all analyzed breast cancer patients. The discovered cells are classified in four different categories (A-D).

	Category			
	A	B	C	D
Patient 1	0	0	3	14
Patient 2	32	0	6	2
Patient 3	0	0	158	13
Patient 4	0	0	0	0
Patient 5	0	2163	0	0
Patient 6	0	1386	0	0
Patient 7	4	1953	0	0
Patient 8	14	0	0	0
Patient 9	0	0	46	18
Patient 10	0	3	10	0
Patient 11	0	0	2	0
Patient 12	7	158	20	0

Figure 14 gives an overview of a selection of keratin+ cells detected in the patients as well as the detected clusters in patient 8 and 12.



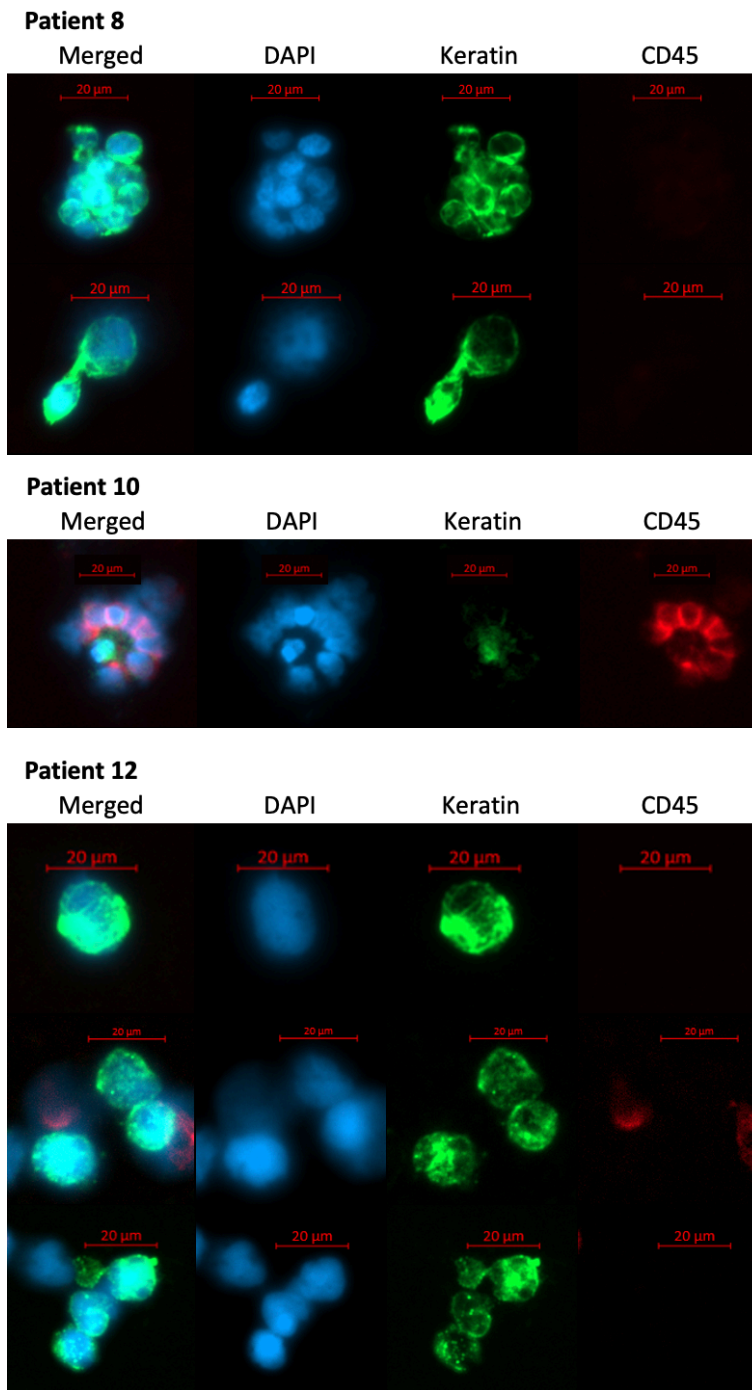


Figure 14 Exemplary pictures of CTCs detected in CTC+ patients after spiral enrichment

To illustrate the heterogeneity of discovered cells after spiral enrichment, this figure shows an overview of a selection of patient-derived CTCs from type A and B. Each cell is shown with a merged picture of all stained markers, as well as with the individual DAPI, keratin and CD45 signals.

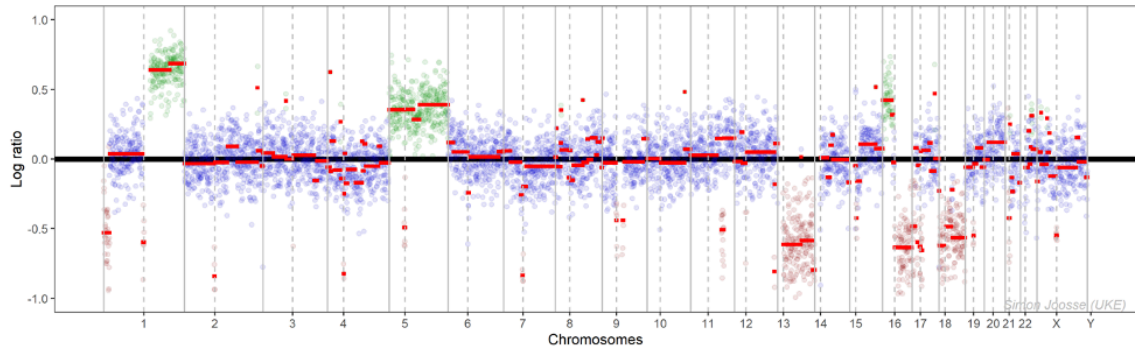
4.3.3 Confirmation of CTC status by next generation sequencing

Potential CTCs were picked from the glass slide and stored at -80° C. Consecutively, the DNA of a selection of 51 of these cells was amplified and DNA quality checked by GAPHD multiplex PCR and electrophoresis. This selection comprised 13 cells of type A, 19 cells of type B, 8 cells of type C and 7 cells of type D. Of these 51 cells, 13 showed two or more PCR fragments after electrophoresis and were therefore classified as suitable for further next generation sequencing analyses. Among these, 6 cells were from category A, 1 from category B, 3 from category C, and 3 from category D. Additionally, 2 clusters of category A cells, were amplified and transmitted for NGS.

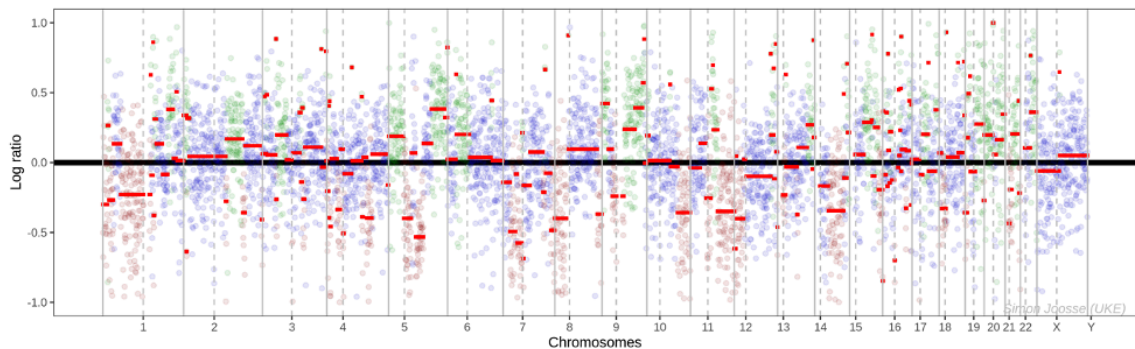
In 2 of the 15 analyzed cells, the data obtained by NGS showed copy number alterations confirming that the identified cells were of malignant origin (Fig. 15).

The cell isolated from patient 2 was classified as a type A cell. This patient suffered from Luminal-A-like breast cancer. After NGS the cell deriving from that patient showed typical CNAs for this molecular subtype, including gain of chromosomes 1q and 16p and loss of chromosome 16q, as well as CNAs typical for G2 histological grade: 13q and 16q loss (Horlings et al., 2010).

For the category B cell from patient number 5, diagnosed with a triple negative breast cancer, the CNA profile included gain of chromosome 6p and loss of chromosomes 4p, 5q and 10q which are also matching this cancer subtype, as well as CNAs typical for grade 3 breast cancer: gain of chromosomes 6p and 17p and loss of chromosome 8p (Horlings et al., 2010).



A CTC patient 2



B CTC patient 5

Figure 15 Copy number alterations in cells confirmed as CTCs

Copy number alterations confirming CTC status could be found in two patients. The x-axes represent the 23 pairs of chromosomes and the y-axes the log ratio of the copy number alterations. Coloured in green are copy number gains and in red copy number losses. Marked in blue are chromosome regions that did not show significant alterations.

Based on the NGS results, cells from category A (DAPI+, strongly keratin+ positive and CD45-) and category B (DAPI+, weakly keratin+ and CD45-) were counted as confirmed CTCs henceforth.

4.3.4 Comparison of CTC counts obtained by slanted spiral and CellSearch® system

To evaluate the efficiency of the slanted spiral, 7.5 ml of blood from 8/12 patients included in the study were analyzed simultaneously by the FDA-cleared CellSearch® System (Table 13). For the other 4 patients CellSearch® performance was not feasible due to too small blood volumes. To compare CellSearch® to slanted spiral results, the spiral enriched keratin-positive CTC counts (category A and B) were scaled down to the concentration per 7.5 ml of blood volume.

Three patient samples were diagnosed to be negative for CTCs by the CellSearch® System, in all three no CTCs were found after enrichment with the spiral as well. Four patient samples

were diagnosed to be positive for CTCs in both the CellSearch® System and after spiral enrichment. Finally, blood of one patient was diagnosed with one CellSearch® System detected CTC, but no CTC could be found after spiral enrichment. Together, there was a fair agreement in CTC status between the two enrichment methods ($k=0.75$, Cohen's kappa). Although many more CTCs could be detected after enrichment using the slanted spiral, not enough samples were investigated to reach statistical significance. In three patient samples, CTC counts after spiral enrichment highly exceeded the discovery rate from the CellSearch® results. Cells observed in these patients showed a comparably weak keratin signal, previously defined as category B cells.

Table 13 Comparison of keratin-positive CTCs detected in breast cancer patients with CellSearch® and slanted spiral

CellSearch® was performed on 7.5 ml of blood while blood volumes for spiral enrichment were varying from 10 ml to 51 ml. Therefore, the total CTC counts in the samples were compared to downscaled CTC counts in 7.5 ml of blood for easier comparison. In four samples no CellSearch® results are available by reason of too small blood volumes.

	CellSearch®	Slanted Spiral		
		Blood volume in ml	Total CTC count	CTC count per 7.5ml
Patient 1	N/A	10	0	0
Patient 2	N/A	10	32	60
Patient 3	0	42	0	0
Patient 4	1	45	0	0
Patient 5	4	10.5	2163	6180
Patient 6	3	10.5	1386	4950
Patient 7	12	18	1957	3262
Patient 8	20	49	14	13
Patient 9	0	51	0	0
Patient 10	N/A	12.5	3	7
Patient 11	0	45	0	0
Patient 12	N/A	11	165	307

4.3.5 Culture of breast cancer CTCs

After showing the suitability of microwells for cultivating tumor cells even from small initial cell counts, we implemented the method on cells extracted from 12 breast cancer patient samples after spiral enrichment.

Table 14 gives an overview of the microwell cultures from breast cancer CTCs after slanted spiral enrichment. The enriched volume of patient number 3 was not transferred into culture. In all the other patients, under bright light microscopy, large cells were apparent in the microwells on the day of seeding. In some cultures, these cells survived the first days of culture and, in a few samples, there was also little proliferation inside the wells.

Table 14 Microwell culture of breast cancer cells after slanted spiral enrichment

Spiral enriched cells of 11 of the 12 breast cancer patients were transferred into microwell culture. Blood volume (ml) transferred into culture, as well as the period (days) the cells were cultivated and their development in culture. In 2/11 patients, weakly keratin positive cells were detected by fluorescence microscopy after culture.

	Blood volume	Days in culture	Development in culture	Keratin+ cells after culture
Patient 1	2.5 ml	33	<ul style="list-style-type: none"> ▪ Large cells in microwells after seeding ▪ Cell survival, proliferation 	<ul style="list-style-type: none"> ▪ No keratin+ cells
Patient 2	6 ml	16	<ul style="list-style-type: none"> ▪ Large cells in microwells after seeding ▪ No survival, no proliferation 	<ul style="list-style-type: none"> ▪ No keratin+ cells
Patient 3	-	-	-	-
Patient 4	33.75 ml	31	<ul style="list-style-type: none"> ▪ Large cells in microwells after seeding ▪ No survival, no proliferation 	<ul style="list-style-type: none"> ▪ No keratin+ cells
Patient 5	7.86 ml	15	<ul style="list-style-type: none"> ▪ Large cells in microwells after seeding ▪ No survival, no proliferation 	<ul style="list-style-type: none"> ▪ No keratin+ cells
Patient 6	8.4 ml	5	<ul style="list-style-type: none"> ▪ Large cells in microwells after seeding ▪ Cell survival and proliferation ▪ Contamination on day 5 	<ul style="list-style-type: none"> ▪ No keratin+ cells
Patient 7	13.5 ml	21	<ul style="list-style-type: none"> ▪ Large cells in microwells after seeding ▪ Cell survival, no proliferation 	<ul style="list-style-type: none"> ▪ No keratin+ cells
Patient 8	40.83 ml	14	<ul style="list-style-type: none"> ▪ Large cells in microwells after seeding ▪ No survival, no proliferation 	<ul style="list-style-type: none"> ▪ No keratin+ cells

Patient 9	27 ml	21	<ul style="list-style-type: none"> ▪ Large cells in microwells after seeding ▪ Cell survival, cell proliferation 	<ul style="list-style-type: none"> ▪ 1 weakly keratin+ cluster
Patient 10	9.375 ml	14	<ul style="list-style-type: none"> ▪ Large cells in microwells after seeding ▪ No survival, no proliferation 	<ul style="list-style-type: none"> ▪ No keratin+ cells
Patient 11	33.33 ml	7	<ul style="list-style-type: none"> ▪ Large cells in microwells after seeding ▪ No survival, no proliferation 	<ul style="list-style-type: none"> ▪ No keratin+ cells
Patient 12	6-97 ml	10	<ul style="list-style-type: none"> ▪ Large cells in microwells after seeding ▪ No survival, no proliferation ▪ Contamination on day 10 	<ul style="list-style-type: none"> ▪ No keratin+ cells

After the culture period the volume from the agar chips was transferred onto microscopic slides, stained, and analyzed under the fluorescence microscope. In one patient a very weakly keratin+ and strongly DAPI+ cluster could be identified (Figure 16). After amplification, this detected cluster passed the quality check described before and was sent for NGS. The performed CNA analysis could not prove the malignant origin of these cells.

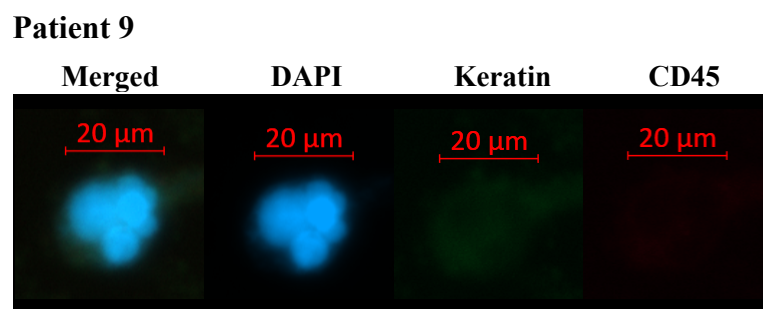


Figure 16 Cell cluster detected in one patient after breast cancer microwell culture

In the microwell culture of the breast cancer patient 9 a weakly keratin positive cell cluster was detected under the fluorescence microscope after culture. Here, it is shown with merged fluorescence signals and individual DAPI, keratin and CD45 marker expression.

The cells of patient number 1 showed cell proliferation and were transferred into one chamber of a 96-wellplate after 20 days to investigate further cell survival outside of the microwells. From this timepoint cells were cultivated under normoxic conditions. In the well plates, cells grew adherent to the flat surface and became apoptotic in the course of a few days (Fig. 17). When taken out of culture and stained for keratins, DAPI and CD45, no fluorescence signal could be observed under the microscope.

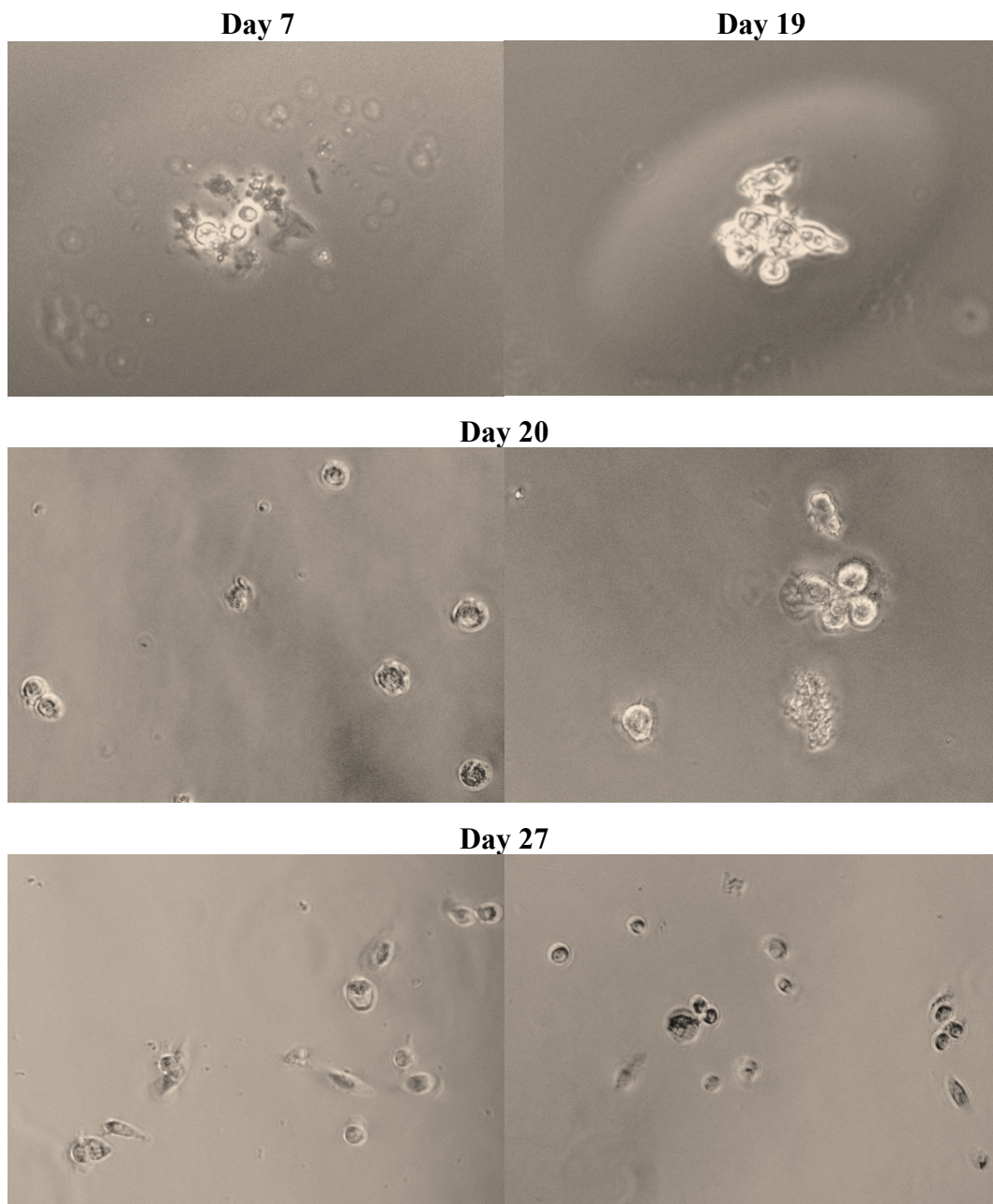


Figure 17 Breast cancer CTC development in culture (Patient 1)

In this figure, the development of CTCs from the first breast cancer patient is illustrated. On day 7 of culture only a few large cells were inside the microwells. On day 19, these cells proliferated, changed phenotype, and seemed to form cell-to-cell adhesions. Subsequently on day 20, all cells from the microwells were transferred into one chamber of a 96-well plate. Here, some of these cells existed in small clusters, others were present as single cells. On day 27, the cells were still alive and there was a clear change of phenotype in some cells, that adhered to the surface of the well plate. Furthermore, some of the cells also achieved proliferation.

4.3.6 Culture of ovarian cancer CTCs

In addition to blood from breast cancer patients, blood from 4 metastatic ovarian cancer patients was processed with the slanted spiral as well, and the entire enriched volume was transferred into the microwell cell culture. Cells were kept under normoxic condition and in two of the microwell cultures proliferation and cluster formation was observed (Table 15).

Table 15 Microwell culture of ovarian cancer cells after slanted spiral enrichment

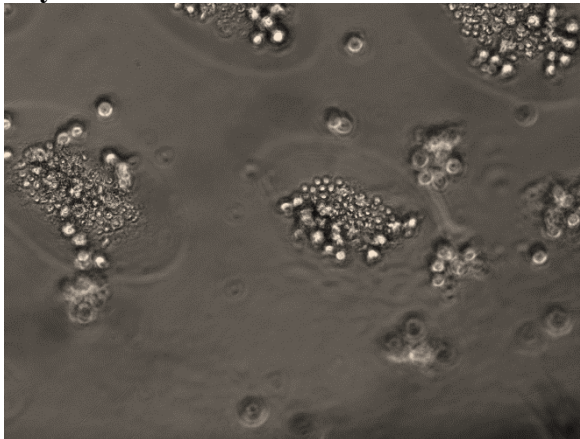
Blood from 4 ovarian cancer patients was enriched with the slanted spiral and directly transferred into microwell culture. Table 15 is providing an overview of the blood volume (ml) transferred into culture, as well as the period (days) the cells were cultivated and their development in culture. In two patients we could observe proliferating cells in many microwells and under fluorescence microscope the clusters also showed expression of keratins.

	Blood volume	Days in culture	Development in culture	Keratin+ cells after culture
Patient 13	56 ml	139	<ul style="list-style-type: none"> ▪ Large cells in microwells after seeding ▪ Cell survival and proliferation 	<ul style="list-style-type: none"> ▪ Singular keratin +, DAPI + cells
Patient 14	52.5 ml	115	<ul style="list-style-type: none"> ▪ Large cells in microwells after seeding ▪ Cell survival and proliferation 	<ul style="list-style-type: none"> ▪ Clusters and singular keratin +, DAPI + cells
Patient 15	60 ml	40	<ul style="list-style-type: none"> ▪ No survival, no proliferation 	<ul style="list-style-type: none"> ▪ No keratin + cells
Patient 16	49 ml	40	<ul style="list-style-type: none"> ▪ No survival, no proliferation 	<ul style="list-style-type: none"> ▪ No keratin + cells

In patient 13, cell growth became apparent on day 37 and in patient 14 on day 24, respectively. The cells of both patients continued proliferation and, once dense clusters had formed inside the microwells, the cells could be transferred to a normal well plate where they adhered to the flat surface and continued proliferation (Fig. 18).

Patient 13

Day 37

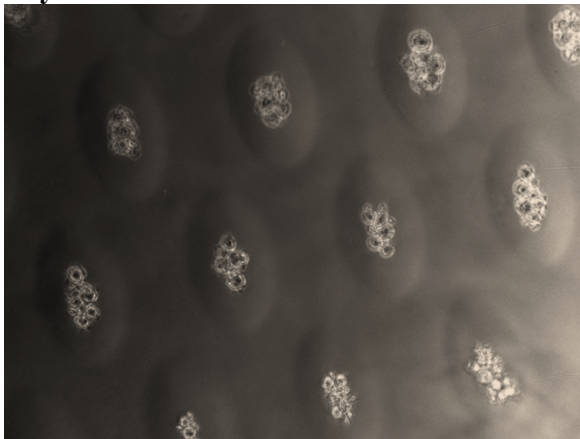


Day 59



Patient 14

Day 26



Day 47

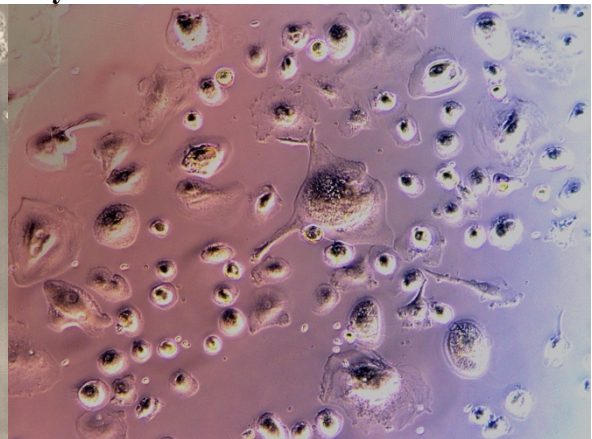


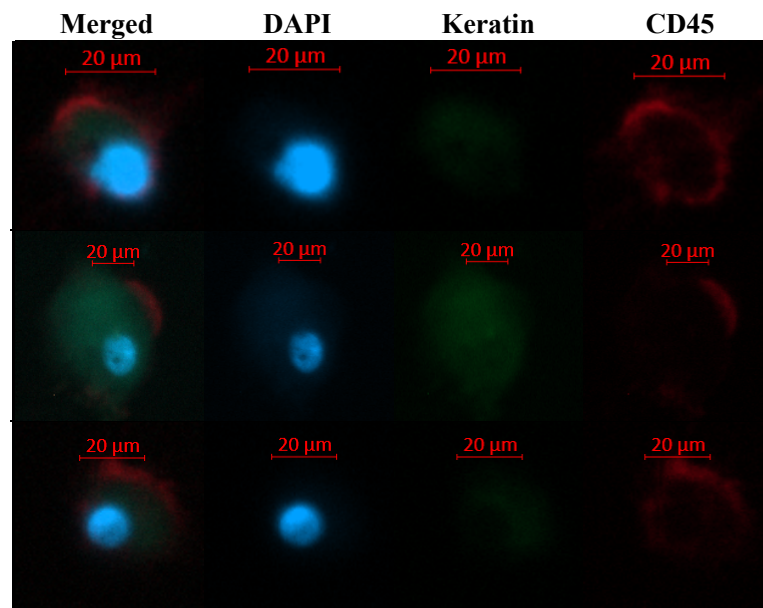
Figure 18 Ovarian CTC progression in microwell culture

In two of the ovarian cancer microwell cultures we observed proliferation in the microwells on day 37 and 24, respectively. These cells could be transferred into regular wellplates where they grew adherent to the surface. This figure presents pictures of the cultures from patient 13 and 14. The pictures on the left show the microwells on the first day of noticeable cell proliferation and on the right there is a follow-up picture after the cells have been transferred into a wellplate.

After 139 and 115 days in culture the cells were removed from culture to perform further analysis. In both patients the cultivated cells were positive for keratin and DAPI (Fig. 19) which proves their epithelial origin. An additional CD45 positivity was observed. Unfortunately, CNA analysis of these cells could not be performed due to insufficient quality and low coverage of the cell's DNA.

The experimental work on the ovarian cancer samples was performed in collaboration with Maximilian C. Wankner.

Patient 13



Patient 14

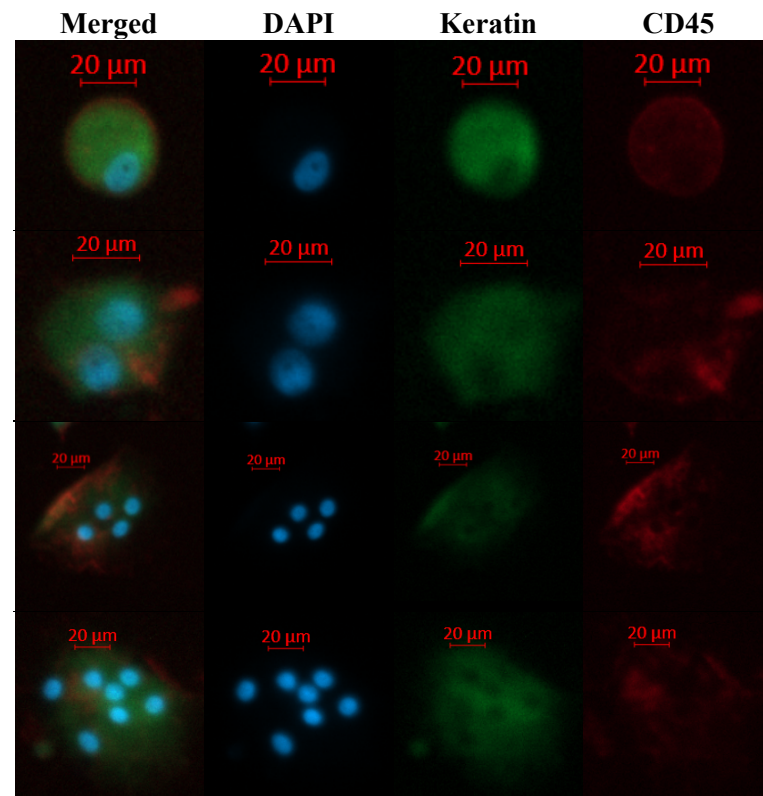


Figure 19 Fluorescence microscopy of cells cultured from ovarian cancer patients

After the ovarian cancer cells were removed from culture, fluorescence staining and microscopic analysis were performed. In Patient 13 only singular cells were discovered which also expressed a less intense keratin signal. In Patient 14 the cultured cells expressed a stronger keratin signal. Here clusters as well as cell couples and singular cells were found. Cells from both patients expressed a CD45 signal together with the keratin markers.

5 Discussion

5.1 Optimal performing conditions of the slanted spiral microfluidic device and potentials in diagnostic leukapheresis enrichment

Despite the great potential of liquid biopsies for the initial diagnosis and treatment of cancer patients, the sensitivity that can be achieved with the current enrichment techniques is still not sufficient enough for its adaptation to the clinical practice (Alix-Panabières and Pantel, 2016; Habli et al., 2020; Lawrence et al., 2023). Enabling the screening of higher blood volumes could not only increase CTC counts per patient, but also identify CTC positive patients with very low CTC numbers (Stoecklein et al., 2016; Yang et al., 2021).

In our study, we demonstrated that the slanted spiral microfluidic device could fulfill this challenge. We showed that this method can easily process higher sample volumes up to 50 ml of blood in mere minutes. Our results show that the highest purity of the enriched fraction is achieved for PBMC concentrations up to 6×10^6 cells/ml. This exceeds the results from the initial spiral presentation where the authors suggested concentrations below $\sim 3.5\text{-}4 \times 10^6$ WBCs/ml (Warkiani et al., 2014a).

In a healthy individual the concentration of leukocytes in pure blood is $4 \times 10^6\text{-}10 \times 10^6$ leukocytes/ml. A 7.5 ml tube of blood will therefore be diluted to a maximum of 12.5 ml of volume after pre-enrichment to reach this concentration. These quantities are very suitable for spiral enrichment as they can be processed in a maximum of 7.35 minutes.

The slanted spiral should also provide a method for rapid and reliable analysis of DLA product. According to previous publications, the DLA harvests a liquid with an average concentration of 50×10^6 to 65.65×10^6 mononuclear cells/ml (Stoecklein et al., 2016, Andree et al. 2018, Fehm et al., 2018). Aiming at a concentration of 6×10^6 PBMCs/ml, one milliliter of DLA product should be diluted by the factor 10. With an average DLA volume of 53 ml in this study, a sample of around 530 ml would have to be processed. The volume of the enriched fraction to be examined for CTCs would still amount to 177 ml. This seems unpractical for clinical practice.

Nevertheless, there are two ways to address this problem. In the present studies, only a fraction of the whole DLA product has been analyzed by the CellSearch® device. Depending on publication, 2.3 ml (Fischer et al., 2013), 2.7 ml (Fehm et al., 2018) or 3.7 ml, (Andree et al. 2018) were used for downstream CellSearch® analysis. As, according to Fehm et al., 5% of the DLA volume in their study is equivalent to 60ml of peripheral blood, analyzing only a fraction of the DLA product already increases CTC detection frequencies and CTC counts immensely (Fischer et al., 2013, Fehm et al., 2018, Andree et al., 2018, Stoecklein et al.,

2016). For example, to process 10% of the DLA volume with the slanted spiral at a concentration of 6×10^6 PBMCs/ml, a dilution to an average of 53 ml would be necessary. This would lead to only 17 ml of volume in the CTC-enriched fraction.

Another option is to increase the PBMC concentration in the processed volume despite the loss of purity. As we showed, a concentration of 25×10^6 PBMCs/ml still provides a PBMC clearance of 85.44%. In contrast to other methods as the CellSearch® system that does not enable the analysis of higher cell concentrations, the slanted spiral is capable of handling increased PBMC inputs. The examiner must only be aware of the increased PBMC contamination in the final product.

A solution to handle these higher PBMC contaminations after the first enrichment cycle could lie in repetitive enrichment cycles. A work of Aya-Bonilla et al. already described a tumor cell loss of 11-33% after a second enrichment step (Aya-Bonilla et al., 2017). Also, the group of Guglielmi et al., who used a so-called “DLA biochip” to perform a CTC enrichment on imitated DLA products, implemented a secondary enrichment cycle in order to increase the purity of the sample. Even though this group used an altered spiral device, they only achieved a tumor cell recovery rate of 47-48% (Guglielmi et al., 2020). We therefore analyzed the effect that repetitive enrichments have on the spiral’s performance and could show that, although multiple cycles are beneficial for further volume and PBMC reduction, the recovery of cancer cells is decreased after every enrichment round. But as a second cycle only decreases CTC recovery by 9.7%, it could give an opportunity to handle the whole DLA volume without increased PBMC concentration and small outcoming volume.

5.2 Recovery rate and impact of internal and external factors

As the slanted spiral is a size-based enrichment method, also previous studies already indicated that the recovery rate of this device depends on CTC cell size with recovery rates ranging from 23% to 90% (Aya-Bonilla et al., 2017; Kulasinghe et al., 2017; Müller Bark et al., 2021; Warkiani et al., 2014a).

As our study was planned to be performed with breast cancer patient samples, recovery studies were conducted with the breast cancer cell line MCF7. The overall recovery of keratin positive cells was 63.4%. However, by examining the cells under the microscope we could see a discrepancy in tumor cell integrity depending on their allocation by the inner or outer outlet. From the MCF7 cells falsely sorted as waste through the outer outlet, a larger proportion showed a torn membrane and a diffuse keratin signal. When counting only MCF7

cells showing an intact membrane and nucleus, the recovery rate was higher with 70.9%. To our knowledge, this differentiation was applied for the first time. A reason for this observation might be the increased deformability of damaged cells leading to a different behavior within the forces of the enrichment process. These findings can be assessed as advantageous with the perspective that only intact cells are suitable for downstream analysis and culture.

Nevertheless, previous researchers could show higher spiral CTC recovery rates in their publications (Table 8). For example, Warkiani et al. presented a MCF7 recovery rate of 85% (Warkiani et al. 2014a). What could have influenced our recovery rate is the staining procedure after the spiral enrichment. Warkiani et al. used green fluorescent protein (GFP) expressing cell lines, which eliminates the potential cell loss during post-enrichment staining. Furthermore, the group used samples spiked with 500 MCF7, whereas in this study only 100 cells were used. Higher initial cancer cell input is positively correlated to the recovery (Kulasinghe et al., 2017) as we also observed in our experiments (Fig. 10). This might be a reason for the discrepancy in the recovery rate. Therefore, starting material with cell counts much higher than usually found in cancer patients should be interpreted carefully. We believe that our experiments reflect the clinical situation more adequately.

There are some limitations of this method that should also be discussed. The biggest downside is given by the size-dependency of the enrichment.

Recovery rates are generally calculated using blood samples provided from healthy individuals spiked with cancer cell line cells. Different groups have performed experiments to calculate spiral efficiency (Table 8). The recovery rates ranged from 23 to 90%, depending on study and cell line. In the original presentation of the slanted spiral by Warkiani et al., there is no annotation until which diameter cells are sorted into the correct outlet (Warkiani et al., 2014a). The group of Müller-Bark et al. state in their experiments, that there is a cutoff size for cells smaller than 14 μm , however it is not evident where this information has been obtained from. In their experiments, they performed spiral enrichment on five different cell lines and show a definite correlation between cell size and recovery rate. Especially cells from their smallest cell line, with an average cell size of 12 μm , could be recovered by only 23-33% (Müller Bark et al., 2021).

Nevertheless, the sizes of cell line cells differ from the in vivo situation, as CTCs can be more heterogeneous depending on origin but also patient, and cells that have undergone EMT can reduce in size and have an increased deformability. For example, breast cancer cell line cells show a diameter of 15 to 17 μm , whereas breast cancer CTCs are reported to have

an average diameter of only 13.1 μm . Prostate cancer CTCs are even smaller with only 10.7 μm (Hao et al., 2018). White blood cells are generally smaller, but depending on subgroup their sizes also overlap with cancer cell line cell and CTC sizes. Leukocytes have diameters of 6-12 μm , granulocytes can measure 8-14 μm and monocytes are the largest blood cells with sizes of 15-20 μm (Welsch et al., 2018). Therefore, modifications that can shift the cutoff, as for example modifying the flowrate, will also have an impact on enrichment purity (Guan et al., 2013), as we could also confirm in this study (Fig. 7).

In conclusion, for future experiments with the slanted spiral the researcher should have in mind that the procedure might not be suitable for cancer entities that are known for small cell sizes (Pei et al., 2020), as e.g., small-cell lung cancer.

Another disadvantage of the presented method, that is shared with other size-based enrichment methods (Werner et al., 2017), is the continued need of fluorescence antibodies for CTC counting after the initial enrichment. The advantage in our method is given by its flexibility regarding the choice of the ideal marker. Depending on cancer entity and experiment design, different antibodies or even a combination of multiple markers can be selected. However, most markers that are currently applied for CTC enumeration are epithelial markers such as EpCAM or keratins. These targets might neither be expressed by cancer stem cells nor by CTCs that have undergone EMT. Up to this date there is still a lack of established markers for these two subgroups (Werner et al., 2017).

Nevertheless, the central advantage the slanted spiral brings to the market is its rapid processing of larger volumes while maintaining cell viability. Subsequent CTC cultures with the opportunity of drug testing may enable an advance regarding personalized cancer medicine (Tellez-Gabriel et al., 2018). For these CTC cultures there is no necessity to perform an additional antibody reliant CTC counting. CTCs can directly be transferred into culture and – in contrary to antibody-dependent enrichment methods as CellSearch® – there is no loss of stem cells or CTCs that have undergone EMT.

During our experiments we experienced that small fibers or dust may enter the spiral loops and lead to clogging of the cross section (Fig. 20). We therefore recommend performing all pre-enrichment steps as well as spiral preparation and sample processing under sterile conditions, even if the slanted spiral is only used for CTC enumeration and no subsequent culture is intended.

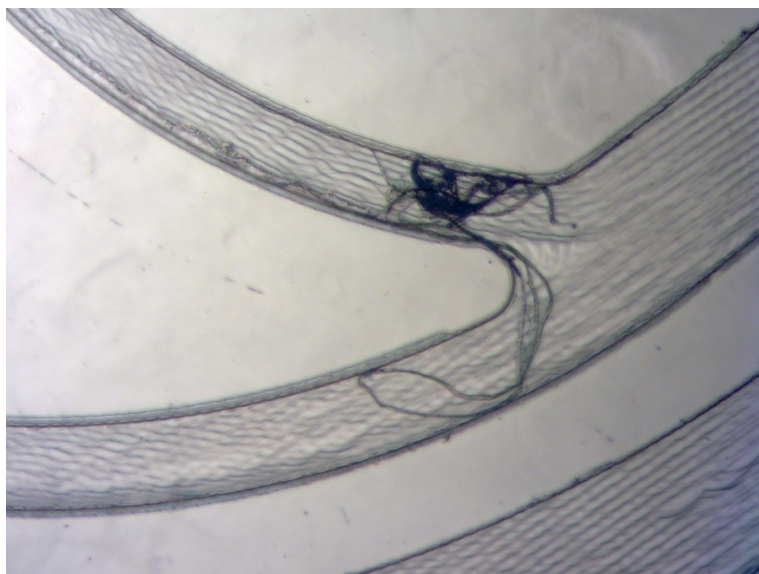


Figure 20 Clogged spiral cross section

A close-up picture of the cross section of the slanted spiral microfluidic device. The grey shaded area are the loops that the fluids are processed through. In the center of the picture the spiral splits into inner and outer outlet. In this picture this cross section is clogged by fibers, leading to its malfunction.

5.3 CTC enrichment from patient samples

When examining patient samples under the microscope after spiral enrichment, we observed differences in the fluorescence characteristics. We discovered cells with the standard CTC attributes of a strong keratin signal and negativity for CD45. These cells were slightly larger than the surrounding blood cells and we could prove that one of these cells had typical copy number aberrations of a Luminal-A type breast cancer, which is also consistent with the patient information.

Despite these typical CTC-like cells, we also found cells that did not meet the criteria but could still not be categorized as normal blood cells. We therefore decided to perform a subgroup analysis. The described above typical CTCs were categorized into subgroup A.

We also discovered cells that were still positive for DAPI and negative for CD45 but a bit smaller in diameter and expressing a fainter keratin signal. These cells were classified as category B cells. In the blood samples of patients that were positive for these cells, there was always a very high number of detectable cells that majorly exceeded any finding of category A cells. One explanation that we considered was a contamination of the liquid biopsy with epithelial skin cells. However, for one of these category B cells, we could prove a cancer origin with typical CNAs of a triple negative breast cancer, which was in concordance with

the patient's disease. We therefore counted cells from this category as CTCs in our analysis. Another explanation for this altered phenotype might be a partial EMT transformation that led to the loss of some, but not all epithelial surface markers. Previous authors described that breast cancer CTCs can lose keratin expression during EMT (Polioudaki et al., 2015) and that breast cancer metastases also show altered keratin expression compared to the primary tumor (Joosse et al., 2012). If the spiral is capable of enrichment and enumeration of cells that have undergone EMT this would give a great advantage in comparison to label-dependent enrichment methods. Further research to prove this hypothesis will be necessary. Interestingly we also found cells that did not express any keratin signal but were neither positive for CD45. This cluster of differentiation is expressed by all nucleated blood cells including immature progenitor cells (Rheinländer et al., 2018). Keratin negative but EpCAM positive CTCs have been described before (Deng et al., 2008). As we did not use a combination of these two fluorescence markers, we are not able to tell if those might be epithelial CTCs which can only be stained with EpCAM or CTCs that have fully transformed to a mesenchymal state and lost all epithelial surface markers. However, we could not prove for any of these cells to have CNAs concordant to a cancer genome after next generation sequencing. We therefore decided to not include them in the analysis as circulating tumor cells.

The last subgroup of cells we found, were very large cells presenting a CD45 signal alongside keratin expression. These, classified as category D cells, could also not be confirmed to be CTCs after next generation sequencing and CNA analysis. The fluorescence characteristics of these cells have been described in the literature in cancer-associated macrophage-like cells (CAMLs). These cells originate from the tumor microenvironment and invade into the blood stream together with the CTCs and have been reported to express CD45, but also keratins and EpCAM (Pereira-Veiga et al., 2022). CAMLs are associated with a worse prognosis when found in a cancer patient's blood (Mu et al., 2017). We did not perform a staining with additional markers typically expressed by CAMLs (CD14+/CD11c+) (Pereira-Veiga et al., 2022), so we cannot prove this hypothesis. The ability to detect those cells after slanted spiral enrichment should be investigated in further research, as their detection might have a prognostic value (Mu et al., 2017), especially when combined with CTC enumeration.

Unfortunately, we could only prove for two of the 15 analyzed cells to exhibit copy number alterations using NGS. Even from the 6 cells of category A, just one was classifiable as a CTC. Furthermore, only one of the category B cells was chosen for NGS, as the rest of the

amplified cells showed low DNA concentrations or less than three bands after electrophoresis. Additionally, none of the category C or D cells could be proven to originate from a carcinoma. A revision of the protocol applied for cell storage and amplification will have to be performed and further patient samples should be analyzed to support the results from this study, especially regarding cells with fainter or no keratin signal.

To evaluate the credibility of the slanted spiral method, we performed a simultaneous CellSearch® analysis of 8/12 breast cancer patients. Due to the low number of investigated cases, a comparison with the CellSearch® system did not show a consistent superiority of either method. Nevertheless, a high number of CTCs with weak keratin signal were observed in the blood of several patients after enrichment with the slanted spiral, but not after CellSearch® system-based enrichment. These findings stress the necessity of implementing new markers and methods for CTC enrichment to increase the accuracy and reliability of the current CTC detection. Additionally, we would perform further experiments with a combination of EpCAM and a keratin cocktail to capture CTCs that only express one of these markers. To validate the trend indicated in these experiments, further analysis with higher case numbers will be necessary.

5.4 CTC culture in microwells

To this date, an obstacle for culturing CTCs and especially for establishing permanent cell lines, is still given by the necessity of high CTC counts in the enriched sample to enable cell growth and survival after enrichment (Cayrefourcq et al., 2015; Cortés-Hernández et al., 2020; Koch et al., 2020b). In this work, we established a protocol to allow culture of cancer cells even from small concentrations.

To prove the suitability of the procedure and cell viability after the enrichment, we initially performed spiking experiments with MCF-7 cell line cells. After spiral enrichment, the captured cells were seeded into microwells providing the advantage that the cells can accumulate in the microwells, develop cell-to-cell adhesions, and form three-dimensional cell clusters (Tu et al., 2014). In our spiking experiments we could observe that single MCF7-cells inside the microwells initiated cell growth and proliferated into a cluster. Cells from already established cancer cell lines are easier to cultivate, so these results may not directly translate to CTC behavior in culture. Nevertheless, also the group of Khoo et al. postulated that one CTC per microwell should be sufficient for the induction of CTC cluster formation (Khoo et al., 2016). As successful CTC-culture depends on high CTC counts in the peripheral blood

(Shimada et al., 2022) this method, which may permit CTC growth also from small cell counts gives a huge opportunity regarding CTC culture in patients with low CTC burden. After demonstrating the suitability of the applied methods, CTC culture was performed on 11 breast cancer and 4 ovarian cancer patient samples. We succeeded in the cultivation of keratin-positive clusters from two of the ovarian cancer patient samples. Besides keratin positivity, the cultured cells were also stainable with a CD45-antibody. Even though this cluster of differentiation is characteristically only expressed by blood cells, previous studies reported CD45 positivity in ovarian cancer cells and their derived cell cultures and an association to cancer stem cell characteristics (Mitra et al., 2018; Ramakrishnan et al., 2013). CD45-positivity was also previously observed in short-term CTC cultures (Shimada et al., 2022).

As NGS and CNA analysis were not yet performed on the cultured cells, there is so far no proof of their CTC character. However, as the cells showed proliferation in cell culture and express typical epithelial surface markers, a CTC status can be assumed. Nevertheless, we failed in establishing sufficient, proliferating CTC cultures from the two other ovarian cancer patients included in this study, as well as from all the breast cancer patients, even in the patients with higher CellSearch® enumerated CTCs. We observed the cell survival and sparse proliferation in a few of the breast cancer patients, but not sufficient enough for downstream culture. As the goal in terms of personalized cancer medicine is a reliable short-term culture of all CTC positive cancer patients, the underlying causes of the unsuccessful cultures should be identified.

When cultivating CTCs from the ovarian cancer patients, some modifications were made regarding sample preparation and cell culture conditions. At first, instead of using a combination of the Ficoll-Paque™ Plus medium and an RBC lysis buffer solution as performed on the breast cancer samples, erythrocyte removal in the ovarian cancer samples was accomplished by only using RBC lysis. Although the purest results could be achieved by combining the two methods, this procedure may have also resulted in a higher stress on the cells and a prolonged sample preparation, which may have led to a loss of cell viability in the breast cancer samples. In addition, the breast cancer samples were kept under hypoxic instead of normoxic conditions which may have also led to a more hostile culture environment. Hypoxic conditions are usually selected to achieve a depletion of the remaining blood cells. Previous successes in long-term and short-term CTC cultures were achieved in normoxic as well as hypoxic conditions. The transfer of the cultures into normoxic conditions within 7 days seems to be generally recommended (Shimada et al., 2022) and

most successful short-term CTC cultures were performed under normoxic conditions (Shimada et al., 2022). Also in our experiments, proliferation of keratin-positive cells could be observed in the ovarian CTC cultures under normoxic conditions, while no proliferation was observed in the breast cancer cultures that have been kept in hypoxia.

In the ovarian cancer CTC cultures that showed cell proliferation we observed cell growth on day 37 and 26. The breast cancer CTC cultures were kept in culture for only 10 to 33 days. It might be possible that the observation period was simply not long enough to capture potential proliferation in the breast cancer patients. In previously published successful microwell cultures, cell growth started on day 8 (Khoo et al., 2015) and day 11 (Khoo et al., 2016). We do not know why proliferation was initiated later in our experiments; however, it seems advisable to observe the cultures for a prolonged period.

Apart from the modifications performed in ovarian CTC culture which may have contributed to successful cell growth, we also did not succeed in establishing a CTC culture from all ovarian cancer samples under these altered conditions. It is therefore plausible, that there are other underlying causes concerning the success of a CTC culture. The collected cells need to possess the ability to initiate proliferation in culture. In the first instance the CTCs need to be in a viable state once they are seeded into the microwells. However, the life span of CTCs is short with a half-life time of under 1.5 hours (Vasantharajan et al., 2021). So even in the only just drawn blood sample, some CTCs might already be apoptotic. Additionally, the process of blood withdrawal, transportation to the laboratory, sample preparation and slanted spiral enrichment takes it time. Furthermore, it must be considered that even if low numbers of cell line cells might be sufficient for the initiation of cell growth in the microwells, this might not be adaptable to CTCs. Most existing CTC-cultures were achieved from samples with high CTC quantity (Shimada et al., 2022). It must therefore be taken into account that the CTC counts in the unsuccessful cultures were simply not sufficient for successful culture establishment.

Despite the importance of cell numbers and cell viability for culture success, it is also possible that not all CTCs have the ability to achieve proliferation in culture. CTCs are very heterogeneous, and it is widely assumed that only a part of these cells, so-termed, metastasis-initiating cells, is capable to induce metastasis (Massagué and Ganesh, 2021). It is therefore plausible that also not all viable CTCs captured by a liquid biopsy are equipped with the right qualities to survive or even proliferate in cell culture.

The optimal CTC culture conditions and the ability of CTCs to initiate cell growth in culture are still not fully understood. Further optimization of the protocol might allow successful culture in a larger proportion of the patient samples.

6 Conclusion

The combination of two innovative techniques, the slanted spiral enrichment device and the microwell culture, represents a promising approach for processing larger sample volumes and the downstream establishment of patient-derived CTC cultures.

Our data shows the suitability of the slanted spiral microfluidic device as an enrichment method for CTCs. It permits the analysis of high sample volumes at a very high throughput while preserving the viability of the enriched cells. Under the established optimal performing conditions of the spiral, a recovery rate of intact MCF-7 cells of 70.9% was achieved. Regarding the analyzed patient samples, in comparison with the FDA-approved CellSearch® device, an agreement in keratin-positive CTC numbers was observed. In a few patients, a high number of weakly keratin-positive CTCs was observed after spiral enrichment but not by CellSearch® analysis. As the method is not label-dependent, it also enables the enrichment of CTCs not expressing the typical epithelial markers as stem cells or cells that have undergone EMT. During this research, cells that expressed neither epithelial keratins nor typical blood cell markers were observed as well. However, we could not identify these cells as CTCs by NGS analysis. A disadvantage of this size-based enrichment is the potential loss of smaller sized CTCs during the enrichment.

In addition, collected cells were also transferred into microwell cell culture after spiral enrichment. Spiking experiments with MCF7 cells could show that very small concentrations of cell line cells are sufficient to initiate cluster formation. Even though achieving successful culture from cell line cells is much simpler than establishing CTC cultures, we also succeeded in the culture of keratin positive cells from two patient samples by using the combination of the spiral enrichment and the microwell culture method. However, we could not yet prove the CTC character of these keratin positive cells.

Summarizing, the possibility of increasing the screened sample volume enables higher CTC yields and spiral enriched cells can proliferate in a downstream microwell-based cell culture. Nevertheless, the procedure needs optimization to enable in-vitro culture from all CTC positive cancer patients.

7 Summary

Cancer is responsible for a quarter of deaths in the German population. Most of these patients do not die from the primary tumor itself but from the consequences of metastatic spread of the localized disease. Metastases are initiated by circulating tumor cells (CTCs) that detach from the original tumor, invade the vascular system, and enable the formation of secondary tumor masses in distant tissues. These CTCs can be detected in the blood with a so-called *liquid biopsy* and be used for downstream analysis. *Ex vivo* culture of CTCs and subsequent drug sensitivity testing could be the next step in realizing personalized cancer medicine.

However, to overcome the limitation of CTC scarcity in most blood samples, it is necessary to increase sample volume and throughput of the CTC enrichment. This research focuses on the suitability of the slanted spiral microfluidic device for processing larger volumes and subsequent in-vitro culture of the enriched CTCs in microwells.

First, a protocol was developed for optimal operation of the device. The highest purity with an average PBMC elimination rate of 97% could be achieved at a cell concentration of 6×10^6 cells per ml and a flowrate of 1.7 ml per minute. The average tumor recovery rate of spiked MCF-7 cells was 71%. Our results indicated that apoptotic cells have a higher chance of elimination than intact cells.

Subsequently, blood samples from 12 metastatic breast cancer patients were processed with the slanted spiral microfluidic device to enrich for CTCs and recovery rates compared to the FDA cleared CellSearch® system. Patient samples with volumes of up to 51 ml were enriched. Compared to CellSearch® results, a fair agreement in CTC number in patient samples was observed (Cohen's kappa=0.75).

Spiral enriched MCF7 cells proliferated in microwell culture by the factor 1000 in 36 days. Furthermore, cell growth was observed in the cultures from ovarian cancer patients. Cells growing in these cultures were positive for keratins and DAPI but could not yet be proven as cancer cells by NGS. No successful culture of keratin-positive cells could be achieved from the breast cancer samples.

8 Zusammenfassung

Krebserkrankungen sind ursächlich für ein Viertel aller Todesfälle in Deutschland. Die meisten Patient:innen versterben nicht an dem Primärtumor, sondern an den Folgen von Tumormetastasen. Diese werden durch zirkulierende Tumorzellen (CTCs) initiiert, welche sich vom Ursprungstumor lösen, in die Blutgefäße einwandern und in peripheren Geweben zu der Bildung von Zweittumoren führen. CTCs können im Patient:innenblut mit einer sogenannten *Liquid Biopsy* detektiert werden und für anschließende Analysen genutzt werden. *Ex vivo* Kulturen in Kombination mit Empfindlichkeitstestungen auf Arzneimittel könnten den nächsten Fortschritt in der personalisierten Krebstherapie bedeuten.

In den meisten Blutproben befindet sich allerdings nur eine geringe Anzahl an CTCs. Diese Einschränkung kann durch eine Steigerung des untersuchten Blutvolumens überwunden werden. In dieser Arbeit soll geprüft werden, ob die *Slanted Spiral* Methode sich zur Prozessierung größerer Proben und anschließender in-vitro Kultivierung von CTCs in *Microwells* eignet.

Zuerst erfolgte die Etablierung eines Protokolls zur optimalen Anwendung der Methode. Die höchste Aufreinigung der Proben mit einer durchschnittlichen PBMC-Eliminierungsrate von 97% konnte bei einer Zellkonzentration von 6×10^6 Zellen pro ml und einer Flussgeschwindigkeit von 1.7 ml pro Minute erzielt werden. Die durchschnittliche Rückgewinnungsrate von MCF-7 Zellen lag bei 71%, wobei unsere Ergebnisse darauf hinwiesen, dass apoptotische Zellen häufiger eliminiert wurden als intakte Zellen.

Anschließend wurden Blutproben von 12 metastasierten Brustkrebspatientinnen mit der *Slanted Spiral* Methode auf CTCs untersucht und Detektionsraten mit der CellSearch® Methode verglichen. Patientinnenproben mit einem Volumen von bis zu 51 ml wurden prozessiert. Verglichen mit CellSearch® Ergebnissen konnte eine Übereinstimmung in CTC-Anzahl gezeigt werden (Cohen's kappa=0.75). Die mit der *Slanted Spiral* Methode angereicherte und in *Microwells* kultivierten MCF-7 Zellen vermehrten sich in 36 Tagen um den Faktor 1000. Außerdem konnte zelluläres Wachstum in zwei Kulturen von Ovarialkarzinompatientinnen beobachtet werden, welche sich unter dem Fluoreszenzmikroskop positiv für Keratine und DAPI zeigten, allerdings noch nicht sicher durch NGS als Krebszellen identifiziert werden konnten. Aus den Proben der Brustkrebspatientinnen konnte keine erfolgreiche Kultur angezchtet werden.

9 References

- Aceto, N., Bardia, A., Miyamoto, D.T., Donaldson, M.C., Wittner, B.S., Spencer, J.A., Yu, M., Pely, A., Engstrom, A., Zhu, H., Brannigan, B.W., Kapur, R., Stott, S.L., Shioda, T., Ramaswamy, S., Ting, D.T., Lin, C.P., Toner, M., Haber, D.A., Maheswaran, S., 2014. Circulating Tumor Cell Clusters are Oligoclonal Precursors of Breast Cancer Metastasis. *Cell* 158, 1110–1122. <https://doi.org/10.1016/j.cell.2014.07.013>
- Alba-Bernal, A., 2020. Challenges and achievements of liquid biopsy technologies employed in early breast cancer 10.
- Alba-Bernal, A., Lavado-Valenzuela, R., Domínguez-Recio, M.E., Jiménez-Rodríguez, B., Queipo-Ortuño, M.I., Alba, E., Comino-Méndez, I., 2020. Challenges and achievements of liquid biopsy technologies employed in early breast cancer. *EBioMedicine* 62, 103100. <https://doi.org/10.1016/j.ebiom.2020.103100>
- Alix-Panabières, C., Pantel, K., 2016. Clinical Applications of Circulating Tumor Cells and Circulating Tumor DNA as Liquid Biopsy. *Cancer Discov* 6, 479–491. <https://doi.org/10.1158/2159-8290.CD-15-1483>
- Allison, K.H., Hammond, M.E.H., Dowsett, M., McKernin, S.E., Carey, L.A., Fitzgibbons, P.L., Hayes, D.F., Lakhani, S.R., Chavez-MacGregor, M., Perlmutter, J., Perou, C.M., Regan, M.M., Rimm, D.L., Symmans, W.F., Torlakovic, E.E., Varella, L., Viale, G., Weisberg, T.F., McShane, L.M., Wolff, A.C., 2020. Estrogen and Progesterone Receptor Testing in Breast Cancer: American Society of Clinical Oncology/College of American Pathologists Guideline Update. *Archives of Pathology & Laboratory Medicine* 144, 545–563. <https://doi.org/10.5858/arpa.2019-0904-SA>
- Al-Ostoot, F.H., Salah, S., Khamees, H.A., Khanum, S.A., 2021. Tumor angiogenesis: Current challenges and therapeutic opportunities. *Cancer Treatment and Research Communications* 28, 100422. <https://doi.org/10.1016/j.ctarc.2021.100422>
- Andree, K.C., Mentink, A., Zeune, L.L., Terstappen, L.W.M.M., Stoecklein, N.H., Neves, R.P., Driemel, C., Lampignano, R., Yang, L., Neubauer, H., Fehm, T., Fischer, J.C., Rossi, E., Manicone, M., Basso, U., Marson, P., Zamarchi, R., Loriot, Y., Lapiere, V., Faugeroux, V., Oulhen, M., Farace, F., Fowler, G., Sousa Fontes, M., Ebbs, B., Lambros, M., Crespo, M., Flohr, P., Bono, J.S., 2018. Toward a real liquid biopsy in metastatic breast and prostate cancer: Diagnostic LeukApheresis increases CTC yields in a European prospective multicenter study (CTCTrap). *Int J Cancer* 143, 2584–2591. <https://doi.org/10.1002/ijc.31752>
- Aya-Bonilla, C.A., Marsavela, G., Freeman, J.B., Lomma, C., Frank, M.H., Khattak, M.A., Meniawy, T.M., Millward, M., Warkiani, M.E., Gray, E.S., Ziman, M., 2017. Isolation and detection of circulating tumour cells from metastatic melanoma patients using a slanted spiral microfluidic device. *Oncotarget* 8, 67355–67368. <https://doi.org/10.18632/oncotarget.18641>
- Bailey, P.C., Martin, S.S., 2019. Insights on CTC Biology and Clinical Impact Emerging from Advances in Capture Technology. *Cells* 8. <https://doi.org/10.3390/cells8060553>
- Birkett, N., Al-Zoughool, M., Bird, M., Baan, R.A., Zielinski, J., Krewski, D., 2019. Overview of biological mechanisms of human carcinogens. *Journal of Toxicology and Environmental Health, Part B* 22, 288–359. <https://doi.org/10.1080/10937404.2019.1643539>

- Bockhorn, M., Jain, R.K., Munn, L.L., 2007. Active versus passive mechanisms in metastasis: do cancer cells crawl into vessels, or are they pushed? *The Lancet Oncology* 8, 444–448. [https://doi.org/10.1016/S1470-2045\(07\)70140-7](https://doi.org/10.1016/S1470-2045(07)70140-7)
- Boeva, V., Popova, T., Bleakley, K., Chiche, P., Cappo, J., Schleiermacher, G., Janoueix-Lerosey, I., Delattre, O., Barillot, E., 2012. Control-FREEC: a tool for assessing copy number and allelic content using next-generation sequencing data. *Bioinformatics* 28, 423–425. <https://doi.org/10.1093/bioinformatics/btr670>
- Boutry, J., Tissot, S., Ujvari, B., Capp, J.-P., Giraudeau, M., Nedelcu, A.M., Thomas, F., 2022. The evolution and ecology of benign tumors. *Biochim Biophys Acta Rev Cancer* 1877, 188643. <https://doi.org/10.1016/j.bbcan.2021.188643>
- Burstein, H.J., Curigliano, G., Thürlimann, B., Weber, W.P., Poortmans, P., Regan, M.M., Senn, H.J., Winer, E.P., Gnant, M., Aebi, S., André, F., Barrios, C., Bergh, J., Bonnefoi, H., Bretel Morales, D., Brucker, S., Burstein, H., Cameron, D., Cardoso, F., Carey, L., Chua, B., Ciruelos, E., Colleoni, M., Curigliano, Giuseppe, Delalogue, S., Denkert, C., Dubsy, P., Ejlertsen, B., Fitzal, F., Francis, P., Galimberti, V., Gamal El Din Mohamed Mahmoud, H., Garber, J., Gnant, Michael, Gradishar, W., Gulluoglu, B., Harbeck, N., Huang, C.-S., Huober, J., Ilbawi, A., Jiang, Z., Johnston, S., Lee, E.S., Loibl, S., Morrow, M., Partridge, A., Piccart, M., Poortmans, Philip, Prat, A., Regan, M., Rubio, I., Rugo, H., Rutgers, E., Sedlmayer, F., Semiglazov, V., Senn, H.-J., Shao, Z., Spanic, T., Tesarova, P., Thürlimann, Beat, Tjulandin, S., Toi, M., Trudeau, M., Turner, N., Vaz Luis, I., Viale, G., Watanabe, T., Weber, Walter P., Winer, Eric P., Xu, B., 2021. Customizing local and systemic therapies for women with early breast cancer: the St. Gallen International Consensus Guidelines for treatment of early breast cancer 2021. *Annals of Oncology* 32, 1216–1235. <https://doi.org/10.1016/j.annonc.2021.06.023>
- Bykov, V.J.N., Eriksson, S.E., Bianchi, J., Wiman, K.G., 2018. Targeting mutant p53 for efficient cancer therapy. *Nat Rev Cancer* 18, 89–102. <https://doi.org/10.1038/nrc.2017.109>
- Castelli, M.S., McGonigle, P., Hornby, P.J., 2019. The pharmacology and therapeutic applications of monoclonal antibodies. *Pharmacol Res Perspect* 7, e00535. <https://doi.org/10.1002/prp2.535>
- Castillo, D.J., Rifkin, R.F., Cowan, D.A., Potgieter, M., 2019. The Healthy Human Blood Microbiome: Fact or Fiction? *Front Cell Infect Microbiol* 9, 148. <https://doi.org/10.3389/fcimb.2019.00148>
- Cayrefourcq, L., Mazard, T., Joosse, S., Solassol, J., Ramos, J., Assenat, E., Schumacher, U., Costes, V., Maudelonde, T., Pantel, K., Alix-Panabières, C., 2015. Establishment and Characterization of a Cell Line from Human Circulating Colon Cancer Cells. *Cancer Res* 75, 892–901. <https://doi.org/10.1158/0008-5472.CAN-14-2613>
- Centre international de recherche sur le cancer (Ed.), 2012. A review of human carcinogens, IARC monographs on the evaluation of carcinogenic risks to humans. International agency for research on cancer, Lyon.
- Chen, S., Zhou, Y., Chen, Y., Gu, J., 2018. fastp: an ultra-fast all-in-one FASTQ preprocessor. *Bioinformatics* 34, i884–i890. <https://doi.org/10.1093/bioinformatics/bty560>
- Cohen, S.J., Punt, C.J.A., Iannotti, N., Saidman, B.H., Sabbath, K.D., Gabrail, N.Y., Picus, J., Morse, M., Mitchell, E., Miller, M.C., Doyle, G.V., Tissing, H., Terstappen, L.W.M.M., Meropol, N.J., 2008. Relationship of circulating tumor cells to tumor

- response, progression-free survival, and overall survival in patients with metastatic colorectal cancer. *J Clin Oncol* 26, 3213–3221.
<https://doi.org/10.1200/JCO.2007.15.8923>
- Cortés-Hernández, L.E., Eslami-S, Z., Alix-Panabières, C., 2020. Circulating tumor cell as the functional aspect of liquid biopsy to understand the metastatic cascade in solid cancer. *Molecular Aspects of Medicine* 72, 100816.
<https://doi.org/10.1016/j.mam.2019.07.008>
- Danecek, P., Bonfield, J.K., Liddle, J., Marshall, J., Ohan, V., Pollard, M.O., Whitwham, A., Keane, T., McCarthy, S.A., Davies, R.M., Li, H., 2021. Twelve years of SAMtools and BCFtools. *GigaScience* 10.
<https://doi.org/10.1093/gigascience/giab008>
- de Bono, J.S., Scher, H.I., Montgomery, R.B., Parker, C., Miller, M.C., Tissing, H., Doyle, G.V., Terstappen, L.W.W.M., Pienta, K.J., Raghavan, D., 2008. Circulating Tumor Cells Predict Survival Benefit from Treatment in Metastatic Castration-Resistant Prostate Cancer. *Clinical Cancer Research* 14, 6302–6309.
<https://doi.org/10.1158/1078-0432.CCR-08-0872>
- Deng, G., Herrler, M., Burgess, D., Manna, E., Krag, D., Burke, J.F., 2008. Enrichment with anti-cytokeratin alone or combined with anti-EpCAM antibodies significantly increases the sensitivity for circulating tumor cell detection in metastatic breast cancer patients. *Breast Cancer Res* 10, R69. <https://doi.org/10.1186/bcr2131>
- Dick, F.A., Rubin, S.M., 2013. Molecular mechanisms underlying RB protein function. *Nat Rev Mol Cell Biol* 14, 297–306. <https://doi.org/10.1038/nrm3567>
- Dillekås, H., Rogers, M.S., Straume, O., 2019. Are 90% of deaths from cancer caused by metastases? *Cancer Medicine* 8, 5574–5576. <https://doi.org/10.1002/cam4.2474>
- Fehm, T.N., Meier-Stiegen, F., Driemel, C., Jäger, B., Reinhardt, F., Naskou, J., Franken, A., Neubauer, H., Neves, R.P.L., van Dalum, G., Ruckhäberle, E., Niederacher, D., Rox, J.M., Fischer, J.C., Stoecklein, N.H., 2018. Diagnostic leukapheresis for CTC analysis in breast cancer patients: CTC frequency, clinical experiences and recommendations for standardized reporting. *Cytometry Part A* 93, 1213–1219.
<https://doi.org/10.1002/cyto.a.23669>
- Ferreira, M.M., Ramani, V.C., Jeffrey, S.S., 2016. Circulating tumor cell technologies. *Mol Oncol* 10, 374–394. <https://doi.org/10.1016/j.molonc.2016.01.007>
- Fischer, J.C., Niederacher, D., Topp, S.A., Honisch, E., Schumacher, S., Schmitz, N., Zacarias Fohrding, L., Vay, C., Hoffmann, I., Kasprovicz, N.S., Hepp, P.G., Mohrmann, S., Nitz, U., Stresemann, A., Krahn, T., Henze, T., Griebisch, E., Raba, K., Rox, J.M., Wenzel, F., Sproll, C., Janni, W., Fehm, T., Klein, C.A., Knoefel, W.T., Stoecklein, N.H., 2013. Diagnostic leukapheresis enables reliable detection of circulating tumor cells of nonmetastatic cancer patients. *Proceedings of the National Academy of Sciences* 110, 16580–16585.
<https://doi.org/10.1073/pnas.1313594110>
- Flavahan, W.A., Gaskell, E., Bernstein, B.E., 2017. Epigenetic plasticity and the hallmarks of cancer. *Science* 357, eaal2380. <https://doi.org/10.1126/science.aal2380>
- Gkountela, S., Castro-Giner, F., Szczerba, B.M., Vetter, M., Landin, J., Scherrer, R., Krol, I., Scheidmann, M.C., Beisel, C., Stirnimann, C.U., Kurzeder, C., Heinzelmann-Schwarz, V., Rochlitz, C., Weber, W.P., Aceto, N., 2019. Circulating Tumor Cell Clustering Shapes DNA Methylation to Enable Metastasis Seeding. *Cell* 176, 98–112.e14. <https://doi.org/10.1016/j.cell.2018.11.046>
- Guan, G., Wu, L., Bhagat, A.A., Li, Z., Chen, P.C.Y., Chao, S., Ong, C.J., Han, J., 2013.

- Spiral microchannel with rectangular and trapezoidal cross-sections for size based particle separation. *Sci Rep* 3. <https://doi.org/10.1038/srep01475>
- Guglielmi, R., Lai, Z., Raba, K., van Dalum, G., Wu, J., Behrens, B., Bhagat, A.A.S., Knoefel, W.T., Neves, R.P.L., Stoecklein, N.H., 2020. Technical validation of a new microfluidic device for enrichment of CTCs from large volumes of blood by using buffy coats to mimic diagnostic leukapheresis products. *Sci Rep* 10. <https://doi.org/10.1038/s41598-020-77227-3>
- Habli, Z., AlChamaa, W., Saab, R., Kadara, H., Khraiche, M.L., 2020. Circulating Tumor Cell Detection Technologies and Clinical Utility: Challenges and Opportunities. *Cancers (Basel)* 12. <https://doi.org/10.3390/cancers12071930>
- Hanahan, D., 2022. Hallmarks of Cancer: New Dimensions. *Cancer Discovery* 12, 31–46. <https://doi.org/10.1158/2159-8290.CD-21-1059>
- Hanahan, D., Coussens, L.M., 2012. Accessories to the Crime: Functions of Cells Recruited to the Tumor Microenvironment. *Cancer Cell* 21, 309–322. <https://doi.org/10.1016/j.ccr.2012.02.022>
- Hanahan, D., Weinberg, R.A., 2011. Hallmarks of Cancer: The Next Generation. *Cell* 144, 646–674. <https://doi.org/10.1016/j.cell.2011.02.013>
- Hao, S.-J., Wan, Y., Xia, Y.-Q., Zou, X., Zheng, S.-Y., 2018. Size-based separation methods of circulating tumor cells. *Advanced Drug Delivery Reviews* 125, 3–20. <https://doi.org/10.1016/j.addr.2018.01.002>
- Heidrich, I., Ačkar, L., Mossahebi Mohammadi, P., Pantel, K., 2021. Liquid biopsies: Potential and challenges. *Int. J. Cancer* 148, 528–545. <https://doi.org/10.1002/ijc.33217>
- Horlings, H.M., Lai, C., Nuyten, D.S.A., Halfwerk, H., Kristel, P., van Beers, E., Joosse, S.A., Klijn, C., Nederlof, P.M., Reinders, M.J.T., Wessels, L.F.A., van de Vijver, M.J., 2010. Integration of DNA Copy Number Alterations and Prognostic Gene Expression Signatures in Breast Cancer Patients. *Clin Cancer Res* 16, 651–663. <https://doi.org/10.1158/1078-0432.CCR-09-0709>
- Hunter, P., 2017. The fourth pillar. *EMBO Rep* 18, 1889–1892. <https://doi.org/10.15252/embr.201745172>
- Hvichia, G.E., Parveen, Z., Wagner, C., Janning, M., Quidde, J., Stein, A., Müller, V., Loges, S., Neves, R.P.L., Stoecklein, N.H., Wikman, H., Riethdorf, S., Pantel, K., Gorges, T.M., 2016. A novel microfluidic platform for size and deformability based separation and the subsequent molecular characterization of viable circulating tumor cells. *Int J Cancer* 138, 2894–2904. <https://doi.org/10.1002/ijc.30007>
- In-Silico Online [WWW Document], 2006. URL <http://in-silico.online/> (accessed 8.4.21).
- Joosse, S.A., Beyer, B., Gasch, C., Nastały, P., Kuske, A., Isbarn, H., Horst, L.J., Hille, C., Gorges, T.M., Cayrefourcq, L., Alix-Panabières, C., Tennstedt, P., Riethdorf, S., Schlomm, T., Pantel, K., 2020. Tumor-Associated Release of Prostatic Cells into the Blood after Transrectal Ultrasound-Guided Biopsy in Patients with Histologically Confirmed Prostate Cancer. *Clinical Chemistry* 66, 161–168. <https://doi.org/10.1373/clinchem.2019.310912>
- Joosse, S.A., Gorges, T.M., Pantel, K., 2015. Biology, detection, and clinical implications of circulating tumor cells. *EMBO Mol Med* 7, 1–11. <https://doi.org/10.15252/emmm.201303698>
- Joosse, S.A., Hannemann, J., Spötter, J., Bauche, A., Andreas, A., Müller, V., Pantel, K., 2012. Changes in Keratin Expression during Metastatic Progression of Breast

- Cancer: Impact on the Detection of Circulating Tumor Cells. *Clin Cancer Res* 18, 993–1003. <https://doi.org/10.1158/1078-0432.CCR-11-2100>
- Kalemkerian, G.P., Narula, N., Kennedy, E.B., Biermann, W.A., Donington, J., Leighl, N.B., Lew, M., Pantelas, J., Ramalingam, S.S., Reck, M., Saqi, A., Simoff, M., Singh, N., Sundaram, B., 2018. Molecular Testing Guideline for the Selection of Patients With Lung Cancer for Treatment With Targeted Tyrosine Kinase Inhibitors: American Society of Clinical Oncology Endorsement of the College of American Pathologists/International Association for the Study of Lung Cancer/Association for Molecular Pathology Clinical Practice Guideline Update. *JCO* 36, 911–919. <https://doi.org/10.1200/JCO.2017.76.7293>
- Kang, Z.-J., Liu, Y.-F., Xu, L.-Z., Long, Z.-J., Huang, D., Yang, Y., Liu, B., Feng, J.-X., Pan, Y.-J., Yan, J.-S., Liu, Q., 2016. The Philadelphia chromosome in leukemogenesis. *Chin J Cancer* 35, 48. <https://doi.org/10.1186/s40880-016-0108-0>
- Keller, L., Pantel, K., 2019. Unravelling tumour heterogeneity by single-cell profiling of circulating tumour cells. *Nat Rev Cancer* 19, 553–567. <https://doi.org/10.1038/s41568-019-0180-2>
- Kharb, R., Haider, K., Neha, K., Yar, M.S., 2020. Aromatase inhibitors: Role in postmenopausal breast cancer. *Arch Pharm* 353, 2000081. <https://doi.org/10.1002/ardp.202000081>
- Khoo, B.L., Greci, G., Jing, T., Lim, Y.B., Lee, S.C., Thiery, J.P., Han, J., Lim, C.T., 2016. Liquid biopsy and therapeutic response: Circulating tumor cell cultures for evaluation of anticancer treatment. *Sci. Adv.* 2, e1600274. <https://doi.org/10.1126/sciadv.1600274>
- Khoo, B.L., Lee, S.C., Kumar, P., Tan, T.Z., Warkiani, M.E., Ow, S.G.W., Nandi, S., Lim, C.T., Thiery, J.P., 2015. Short-term expansion of breast circulating cancer cells predicts response to anti-cancer therapy. *Oncotarget* 6, 15578–15593.
- Koch, C., Joosse, S.A., Schneegans, S., Wilken, O.J.W., Janning, M., Loreth, D., Müller, V., Prieske, K., Banys-Paluchowski, M., Horst, L.J., Loges, S., Peine, S., Wikman, H., Gorges, T.M., Pantel, K., 2020a. Pre-Analytical and Analytical Variables of Label-Independent Enrichment and Automated Detection of Circulating Tumor Cells in Cancer Patients. *Cancers (Basel)* 12, 442. <https://doi.org/10.3390/cancers12020442>
- Koch, C., Kuske, A., Joosse, S.A., Yigit, G., Sflomos, G., Thaler, S., Smit, D.J., Werner, S., Borgmann, K., Gärtner, S., Mossahebi Mohammadi, P., Battista, L., Cayrefourcq, L., Altmüller, J., Salinas-Riester, G., Raithatha, K., Zibat, A., Goy, Y., Ott, L., Bartkowiak, K., Tan, T.Z., Zhou, Q., Speicher, M.R., Müller, V., Gorges, T.M., Jücker, M., Thiery, J., Brisken, C., Riethdorf, S., Alix-Panabières, C., Pantel, K., 2020b. Characterization of circulating breast cancer cells with tumorigenic and metastatic capacity. *EMBO Mol Med* 12, e11908. <https://doi.org/10.15252/emmm.201911908>
- Krewski, D., Bird, M., Al-Zoughool, M., Birkett, N., Billard, M., Milton, B., Rice, J.M., Grosse, Y., Coglianò, V.J., Hill, M.A., Baan, Robert.A., Little, J., Zielinski, J.M., 2019. Key characteristics of 86 agents known to cause cancer in humans. *Journal of Toxicology and Environmental Health, Part B* 22, 244–263. <https://doi.org/10.1080/10937404.2019.1643536>
- Kulasinghe, A., Tran, T.H.P., Blick, T., O’Byrne, K., Thompson, E.W., Warkiani, M.E., Nelson, C., Kenny, L., Punyadeera, C., 2017. Enrichment of circulating head and neck tumour cells using spiral microfluidic technology. *Sci Rep* 7.

<https://doi.org/10.1038/srep42517>

- Lawrence, R., Watters, M., Davies, C.R., Pantel, K., Lu, Y.-J., 2023. Circulating tumour cells for early detection of clinically relevant cancer. *Nat Rev Clin Oncol* 20, 487–500. <https://doi.org/10.1038/s41571-023-00781-y>
- Lee, Y.T., Tan, Y.J., Oon, C.E., 2018. Molecular targeted therapy: Treating cancer with specificity. *European Journal of Pharmacology* 834, 188–196. <https://doi.org/10.1016/j.ejphar.2018.07.034>
- Liu, H.-Y., Koch, C., Haller, A., Joosse, S.A., Kumar, R., Vellekoop, M.J., Horst, L.J., Keller, L., Babayan, A., Failla, A.V., Jensen, J., Peine, S., Keplinger, F., Fuchs, H., Pantel, K., Hirtz, M., 2020. Evaluation of Microfluidic Ceiling Designs for the Capture of Circulating Tumor Cells on a Microarray Platform. *Advanced Biosystems* 4, 1900162. <https://doi.org/10.1002/adbi.201900162>
- Łukasiewicz, S., Czezelewski, M., Forma, A., Baj, J., Sitarz, R., Stanisławek, A., 2021. Breast Cancer—Epidemiology, Risk Factors, Classification, Prognostic Markers, and Current Treatment Strategies—An Updated Review. *Cancers (Basel)* 13, 4287. <https://doi.org/10.3390/cancers13174287>
- Mader, S., Pantel, K., 2017. Liquid Biopsy: Current Status and Future Perspectives. *Oncol Res Treat* 40, 404–408. <https://doi.org/10.1159/000478018>
- Martincorena, I., Campbell, P.J., 2015. Somatic mutation in cancer and normal cells. *Science* 349, 1483–1489. <https://doi.org/10.1126/science.aab4082>
- Massagué, J., Ganesh, K., 2021. Metastasis-Initiating Cells and Ecosystems. *Cancer Discovery* 11, 971–994. <https://doi.org/10.1158/2159-8290.CD-21-0010>
- Md, V., Misra, S., Li, H., Aluru, S., 2019. Efficient Architecture-Aware Acceleration of BWA-MEM for Multicore Systems. *arXiv:1907.12931 [cs, q-bio]*.
- Miller, M.C., Robinson, P.S., Wagner, C., O’Shannessy, D.J., 2018. The Parsortix™ Cell Separation System—A versatile liquid biopsy platform. *Cytometry A* 93, 1234–1239. <https://doi.org/10.1002/cyto.a.23571>
- Mitra, T., Prasad, P., Mukherjee, P., Chaudhuri, S.R., Chatterji, U., Roy, S.S., 2018. Stemness and chemoresistance are imparted to the OC cells through TGFβ1 driven EMT. *J of Cellular Biochemistry* 119, 5775–5787. <https://doi.org/10.1002/jcb.26753>
- Mu, Z., Wang, C., Ye, Z., Rossi, G., Sun, C., Li, L., Zhu, Z., Yang, H., Cristofanilli, M., 2017. Prognostic values of cancer associated macrophage-like cells (CAML) enumeration in metastatic breast cancer. *Breast Cancer Res Treat* 165, 733–741. <https://doi.org/10.1007/s10549-017-4372-8>
- Müller Bark, J., Kulasinghe, A., Hartel, G., Leo, P., Warkiani, M.E., Jeffree, R.L., Chua, B., Day, B.W., Punyadeera, C., 2021. Isolation of Circulating Tumour Cells in Patients With Glioblastoma Using Spiral Microfluidic Technology – A Pilot Study. *Front Oncol* 11, 681130. <https://doi.org/10.3389/fonc.2021.681130>
- Nagini, S., 2017. Breast Cancer: Current Molecular Therapeutic Targets and New Players. *ACAMC* 17, 152–163. <https://doi.org/10.2174/1871520616666160502122724>
- Nath, S., Devi, G.R., 2016. Three-Dimensional Culture Systems in Cancer Research: Focus on Tumor Spheroid Model. *Pharmacol Ther* 163, 94–108. <https://doi.org/10.1016/j.pharmthera.2016.03.013>
- Nurmik, M., Ullmann, P., Rodriguez, F., Haan, S., Letellier, E., 2020. In search of definitions: Cancer-associated fibroblasts and their markers. *Int. J. Cancer* 146, 895–905. <https://doi.org/10.1002/ijc.32193>

- Pei, H., Li, L., Han, Z., Wang, Y., Tang, B., 2020. Recent advances in microfluidic technologies for circulating tumor cells: enrichment, single-cell analysis, and liquid biopsy for clinical applications. *Lab Chip* 20, 3854–3875. <https://doi.org/10.1039/D0LC00577K>
- Pereira-Veiga, T., Schneegans, S., Pantel, K., Wikman, H., 2022. Circulating tumor cell-blood cell crosstalk: Biology and clinical relevance. *Cell Reports* 40, 111298. <https://doi.org/10.1016/j.celrep.2022.111298>
- Phan, T.G., Croucher, P.I., 2020. The dormant cancer cell life cycle. *Nat Rev Cancer* 20, 398–411. <https://doi.org/10.1038/s41568-020-0263-0>
- Polioudaki, H., Agelaki, S., Chiotaki, R., Politaki, E., Mavroudis, D., Matikas, A., Georgoulas, V., Theodoropoulos, P.A., 2015. Variable expression levels of keratin and vimentin reveal differential EMT status of circulating tumor cells and correlation with clinical characteristics and outcome of patients with metastatic breast cancer. *BMC Cancer* 15, 399. <https://doi.org/10.1186/s12885-015-1386-7>
- Pon, J.R., Marra, M.A., 2015. Driver and Passenger Mutations in Cancer. *Annual Review of Pathology: Mechanisms of Disease* 10, 25–50. <https://doi.org/10.1146/annurev-pathol-012414-040312>
- Prasetyanti, P.R., Medema, J.P., 2017. Intra-tumor heterogeneity from a cancer stem cell perspective. *Mol Cancer* 16, 41. <https://doi.org/10.1186/s12943-017-0600-4>
- Prior, I.A., Hood, F.E., Hartley, J.L., 2020. The Frequency of Ras Mutations in Cancer. *Cancer Research* 80, 2969–2974. <https://doi.org/10.1158/0008-5472.CAN-19-3682>
- Ramakrishnan, M., Mathur, S.R., Mukhopadhyay, A., 2013. Fusion-Derived Epithelial Cancer Cells Express Hematopoietic Markers and Contribute to Stem Cell and Migratory Phenotype in Ovarian Carcinoma. *Cancer Research* 73, 5360–5370. <https://doi.org/10.1158/0008-5472.CAN-13-0896>
- Rheinländer, A., Schraven, B., Bommhardt, U., 2018. CD45 in human physiology and clinical medicine. *Immunology Letters* 196, 22–32. <https://doi.org/10.1016/j.imlet.2018.01.009>
- Robert Koch-Institut (Hrsg) und die Gesellschaft der epidemiologischen Krebsregister in Deutschland e.V. (Hrsg), 2019. *Krebs in Deutschland | 2015/2016*.
- Rushton, A.J., Nteliopoulos, G., Shaw, J.A., Coombes, R.C., 2021. A Review of Circulating Tumour Cell Enrichment Technologies. *Cancers* 13, 970. <https://doi.org/10.3390/cancers13050970>
- Sahai, E., Astsaturov, I., Cukierman, E., DeNardo, D.G., Egeblad, M., Evans, R.M., Fearon, D., Greten, F.R., Hingorani, S.R., Hunter, T., Hynes, R.O., Jain, R.K., Janowitz, T., Jorgensen, C., Kimmelman, A.C., Kolonin, M.G., Maki, R.G., Powers, R.S., Puré, E., Ramirez, D.C., Scherz-Shouval, R., Sherman, M.H., Stewart, S., Tlsty, T.D., Tuveson, D.A., Watt, F.M., Weaver, V., Weeraratna, A.T., Werb, Z., 2020. A framework for advancing our understanding of cancer-associated fibroblasts. *Nat Rev Cancer* 20, 174–186. <https://doi.org/10.1038/s41568-019-0238-1>
- Samavat, H., Kurzer, M.S., 2015. Estrogen metabolism and breast cancer. *Cancer Letters* 356, 231–243. <https://doi.org/10.1016/j.canlet.2014.04.018>
- Schiliro, C., Firestein, B.L., 2021. Mechanisms of Metabolic Reprogramming in Cancer Cells Supporting Enhanced Growth and Proliferation. *Cells* 10, 1056. <https://doi.org/10.3390/cells10051056>
- Sepulveda, A.R., Hamilton, S.R., Allegra, C.J., Grody, W., Cushman-Vokoun, A.M.,

- Funkhouser, W.K., Kopetz, S.E., Lieu, C., Lindor, N.M., Minsky, B.D., Monzon, F.A., Sargent, D.J., Singh, V.M., Willis, J., Clark, J., Colasacco, C., Rumble, R.B., Temple-Smolkin, R., Ventura, C.B., Nowak, J.A., 2017. Molecular Biomarkers for the Evaluation of Colorectal Cancer: Guideline From the American Society for Clinical Pathology, College of American Pathologists, Association for Molecular Pathology, and the American Society of Clinical Oncology. *JCO* 35, 1453–1486. <https://doi.org/10.1200/JCO.2016.71.9807>
- Shimada, Y., Sudo, T., Akamatsu, S., Sunada, T., Myomoto, A., Okano, K., Shimizu, K., 2022. Cell Lines of Circulating Tumor Cells: What Is Known and What Needs to Be Resolved. *JPM* 12, 666. <https://doi.org/10.3390/jpm12050666>
- Siersbæk, R., Kumar, S., Carroll, J.S., 2018. Signaling pathways and steroid receptors modulating estrogen receptor α function in breast cancer. *Genes Dev.* 32, 1141–1154. <https://doi.org/10.1101/gad.316646.118>
- Smit, D.J., Pantel, K., Jücker, M., 2021. Circulating tumor cells as a promising target for individualized drug susceptibility tests in cancer therapy. *Biochemical Pharmacology* 188, 114589. <https://doi.org/10.1016/j.bcp.2021.114589>
- Sobierajska, K., Ciszewski, W.M., Sacewicz-Hofman, I., Niewiarowska, J., 2020. Endothelial Cells in the Tumor Microenvironment, in: Birbrair, A. (Ed.), *Tumor Microenvironment: Non-Hematopoietic Cells*, Advances in Experimental Medicine and Biology. Springer International Publishing, Cham, pp. 71–86. https://doi.org/10.1007/978-3-030-37184-5_6
- Statistisches Bundesamt, 2021. Krebs war 2019 für ein Viertel aller Todesfälle in Deutschland verantwortlich. URL https://www.destatis.de/DE/Presse/Pressemitteilungen/2021/02/PD21_N010_231.html (accessed 12.27.22).
- Stoecklein, N.H., Fischer, J.C., Niederacher, D., Terstappen, L.W.M.M., 2016. Challenges for CTC-based liquid biopsies: low CTC frequency and diagnostic leukapheresis as a potential solution. *Expert Review of Molecular Diagnostics* 16, 147–164. <https://doi.org/10.1586/14737159.2016.1123095>
- Stratton, M.R., Campbell, P.J., Futreal, P.A., 2009. The cancer genome. *Nature* 458, 719–724. <https://doi.org/10.1038/nature07943>
- Strilic, B., Offermanns, S., 2017. Intravascular Survival and Extravasation of Tumor Cells. *Cancer Cell* 32, 282–293. <https://doi.org/10.1016/j.ccell.2017.07.001>
- Swennenhuis, J.F., van Dalum, G., Zeune, L.L., Terstappen, L.W.M.M., 2016. Improving the CellSearch® system. *Expert Review of Molecular Diagnostics* 16, 1291–1305. <https://doi.org/10.1080/14737159.2016.1255144>
- Tellez-Gabriel, M., Cochonneau, D., Cadé, M., Jubelin, C., Heymann, M.-F., Heymann, D., 2018. Circulating Tumor Cell-Derived Pre-Clinical Models for Personalized Medicine. *Cancers (Basel)* 11. <https://doi.org/10.3390/cancers11010019>
- Tibbe, A.G.J., Miller, M.C., Terstappen, L.W.M.M., 2007. Statistical considerations for enumeration of circulating tumor cells. *Cytometry Part A* 71A, 154–162. <https://doi.org/10.1002/cyto.a.20369>
- Toivola, D.M., Boor, P., Alam, C., Strnad, P., 2015. Keratins in health and disease. *Current Opinion in Cell Biology, Cell architecture* 32, 73–81. <https://doi.org/10.1016/j.ceb.2014.12.008>
- Tomasetti, C., Vogelstein, B., 2015. Variation in cancer risk among tissues can be explained by the number of stem cell divisions. *Science* 347, 78–81.

- <https://doi.org/10.1126/science.1260825>
- Tu, T.-Y., Wang, Z., Bai, J., Sun, W., Peng, W.K., Huang, R.Y.-J., Thiery, J.-P., Kamm, R.D., 2014. Rapid Prototyping of Concave Microwells for the Formation of 3D Multicellular Cancer Aggregates for Drug Screening. *Adv. Healthcare Mater.* 3, 609–616. <https://doi.org/10.1002/adhm.201300151>
- Valencia, A.M., Kadoch, C., 2019. Chromatin regulatory mechanisms and therapeutic opportunities in cancer. *Nat Cell Biol* 21, 152–161. <https://doi.org/10.1038/s41556-018-0258-1>
- Varol, U., Kucukzeybek, Y., Alacacioglu, A., Somali, I., Altun, Z., Tarhan, M.O., 2018. BRCA genes: BRCA 1 and BRCA 2.
- Vasantharajan, S.S., Eccles, M.R., Rodger, E.J., Pattison, S., McCall, J.L., Gray, E.S., Calapre, L., Chatterjee, A., 2021. The Epigenetic landscape of Circulating tumour cells. *Biochimica et Biophysica Acta (BBA) - Reviews on Cancer* 1875, 188514. <https://doi.org/10.1016/j.bbcan.2021.188514>
- Vinay, D.S., Ryan, E.P., Pawelec, G., Talib, W.H., Stagg, J., Elkord, E., Lichtor, T., Decker, W.K., Whelan, R.L., Kumara, H.M.C.S., Signori, E., Honoki, K., Georgakilas, A.G., Amin, A., Helferich, W.G., Boosani, C.S., Guha, G., Ciriolo, M.R., Chen, S., Mohammed, S.I., Azmi, A.S., Keith, W.N., Bilsland, A., Bhakta, D., Halicka, D., Fujii, H., Aquilano, K., Ashraf, S.S., Newsheen, S., Yang, X., Choi, B.K., Kwon, B.S., 2015. Immune evasion in cancer: Mechanistic basis and therapeutic strategies. *Seminars in Cancer Biology* 35, S185–S198. <https://doi.org/10.1016/j.semcancer.2015.03.004>
- Warburg, O., 1925. The Metabolism of Carcinoma Cells1. *The Journal of Cancer Research* 9, 148–163. <https://doi.org/10.1158/jcr.1925.148>
- Warkiani, M.E., Guan, G., Luan, K.B., Lee, W.C., Bhagat, A.A.S., Kant Chaudhuri, P., Tan, D.S.-W., Lim, W.T., Lee, S.C., Chen, P.C.Y., Lim, C.T., Han, J., 2014a. Slanted spiral microfluidics for the ultra-fast, label-free isolation of circulating tumor cells. *Lab Chip* 14, 128–137. <https://doi.org/10.1039/C3LC50617G>
- Warkiani, M.E., Khoo, B.L., Tan, D.S.-W., Bhagat, A.A.S., Lim, W.-T., Yap, Y.S., Lee, S.C., Soo, R.A., Han, J., Lim, C.T., 2014b. An ultra-high-throughput spiral microfluidic biochip for the enrichment of circulating tumor cells.
- Welsch, U., Kummer, W., Deller, T., 2018. *Histologie - Das Lehrbuch*, 5th ed. Elsevier.
- Werner, S., Stenzl, A., Pantel, K., Todenhöfer, T., 2017. Expression of Epithelial Mesenchymal Transition and Cancer Stem Cell Markers in Circulating Tumor Cells, in: Magbanua, M.J.M., Park, J.W. (Eds.), *Isolation and Molecular Characterization of Circulating Tumor Cells*. Springer International Publishing, Cham, pp. 205–228. https://doi.org/10.1007/978-3-319-55947-6_11
- Wu, S., Zhu, W., Thompson, P., Hannun, Y.A., 2018a. Evaluating intrinsic and non-intrinsic cancer risk factors. *Nat Commun* 9, 3490. <https://doi.org/10.1038/s41467-018-05467-z>
- Wu, S., Zhu, W., Thompson, P., Hannun, Y.A., 2018b. Evaluating intrinsic and non-intrinsic cancer risk factors. *Nat Commun* 9, 3490. <https://doi.org/10.1038/s41467-018-05467-z>
- Yang, Y.-P., Giret, T.M., Cote, R.J., 2021. Circulating Tumor Cells from Enumeration to Analysis: Current Challenges and Future Opportunities. *Cancers (Basel)* 13, 2723. <https://doi.org/10.3390/cancers13112723>
- Yu, W., Hurley, J., Roberts, D., Chakraborty, S.K., Enderle, D., Noerholm, M.,

Breakefield, X.O., Skog, J.K., 2021. Exosome-based liquid biopsies in cancer: opportunities and challenges. *Annals of Oncology* 32, 466–477. <https://doi.org/10.1016/j.annonc.2021.01.074>

Zhang, L., Riethdorf, S., Wu, G., Wang, T., Yang, K., Peng, G., Liu, J., Pantel, K., 2012. Meta-Analysis of the Prognostic Value of Circulating Tumor Cells in Breast Cancer. *Clin Cancer Res* 18, 5701–5710. <https://doi.org/10.1158/1078-0432.CCR-12-1587>

10 Acknowledgements

First of all, I would like to give a special thank you to my supervisor PD Dr. Simon A. Joosse who made this work possible. Thanks for the support during the experimental work in the lab, the assistance along the writing process of this thesis, always being available for questions and being my scientific mentor these last four years.

I am very grateful to Prof. Dr. med Klaus Pantel for supporting me in this project as head of the institute. I really appreciate the regular support, opportunity to discuss questions and interest on the current state of the project in the weekly meetings.

I also want to thank my work group, for the great experience and the wonderful time in the lab. Especially, Gresa Hasani and Nikhil Kalra who have supported me with the experimental work, but also with advice and new ideas during the laboratory work. Thanks as well to Maximilian C. Wankner and Paul N. Rademacher for collaborating with me on this project and to our technician assistant Sandra Lenz for the help with my experiments and always bringing a cheerful mood into the lab.

The fellowship of the *Deutsche Krebshilfe* enabled me to completely focus on my experimental work in the lab for a year and I really appreciate this generous funding.

11 Eidesstattliche Versicherung

Ich versichere ausdrücklich, dass ich die Arbeit selbständig und ohne fremde Hilfe verfasst, andere als die von mir angegebenen Quellen und Hilfsmittel nicht benutzt und die aus den benutzten Werken wörtlich oder inhaltlich entnommenen Stellen einzeln nach Ausgabe (Auflage und Jahr des Erscheinens), Band und Seite des benutzten Werkes kenntlich gemacht habe.

Ferner versichere ich, dass ich die Dissertation bisher nicht einem Fachvertreter an einer anderen Hochschule zur Überprüfung vorgelegt oder mich anderweitig um Zulassung zur Promotion beworben habe.

Ich erkläre mich einverstanden, dass meine Dissertation vom Dekanat der Medizinischen Fakultät mit einer gängigen Software zur Erkennung von Plagiaten überprüft werden kann.

Unterschrift: